Response to referees for, "Ozonolysis of α-phellandrene, Part 1: Gas- and particle-phase characterisation" by Mackenzie-Rae et al.

The authors would like to thank the referees for their time reviewing the manuscript, and for the thoughtful feedback provided. Based on their recommendations a number of significant modifications have been made to improve the manuscript, which we believe has substantially improved the interpretation of this study. Presented below are the specific comments made by the reviewers (italicised) and our corresponding responses (non-italicised).

Referee #1

General comments
This paper presents experimental results on the formation of gaseous organic species, OH radicals and secondary organic aerosols (SOA) during a-phellandrene ozonolysis. Various dark ozonolysis experiments were performed in an indoor smog chamber facility (with or without OH scavengers, CI scavengers and NOx). Gas-phase species were monitored using a PTR-TOF-MS, SOA size distributions with a SMPS and aerosol compositions with an AMS. Measurements were used to calculate yields for a few gaseous organic species, OH yields from a-phellandrene and its first-generation products, and rate coefficient of first-generation products. Aerosol yields and effective density of SOA are also provided. The reactivity of a-phellandrene with ozone, as well as its impact on HOx and SOA formation has currently not been studied in the scientific community. This paper provides experimental data that are valuable to better understand the environmental impact of biogenic compound ozonolysis and could therefore be of interest to the scientific community. However, the manuscript suffers from a lack of clarity, precision and discussion in several places. In particular, the current knowledge on a-phellandrene ozonolysis is not enough presented, the purpose of the selected type of experiments are not explained, the methodology used to calculate yields or kinetic constants should be clarified and conclusions reached by the author should be better justified by comparison with previous work. All of this make that even if the results may well be fully valid, an explanation of the methodologies and a justification of conclusions are needed to support the results. Major revisions are therefore required before publication in ACP.

> We appreciate the referee's feedback and their recognition of the value that the study offers the scientific community. We will now address their specific concerns to improve the precision, clarity and discussion of the manuscript.

Specific comments
The chemical reactions expected to occur during a-phellandrene ozonolysis according to the literature are never described rigorously in the manuscript. The discussion and the Figure in S4 should be presented before section 2 (and not in section 3 where it is difficult to make the difference between our knowledge, the coherence of the observations shown in this study and the novelty of the results). This figure should be used in section 3 to justify the detection of some species and could be coupled with in Fig. 7 to explain the formation of the "new" species

detected in this study and with Fig. 6. The structure of a-phellandrene can also be presented from this figure, allowing to remove Figure 1 which is not really useful.

Upon review it is clear that both the general ozonolysis mechanism, and the specific processes involved in α-phellandrene's degradation are not included or are included too late in the manuscript to prove efficient. To address the lack of background mechanism information, the following paragraph was added to the introduction.

p.2 l.20: "Ozonolysis is generally agreed to occur through a concerted cycloaddition of ozone to the olefin bond, forming a 1,2,3-trioxolane intermediate species referred to as a primary ozonide (POZ) (Calvert et al., 2000; Johnson and Marston, 2008). Addition of ozone is highly exothermic with excess energy retained in the POZ structure, resulting in rapid decomposition through homolytic cleavage of the C–C and one of the O–O bonds, which forms, in the case of asymmetrically substituted alkenes, a pair of products containing a carbonyl and reactive Criegee Intermediate (CI). Sufficient vibrational and rotational excitation exists in the CI to permit further unimolecular decomposition which typically occurs through one of two channels; firstly excited CIs can cyclise to a dioxirane, which then decomposes to a carboxylic acid, ester or lactone depending on neighbouring substituents in what is known as the ester or `hot' acid channel, or secondly, when available, excited CIs can isomerise via a 1,5-hydrogen shift to form a vinylhydroperoxide, which subsequently decomposes into a vinoxy radical and a hydroxyl radical in what is known as the hydroperoxide channel. Alternatively excited CIs can be collisionally stabilised, such that bimolecular reactions with trace species (e.g. H_2O, NO_2, aldehydes, acids) becomes important (Johnson and Marston, 2008). The relative prevalence of these two channels is strongly linked to the structure and conformation of the CI (Vereecken et al., 2015), with the various mechanistic pathways summarised in Fig. 1."

Furthermore the following sentence was added on p.3 l.8. to introduce the reactions expected to occur during α-phellandrene's ozonolysis before section 2.

p.3 l.8: "A basic overview of the reaction pathways is provided in Fig. 1, with a comprehensive discussion of the reaction mechanism of α-phellandrene with ozone based on the findings of Mackenzie-Rae et al. (2016) pertinent to this study provided in the Supplementary Information S.1."

Rather than discarding, Figure 1 was amended (shown below) to include an overview of processes involved in the degradation of α-phellandrene through ozonolysis. The revised figure is accompanied by direction in the main text to the Supplementary information S1 (previously S4), for those readers seeking a more exhaustive description of the mechanistic processes involved in α-phellandrene's degradation through ozonolysis. Furthermore the coupling between the various mechanistic figures was

improved to assist in overall readability. The lines starting at p.5 l.22 were amended to:

p.5 l.22: "Ignoring conformational isomerism, the ozonolysis of α-phellandrene can yield four unique CIs (Fig. 1) (Mackenzie-Rae et al., 2016), with the degradation mechanism of **CI3** provided in Fig. 7. Detailed schematics of the remaining CIs are provided in the Supplementary Information (S1), and lead to products isomeric to those shown in Fig. 7."
The caption of Figure 7 was then changed to:

Fig. 7: "Partial mechanism for the ozonolysis of α-phellandrene starting from **CI3**, yielding product masses detected by the PTR-TOF. Similar constructs for the remaining CIs are provided in the Supplementary Information (S.1)."

Similarly the caption of Figure S.1.1 (formally S.4.1) was adjusted to link into the degradation scheme provided in the main text, by adding the following sentence to the end of the caption:

Fig. S.1.1: "A more exhaustive description of the mechanism originating from **CI3** is provided in Fig. 7 of the main text."

A rigorous description of the mechanism is not the goal of this paper, and is more or less covered in the theoretical paper, 'Computational investigation into the gas-phase ozonolysis of the conjugated monoterpene α-phellandrene' by Mackenzie-Rae et al. (2016). However with the updates we now think that the introduction provides the reader with the necessary background knowledge to understand the mechanistic aspects and discussion provided in Section 3, and improves the overall clarity of the manuscript.

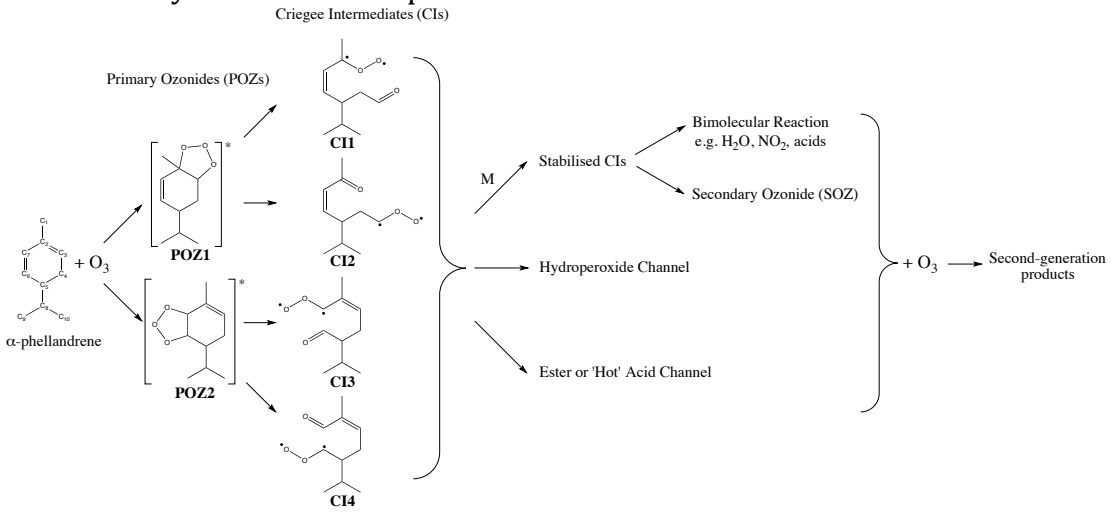

Figure 1. Simplified mechanism showing reaction processes involved during ozone addition to α-phellandrene within conventional frameworks (adapted from Mackenzie-Rae et al. (2016)). Carbon labels on α-phellandrene are referred to in the main text.

The various experiments are listed but the objective of each different type as well as

the expected impact on the chemical system should be discussed (why several O3 injections, NO2 addition? what is the expected impact of an OH and a Criegee intermediate (CI) scavenger on the chemistry? how much of the CI is expected to be scavenged by the used amount of formic acid?). The observed influences of OH and CI scavengers, NO2 or the several O3 additions are not enough shown or discussed, questioning the interest of including exp. 6, 7, 9 and 11 in the paper. Do the authors see expected or unexpected differences in gaseous secondary organic and OH yields, SOA formation…?

We thank the referee for noticing these points; justification of the experimental design and their consequences were not sufficiently addressed in the original manuscript. With respect to the several additions of ozone in some experiments (it was only ever one additional addition) the following lines were added/amended:

p.3 l.25: "α-phellandrene was injected prior to admission of O_3 into the chamber, with O_3 added through two separate additions in experiments 7 and 10 to facilitate the identification of detected species as either first- or second-generation products."

p.5 l.34: "This continual increase remained true in experiments which added a large secondary dose of ozone after commencement of the reaction (Fig. S.4.1), confirming the ions discussed as saturated."

With respect to NO_2 addition the following lines were added/amended:

p.3 l.29: "Prior to O_3 addition in experiment 11, 385 ppb of NO_2 was added through a septum installed in one of the injection ports using a gas-tight syringe, with the inclusion providing an alternative representation of tropospheric nocturnal chemistry in a polluted environment."

p.7 l.10: "A comparison of rate constants of O_3 with α-phellandrene (3.0×10^{-15} cm^3 $molecule^{-1}$ s^{-1}) and NO_2 (3.5×10^{-17} cm^3 $molecule^{-1}$ s^{-1}) suggests that the majority of O_3 will be consumed by α-phellandrene, with formation of the nitrate radical relatively minor. Nevertheless NO_2 is in excess in the system, with a systematic reduction in product yields indicative of a shift towards RO_2+NO_2 chemistry, producing peroxy nitrate containing products (Draper et al., 2015)."

Reference Added:
Draper, D. C., Farmer, D. K., Desyaterik, Y., and Fry, J. L.: A qualitative comparison of secondary organic aerosol yields and composition from ozonolysis of monoterpenes at varying concentrations of NO_2, Atmos. Chem. Phys., 15, 12 267-12 281, 2015.

p.7 l.21: "…while addition of NO_2 to the system in experiment 11 resulted in significantly reduced yields, although overall distribution remained similar with no new peaks or evidence of nitrate containing compounds observed, indicating that ozonolysis products remain dominant."

p.12 l.23: “Similarly there is a reduction in the α-phellandrene normalised number distribution when NO_2 is added (Fig. 11). Like formic acid, NO_2 can also react with sCIs (Johnson and Marston, 2008) and therefore potentially inhibit particle formation and growth. If this were the case then results from this ozonolysis study likely represent an upper limit to SOA formation under ambient conditions, although more experiments are necessary to confirm the impact of NO_2 on SOA formation in the α-phellandrene system.”

In addition Fig. 11a was amended to show the impact that NO_2 has with respect to the other experiments.

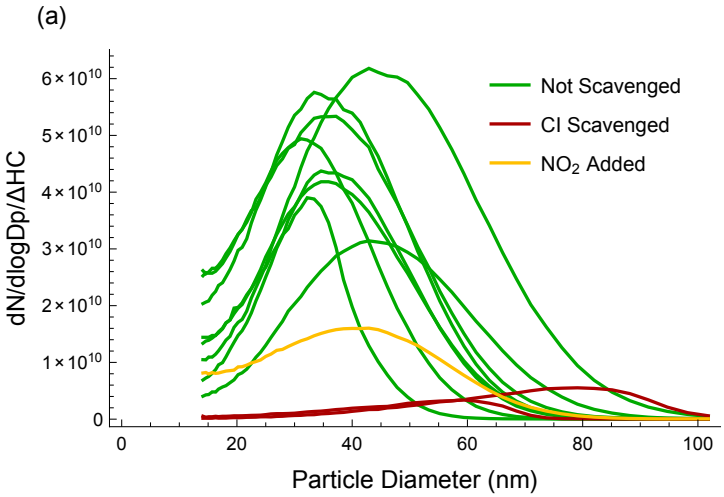

p.15 l.23: “Nitrogen containing species were found to make little contribution to the aerosol formed in experiment 11, with an average N/C ≈ 0.002 during this experiment. Nitrate functionality is believed to significantly reduce the vapour pressure of constituents (Capouet and Müller, 2006; Pankow and Asher, 2008), with the result implying a small gas-phase concentration. Nevertheless there exists evidence that organic nitrate contribution to SOA may be kinetically, rather than volatility driven (Perraud et al., 2012)”

Reference Added:
Perraud, V., Bruns, E. A., Ezell, M. J., Johnson, S. N., Yu, Y., Alexander, M. L., Zelenyuk, A., Imre, D., Chang, W. L., Dabdub, D., Pankow, J. F., and Finlayson-Pitts, B. J.: Nonequilibrium atmospheric secondary organic aerosol formation and growth, Proc. Natl. Acad. Sci., 109, 2836-2841, 2012.

With respect to formic acid addition it is difficult to estimate the amount of sCI that is expected to be scavenged, as this would require knowledge of sCI formation rates and rate constants of the various competing pathways (bimolecular reactions, unimolecular decomposition, reaction with formic acid), none of which currently exists in the literature for α-phellandrene. For this reason the information is not given, however the amount of formic acid has now been added to Table 1, with the ratio of formic acid to α-phellandrene added comparable to similar studies where

it has been used as a sCI scavenger (e.g. Bonn et al., 2002; Winterhalter et al., 2009). The following lines were also added/amended to strengthen the argument for its inclusion and discussion of its impact:

p.3 l.27: "Formic acid (J&K Scientific Ltd., 98%) was added to experiments 6 and 7 as a stabilised Criegee Intermediate (sCI) scavenger to better understand the role of sCIs on gas-phase species distribution and importantly particle-phase formation and growth, for which it has been identified as a significant precursor (Bonn et al., 2002; Bateman et al., 2009; Sakamoto et al., 2013; Wang et al., 2016)."

p.7 l.8: "The addition of a sCI scavenger was found to have little impact on product distribution or yields, suggesting that the sCI-formic acid complexes ultimately decompose to yield similar gas-phase products as sCIs that degrade through conventional channels. Whether this decoupling of the complex occurs inside the reactor or upon protonation in the PTR-TOF remains unknown."

The addition of cyclohexane as an OH scavenger in ozonolysis experiments is fairly common practice in the field (e.g. Bonn et al., 2002; Keywood et al., 2004; Saathoff et al., 2009; Winterhalter et al., 2009) and so validation of its inclusion is not necessary. However with regards to experiment 9 it is rightly noted by the referee that validation of its inclusion and impact on the gas-phase were not included, with the following lines added/amended to rectify this.

p.3 l.25: "Anhydrous cyclohexane (Sigma-Aldrich, 99.5%) was added in sufficient quantity in all but two experiments to scavenge > 95% of OH radicals (Aschmann et al., 1996; Herrmann et al., 2010), with the remaining experiments used to assess the impact of cyclohexane's inclusion."

p.7 l.9: "Similarly no significant differences in yields were observed between experiment 9 and OH-scavenged experiments, with decomposition into smaller carbon species counter intuitively invariant to action by the OH radical; strengthening the argument that fragmentation inside the PTR-TOF is non-negligible"

p.7 l.21: "Again the presence of OH radicals in experiment 9 had little effect on product yields…"

What is the typical volume of the chamber at the end of an experiment? (p.3 l.31).

Varies for each experiment, but typically between 6 – 8 m^3. This information was added to the end of p.3 l.31.

Numerous figures and tables are discussed before or without being presented. Each Figure or Table should be clearly introduced in the text before being discussed.

Yes, upon re-reading we agree that the integration of figures/tables into text definitely requires improvement in multiple places. The following changes were made to address this:

The premature reference to Fig. 2 on p.5 l.6 was removed, with the proper introduction to the figure remaining at p.5 l.20.

Figures 3, 4, 5, 6 and 7 were renumbered to Figs 4, 6, 7, 5 and 3 respectively, so that the order of introduction in the text matches the figure number. This makes logical sense in the scheme of the manuscript and ensures figures have properly been introduced before discussion, improving general readability.

Additionally the following sentences were changed to better introduce the figures.

p.8 l.6: "An example showing this from a proposed first-generation product is provided in Fig. 5."

p.11 l.28: "Nevertheless rapid aerosol formation is observed upon reaction of α-phellandrene and ozone as shown in Fig. 10, with sharp increases in particle number (dN/dlogDp) and volume (dV/dlogDp) concentrations observed."

p.15 l.16: "Figure 16 shows the typical temporal profile of aerosol composition observed over an experiment."

p.16 l.27: "The carbon mass balance for each experiment is shown in Fig. 19. It was calculated by…"

The lines p.4 l.30-33 that introduce Table 1 have been moved to p.3 l.31, with the earlier reference to the table on p.3 l.24 removed.

Reference to Table 2 on p.5 l.9 was removed, as it was unnecessary and occurred before Table 2 was properly introduced on line 18 of that page.

Table 3 is now properly introduced on p.6 l.18 by adding the following, with the old reference on p.6 l.28 removed.

p.6 l.18: "The average yield from sequential ozonolysis is therefore calculated with results provided in Table 3. In practice however calculations are…"

The temporal evolution of the PTR-TOF-MS signals presented in Fig 2 should be described in the text at the beginning of the section 3.1.1. In particular, Why are all concentrations at around 35 min going to 0 except m/z = 42 and 137? Why does the precursor's concentration decrease at the same time? The m/z 42 signal is not impacted. Why? Is the linear decrease of O3 (after 70 min) due to wall loss?

Yes Fig. 2 was not discussed in depth in the text. This was partly because it shows time profiles from one of eleven experiments, nonetheless as the referee pointed out there are some common trends which are worth discussing. For this reasons the line starting at p.5 l.20 was expanded to the following.

p.5 l.20: "Figure 2 shows time profiles of major species detected by the PTR-TOF during the ozonolysis of α-phellandrene. For clarity peaks have been corrected for background readings recorded prior to the introduction of ozone. Upon the injection of ozone, α-phellandrene is rapidly oxidised forming a number of product ions at low concentrations that continually increase throughout the experiment. Meanwhile ozone, after rapid initial consumption, slowly decreases throughout the experiment in part due to losses to the reactor walls (Wang et al., 2014). The stability of acetonitrile and cyclohexane signals supports the finding of Wang et al. (2014) that wall losses are relatively minor for volatile organics in the GIG-CAS chamber."

With regards to the precursors concentration decreasing at the start and the corresponding m/z 42 signal remaining unchanged, this was an irregularity experienced in this experiment caused by the fans being switched on after α-phellandrene's injection. As the sampling port is near to the injection port, upon addition of α-phellandrene its concentration was read erroneously high. When switched on the fans quickly dispersed α-phellandrene causing its concentration to fall and stabilise. As the fans were switched on prior to acetonitrile injection such an effect was not seen. Justification of this was thus added to the caption of Fig 2.

Fig. 2: "The peak of α-phellandrene observed upon its addition was the result of the reactor fans being switched on immediately prior to the introduction of acetonitrile in this experiment."

With regards to impact all concentrations and physical conditions (e.g. temperature, humidity) were stable prior to injection of ozone, so the delayed start of the fans in this experiment had no impact on findings.

In OH scavenged experiment, the reactivity of the system is expected to stop when the two a-phellandrene double bonds have each been reacting with O3. PTR-TOF-MS measurements show an increase of all the m/z signals (also for small molecules), except for the m/z assigned to the precursor and the inert gas. Some of these m/z could be assigned to first generation products (and also maybe second generation?) expected to be formed during scavenged a-phellandrene + O3 experiments. These first and also second generation species are expected to stop growing when no double bond remain in the molecule considering the known chemistry. The authors claim at several places in the paper that the observed increase suggests that these compounds are second-generation or higher generation species (e.g. p.5 l.25, l.35 and below in the paper) or that this unique profile implies that they derived from a source secondary to ozonolysis, such as gas-phase accretion (e.g. p7 l.35., table 2, S3...). The authors should be careful in

drawing their conclusions. Why an increasing signal makes the species a second-generation compound?

In the majority of experiments ozone is added in excess ([O_3] = 2x[α-phellandrene]). Therefore first-generation products, containing one residual double bond, are expected to further react resulting in a time-profile that reaches a peak sometime after initiation, before decaying as the first-generation product is consumed by ozone (e.g. Lee et al., 2006; Ng et al., 2006; Camredon et al., 2010). Because such time profiles were not observed it can be concluded that either (i) all observed species have second-generation contribution or (ii) experimental run times were not long enough to see the consumption of first-generation products. The simple modelling study described in the manuscript shows (ii) not to be true. The same thought process, whereby increasing signals were argued to have second-generation contributions was made in Lee et al. (2006). This distinction was not made clear on p.5 l.25 and l.33, with the following changes made:

p.5 l.25: "…however none of the product ions detected were observed to decrease over the course of the chamber experiments, suggesting that detected ions in part correspond to second-generation products."

p.5 l.33: "Both these ions were detected in the PTR-TOF but again had concentrations which increased throughout the experiments, suggesting that they have large contributions from saturated species."

The study of Ng et al. (2006), whilst referenced in the manuscript, was not used as an additional example of a study where first-generation products were observed with a PTR-MS for all terpenes investigated except for the most reactive poly-alkenes (in their case α-terpinene, α-humulene and β-caryophyllene). The reference was thus incorporated into p.6 l.1 alongside that of Lee et al. (2006).

If this increasing signal comes from the formation of dimers, why is an increase also observed for the low m/z signals (m/z = 47, 59, 61…)?

An increasing signal does not necessarily mean it comes from dimers, we argue that it purely means it likely comes from a saturated species. We hope that the above changes make this clearer. Instead dimers are used to explain the higher mass signals (*m/z* 167, 169 and 185) as due to fragmentation upon the second addition of ozone products of these masses are unlikely to form in large amounts (requires ~5 oxygens on a C_7 or less backbone). Furthermore as Fig. S.3.1 shows the rate of formation of these products is relatively unperturbed by a second addition of ozone, whilst direct second-generation products (e.g. *m/z* 47, 59, 61) all show a marked increase. Because of this a higher generation process, such as accretion, is inferred. P.7 l.32 and the supplementary entry S.3 were changed to better convey this.

p.7 l.32: "…have relatively constant temporal profiles which also lack an accelerated increase upon a second addition of ozone; a feature that is apparent among lighter product ions (Fig. S. 3. 1). Their unique time profiles imply that they are derived from a source secondary to ozonolysis such as gas-phase accretion reactions, with modeling support for this provided in the Supplementary Information (S.3).

S.3: "Signals at *m/z* 167, 169 and 185 are relatively invariant to a second addition of ozone to the reactor, lacking the characteristic rapid increase in concentration observed for lighter product ions (Figure S.3.1). This suggests that the peaks are formed through a process supplementary to direct ozonolysis."

The hypothesis of some chamber wall artefacts is never discussed in the paper. Have the author already tested the impact of chamber teflon walls on the off-gassing of radical and/or organic species in the gas phase? Could it be a possible explanation of the increasing m/z signals?

It is not mentioned in the paper but off-gassing of radicals/organics from the reactor walls is not expected to be important under the dark, dry conditions used, especially given the extensive cleaning process between experiments (Section 2.1). Characterisation of the chamber auxiliary process is described in depth in Wang et al. (2014), with off-gassing expected to be predominantly a light driven process. Wang et al. (2014) showed that propene remains stable in concentration, whilst we conducted a similar experiment with α-phellandrene whose concentration was also stable inside a clean reactor, suggesting that off-gassing of radicals is minor. This is somewhat shown in Fig. 2, where both α-phellandrene and product signals remain stable in the ~30 minutes prior to ozone addition. To address this in the manuscript the following line was added.

p.3 l.19: "…with the impact of off-gassing of radicals from the reactor walls during experiments under the dark, dry conditions used negligible (Wang et al., 2014)."

Experimental results are used to provide various yields. The yields are however not always clearly defined in the paper. For secondary organic species (SOC), Y would be usually defined as: Y = Δ [SOC]/ Δ [COV]. Here Y is calculated from the amount of O3 that has reacted as Y = Δ [SOC]/ Δ [O3]. Has the Δ [O3] to be divided by a factor of 2 to correspond to the Δ [COV] or not? Has this method been used previously? How do you deal with experiments without OH scavenger or with various additions of O3? The initial concentration of O3 is not known. Does this have an impact on the calculated yields? Looking at Fig. 3, no data is used at the beginning of the experiment when the system is the most reactive, i.e. before Δ [O3]=40 ppb. Why? The intercept of the regression lines is different of 0. Why? The all length of the experiment is used to optimize regression lines and therefore to get the yield. 4/5 of these measured data correspond to a decrease of O3 concentration due to wall loss and an increase of secondary organic species which is difficult to understand. Is

that not an issue to keep these points for the optimization?

We assume that the referee is defining SOC as secondary organic compound and means VOC instead of COV? If so, then the yield equation provided is correct for determining yields with respect to α-phellandrene (and was used for OH yields in this work). However $\Delta[O_3]$ was used as opposed to Δ[VOC] in calculating gas-phase product yields in this study because of the high reactivity of α-phellandrene. For all species, most of the growth occurs after α-phellandrene is more or less completely consumed; therefore if the primary hydrocarbon were used in the denominator unrealistically high yields would be obtained. The use of $\Delta[O_3]$ provided much cleaner, more consistent results – however as far as the authors are aware it is the first time this method has been used. The implication of using $\Delta[O_3]$ is stated on p.6 l.18, 'The average yield from sequential ozonolysis is therefore calculated'. This statement implies $\Delta[O_3]$ was not divided by a factor of 2, this is because this action would implicitly assume that half of each product yield is attributable to α-phellandrene. Obviously this is going to be different for each product ion, and so making this assumption would be incorrect. The wall loss of ozone was frequently calibrated and corrected for in all calculations (p.6 l.17). The fact that 4/5 of the data occurs after α-phellandrene's consumption is an issue for optimisation as it results in fitted yield plots being dominated by reaction of first-generation products, however this shortcoming is noted on p.6 l.19. The difference in methodologies when comparing results is now noted on p.6 l.30.

p.6 l.30: "…although a subtle difference in methodology should be noted with Lee et al. (2006) calculating yields with respect to the parent hydrocarbon."

For experiments with two additions of O_3 separate yield lines were fitted, one for each addition. Differences were observed, as the yield plot from the first addition contains a much greater influence from α-phellandrene, whilst the second addition is impacted to a greater extent by first-generation products. However in keeping with the remaining data the two yields were averaged to get an overall yield from the system. This subtle change in methodology is now included in p.6 l.23.

p.6 l.23: "For experiments that had two additions of ozone (7 and 10), separate yield lines were fitted for data after each addition of ozone with the results then averaged, therefore maintaining the reported yield as an average of the entire ozonolysis system."

For the two experiments where no OH radical scavenger was added no change in analysis methodology was made, with the impact of OH radicals an obvious unaccounted for uncertainty. This impact is implicit in the new inclusions of p.7 l.9 and p.7 l.21 described on page 6 of this document.

Whilst it is true that the initial concentration of O_3 is not known it has no

impact on results, as it is the change in [O_3] between data points that is important. With regards to Fig. 3, it is well noted that no data points are used when the system is at its most reactive ($\Delta[O_3] < 40$ ppb). This is because of the finite mixing time of the reactor, with the first few minutes of data not used to ensure [O_3] readings are accurate (mentioned on p.6 l.20). For the plotted experiment (#5), this resulted in a difference of 38 ppb between the peak [O_3] reading and first data point used. The intercepts are non-zero because of this; with the majority of data points used corresponding to reaction of first-generation products. The impact of excluding data from the first few minutes, predominantly involving product production from α-phellandrene, ultimately yields non-zero intercepts. This was observed across all experiments.

Two OH yields are calculated, one for a-phellandrene and another one for its first-generation products using the methodology presented in Herrmann et al. (2010). The methodology used here should be presented using the Herrmann et al. (2010) reference with the two reactions p.8 l.34, before the presentation of the OH yield results.

We agree this change will improve the flow of the manuscript. The sentence referring to the results on p.8 l.18 is therefore moved to p.9 l.12, so that results are presented after the method.

How do you define the end of the a-phellandrene dominated zone (Fig. 4)? Why is the intercept of the regression line different of 0 in Fig 5.a.? The intercept could be 0 with a good correlation coefficient if the end of the a-phellandrene dominated zone stops before.

The end of the α-phellandrene dominated zone for each experiment is chosen qualitatively, however a correlation coefficient (R^2) greater than 0.9 is always maintained. The intercept of the regression line in Fig. 5a is different from zero due to a delay in OH radical detection by the PTR-TOF. There appears to be little change in OH radical production over the first 3 data points, corresponding to a 6 second delay with respect to α-phellandrene consumption. OH radicals do have to react with cyclohexane to form cyclohexanone to be detected, although 6 seconds to do this does seem too long given the rapid reactions of radicals. Nevertheless similar delay lengths were observed in all experiments.

How do you define the end of the product dominated zone (Fig. 4)? Is that not when the observations are difficult to understand and when we do not look at ozonolysis?

The product dominated zone had no end-point. We propose in theory it would be when the products are no longer reacting, being when all species are saturated in an ozonolysis experiment, although this point was never reached during chamber simulations considered here. For example Fig. 5b shows all data points until termination of experiment 3. It is not defined as a point when "observations are difficult to understand".

In Fig 5.b, shouldn't the OH and O3 concentration variations be looked starting from the beginning of the product dominated zone (and not from the beginning of the experiment) and why is the intercept of the regression line far from 0?

In Fig. 5b the variation of OH and O_3 are looked at from the start of the product-dominated regime. That is why both [OH] and [O_3] are non-zero. The intercept of the regression line for this is far from zero because it does start from the beginning of the product-dominated regime, with [OH] therefore having received contributions from α-phellandrene. As the OH yield from α-phellandrene is higher than the yield from first-generation products (Herrmann et al. 2010), a positive y-intercept is produced upon fitting the data.

The kinetic constant for the reaction of the secondary products with O3 was optimized giving again most of the weight to the to the part of the experiment we do not understand. Is that not an issue?

The beauty with the modeling study is that due to its simplicity, all parameters have to be more or less correct to get a time-profile that matches experiments. Whilst the majority of data pertains to the end of the experiment, the constants concerning the reaction of α-phellandrene with ozone are extremely important in determining overall shape and magnitude of the profiles. Indeed these parameters were found to be extremely sensitive and more difficult to fit. Therefore the quantity of data in the latter part of the experiment is not an issue.

What is the objective of all the section 3.2? No particle phase chemistry was studied in the paper. Please, change the title 3.2. Most of the sentences in section 3.2 are generalities, figures are listed but poorly discussed and the selected figures do not justify the reached conclusions. The writing of this section has to be largely improved with clear objectives and appropriated figures, discussion of the results and comparisons with literature.

Correct no particle-phase chemistry is discussed in Section 3.2, with this aspect reserved for the companion paper. Section 3.2 is thus renamed, 'Particle-phase Analysis', inline with the naming of Section 3.1, 'Gas-phase Analysis'.

A large portion of the generality discussion occurs when using metrics to assess the particle-phase. It is true that these parts are very qualitative, offering mere insights with strong conclusions not reached. For this reason the text from p.14 l.31 – p.15 l.11, discussing the CO_2^+ to $C_2H_3O^+$ ratios, and text on p.16 l.1 – p.16 l.12, discussing the double bond index, are removed from the discussion. This includes removal of Fig. 15 and the line corresponding to it in the abstract p.1 l.18. In total 29 lines were removed with no major implication on the overall discussion, making Section 3.2 much more succinct with clear objectives.

The introduction of the AMS data in the discussion was also heavily

modified, with large portions removed, including reference to and inclusion of Fig. 14. The paragraph starting at p.14 l.21 has been replaced with:

p.14 l.21: "Resolution in the W-mode of the AMS is sufficient to unambiguously identify chemical formulae of detected ions (DeCarlo et al., 2006; Aiken et al., 2007). Ions are formed however using high-energy electron impact ionisation (70 eV), resulting in significant fragmentation. The complexity of aerosol produced, along with an unknown number of fragmentation pathways including the possibility of charge migration and other internal rearrangements, makes it exceedingly difficult to obtain clear structural information about SOA constituents from the AMS. For this reason filter samples were collected and analysed to identify SOA constituents, with results to be published in a companion paper. Nevertheless the AMS remains useful for analysing bulk properties of the aerosol to gain further insight into the system."

Furthermore minor improvements were made to the remaining text to improve clarity and the overall discussion.

p.12 l.17: To improve flow and readability the text, 'whether uni- or bi-molecular' was removed.

p.13 l.27: Further references added to show utility of result.

Tsigaridis, K. and Kanakidou, K.: Global modeling of secondary organic aerosol in the troposphere: a sensitivity analysis, Atmos. Chem. Phys., 3, 1849-1869, 2003.

Henze, D. K. and Seinfeld, J. H.: Global secondary organic aerosol from isoprene oxidation, Geophys. Res. Lett., 33, L09812, 2006.

Jathar, S. H., Cappa, C. D., Wexler, A. S., Seinfeld, J. H., and Kleeman, M. J.: Simulating secondary organic aerosol in a regional air quality model using the statistical oxidation model – Part 1: Assessing the influence of constrained multi-generational ageing. Atmos. Chem. Phys., 16, 2309-2322, 2016.

p.13 l.31: Line added, "Nevertheless yields from the two experiments differ by almost a factor of two despite having similar starting conditions, with further experiments necessary to better quantify the impact of sCIs on yields."

p.15 l.29: To make reference to the literature stronger, "Figure 17 shows that the OS_c decreases from -0.61 to -1.00 as the particle loading increases from 21.5 to 658.1 μg m^{-3}, suggesting a strong link between mass loading and degree of functionalisation consistent with the findings of Shilling et al. (2009) for the ozononlysis of α-pinene."

p.16 l.26: References added:

Turpin, B. J., Saxena, P., and Andrews, A.: Measuring and simulating particulate organics in the atmosphere: Problems and prospects,

Atmos. Environ., 34, 2983-3013, 2000.
Kirchsetter, T. W., Corrigan, C. E., and Novakov, T.: Laboratory and field investigation of the adsorption of gaseous organic compounds onto quartz filters, Atmos. Environ., 35, 1663-1671, 2001.

Why are the activity coefficients needed (p.11 l.20)?

Activity coefficients affect the vapour pressure of SVOCs in the condensed organic phase (Pankow, 1994), with activity coefficient estimations therefore required for calculating saturation vapour concentrations. From the theory of Pankow (1994):

$$p_i = X_{i,om}\zeta_i p^0_{L,i}$$

where p_i is the gas-phase pressure of compound i, $X_{i,om}$ is its mole fraction in the organic matter phase and ζ_i is its activity in the organic matter phase.

In the two product parameterization, a1=a2 and Kom1=Kom2. What optimization method has been used? Does this mean that one product is enough to parameterized SOA formation? How can this be explained?

The parameters in Equation 2 in the manuscript were optimised for a two-product model using the NonlinearModelFit function in Wolfram Mathematica software, constraining each variable to be positive. Corresponding fitted parameters did not differ within the first five decimal points and so were reported as the same. A two-product model was reported, as is convention in the field (Odum et al., 1996). However because the parameters are the same it does result in a one-product model producing an identical fit:

$$Y = \Delta M_o \left(\frac{0.60 \times 0.022}{1 + 0.022\ \Delta M_o} + \frac{0.60 \times 0.022}{1 + 0.022\ \Delta M_o}\right) = 2\Delta M_o \frac{0.60 \times 0.022}{1 + 0.022\ \Delta M_o} = \Delta M_o \frac{1.2 \times 0.022}{1 + 0.022\ \Delta M_o}$$

where $\alpha_1 = 1.2$ and $K_{om,1} = 0.022$. Upon the referees recommendation the manuscript was changed to reflect this, with a more economical one-product fit now included.

Technical corrections
- p.2 l.32: change "µ g m3" into "µ g m-3"

Thank you, it has been corrected.

- p.3 l.9: I don't see a link between this study and the "theoretical foundation" you are talking about. I would remove "theoretical foundation".

The line, 'With a theoretical foundation', has been removed.

-p.3 l.27: "formic acid was added to experiment 6 and 7 to ascertain the role of SCI". What do you mean by "ascertain the role of SCI"? Are you talking about the role of CI?

Yes, the impact of stabilised Criegee intermediates on the reaction

mechanism and subsequent gas- and particle-phase observations. This line has been amended to improve clarity, with the revision provided on page 5 of this document.

-p.7 l.9: change "acetaldhyde" into "acetaldehyde"

Thank you, it has been corrected.

-p.8 l.15: this part of the sentence "So whilst the complete product distribution will likely consist of a myriad of species (Aumont et al., 2005)" is off-topic.

Agreed, it has been removed.

-p.36 Fig.10: in the legend, "µg m-3" has to be changed in a concentration in volume.

Thank-you, has been changed to $\mu m^3\ m^{-3}$.

-p.31 Fig.5: Δ[OH] on the y axis?

[OH] starts at zero in the reactor, so [OH] = Δ[OH]. However the change was made for clarity, and for consistency with Fig. 4 where it was used.

- Check that the concentrations and the variation of the concentration are written as [X] and not X .

Amendments were made to Fig. 2 legend, Fig. 3 axis and legend, Fig. 4 axis, Fig. 5 axis and legend and Fig. 8 axis and legend.

Whilst strictly M_o and HC are concentrations on p.14 and so should be written as [M_o] and [HC], they are presented in the form standard in the literature and so brackets are not included (e.g. Odum et al., 1996; Griffin et al., 1999; Kroll et al., 2008). This additionally extends to the y-axis label in Fig. 13.

Referee #2

General Comments
In this manuscript the authors describe results of a series of environmental chamber experiments in which a-phellandrene was reacted with ozone under a variety of conditions. Gas phase products were monitored with a PTR-MS and aerosol composition with an AMS. Yields for a number of low molecular weight gas phase products, OH radicals, and SOA were measured, and the rate constants for the reaction of a-phellandrene and first generation products with ozone were determined. A large number of higher molecular weight gas phase products were also observed, but could not be identified. Aerosol elemental composition, carbon oxidation state, and density were also measured. Overall, these experiments were well done and generated a large volume of data on gas and aerosol composition. The data analysis is very thorough and the authors have extracted about as much from this study as possible. The manuscript reports useful new information on an important monoterpene emission, which may be an important contributor to nucleation and SOA formation in some forested areas. When combined with results of ongoing molecular analysis of SOA products should provide a more complete picture of the chemistry. I think the manuscript is suitable for publication, but suggest the following comments be addressed.

Thank-you. We will now address the specific comments.

Specific Comments
1. Page 5, lines 23–25; Page 6, lines 5–9: What role might gas-wall partitioning of products play in these observations? It is now well established that this can be important for oxidized compounds. The authors could explore the extent to which their products might partition to the walls using empirical approaches that have recently been developed (e.g., Krechmer et al. ES&T, 2016).

The loss of volatile organics to the reactor walls was addressed in a response to the first referee on page 7. However rightly pointed out, a substantial discussion of the impact of gas-wall partitioning in the system is missing from the original manuscript. The extent to which gas-wall portioning occurs depends heavily on the equivalent organic mass concentration of the Teflon walls (C_w), which has not been measured for the GIG-CAS reactor. Values for C_w vary considerably in the literature, and so no formal parameterisation of the effect was undertaken. Nevertheless based on recent literature, it is likely that gas-wall partitioning of oxidised organics has a large impact on the results of the study, with the following updates and amendments made to the original manuscript to reflect this.

p.6 l.7: "Recent literature has shown that functionalised organic species experience considerable losses to Teflon chamber walls through gas-wall partitioning (e.g., Matsunaga and Ziemann, 2010; Zhang et al., 2014; Yeh and Ziemann, 2015; Krechmer et al., 2016; La et al., 2016). Observations indicate that organic compounds are not lost to the reactor walls, but rather partition between the gas-phase and Teflon walls in a reversible process that eventually reaches equilibrium, the speed of which is

dependent on reactor geometry, turbulence and species diffusivity, and penetration and accommodation in the reactor walls. Based on the work of Krechmer et al. (2016) the time scale for reaching gas-wall equilibrium in these experiments is thought to be less than 600 s. Gas-wall partitioning therefore operates quick enough to affect the considered chamber experiments and detection of first-generation products. The relative impact of gaseous wall losses is further explored in Section 3.2.1, nonetheless partitioning is strongly dependent on volatility with losses of highly-functionalised first-generation products of α-phellandrene to reactor walls and/or sample lines during transfer into and detection by the PTR-TOF expected (Yeh and Ziemann, 2015; Krechmer et al., 2016; La et al., 2016)."

p.7 l.21: "Calculated yields for these larger products were in general < 5%, with detected products sufficiently volatile such that gas-wall partitioning losses are thought to be minor (see Fig. 9)."

p.11 l.23: "Gas-particle partitioning occurs in competition with gas-wall partitioning, a process that is also dependent on species saturation vapour concentrations (Supplementary Information S.6). In parameterising gas-wall partitioning, the Teflon film is often considered to have an equivalent organic aerosol mass concentration (C_w). Values for C_w vary significantly in the literature, with Ziemann and co-workers reporting values of $C_w \sim 2 - 40$ mg m^{-3} (Matsunaga and Ziemann, 2010; Yeh et al., 2015), Zhang et al. (2014) reporting C_w values from 0.0004 – 300 mg m^{-3} and Krechmer et al. (2016) showing values of C_w to vary with C*, from C_w = 0.016 mg m^{-3} for C* < 1 up to 30 mg m^{-3} for C* > 10^4. The reasons for the large discrepancies between studies are unknown, however are likely due to differing deformation and activities of the Teflon walls (Krechmer et al., 2016). Nonetheless comparing reported values to SOA loadings generated during the chamber experiments in this work, it is evident that gas-wall partitioning is at least competitive, if not dominant compared to gas-particle partitioning. The impact is shown in Fig. 9 by plotting the fraction of an organic species that remains in the gas-phase over different saturation vapour concentrations using C_w = 5 mg m^{-3} and an SOA loading of 200 μg m^{-3}. Under this scenario gas-wall partitioning dominates, with compounds having C* < 10^2 μg m^{-3} predominantly residing in the walls with a small fraction in the aerosol phase after equilibrium is established, whereas species with C* > 10^6 μg m^{-3} remain almost entirely in the gas-phase. Compounds with 10^2 < C* < 10^6 μg m^{-3} will partition to varying extents depending on their volatility and functional group composition between the wall, gas- and particle-phases (Krechmer et al., 2016). However no corrections for gas-particle partitioning are made in the present study, given that no product vapour loss rate measurements were made for the GIG-CAS chamber and the large variability in literature values of C_w. Without correcting for vapour wall losses SOA yields are likely to be underestimated (Matsunaga and Ziemann, 2010; Zhang et al., 2014; La et al., 2016)."

Figure 9 was amended to include the fraction of organic species in the gas phase for different C*. This incorporates partitioning into both SOA and the Teflon walls.

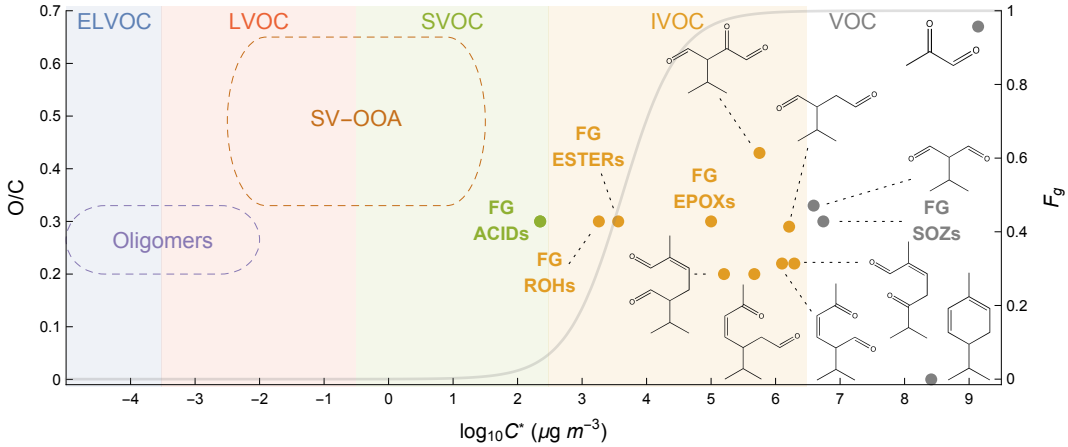

Figure 9. Dots show predicted first-generation and detected second-generation products from the ozonolysis of α-phellandrene in Donahue et al. (2006) space. Grey line shows the fraction of species of different saturation vapour concentrations in the gas-phase (F_g) after gas-wall and gas-particle equilibrium is reached, using C_w = 5 mg m^{-3} and an SOA loading of 200 μg m^{-3}. Formulation of F_g is given in the Supplementary Information (S.6).

The following entry was added to the Supplementary Information.

"S.6 Discussion of Gas-Wall Losses

The volatile species α-phellandrene, propene, acetonitrile and cyclohexane were not observed to experience losses inside the GIG-CAS reactor (this study, Wang et al., 2014). Nevertheless recent studies have shown that low volatility organic gases experience considerable losses onto reactor Teflon wall surfaces (e.g., Matsunaga and Ziemann, 2010; Zhang et al., 2014; Yeh and Ziemann, 2015; Krechmer et al., 2016; La et al., 2016). Studies have observed that organic compounds are not lost to the reactor walls, but rather partition between the gas-phase and Teflon walls in a reversible process that eventually reaches equilibrium. The time required for equilibrium depends on reactor geometry, pressure, turbulence inside the reactor and diffusion coefficients. Sorption of gaseous organic compounds to the wall and corresponding desorption from the wall back to the gas-phase can be parameterised using Raoult's law, treating the wall as a phase into which the organic compounds can partition (Matsunaga and Ziemann, 2010). The equilibrium state thus depends on compound volatility and can be modelled analogously to gas-particle absorptive partitioning, originally developed by Pankow (1994). Matsunaga and Ziemann (2010) argued that the fraction of an organic compound X that partitions into the walls at equilibrium is represented by:

$$\frac{[X]_w}{[X]_g} = K_w C_w = \frac{C_w}{C_w^*} = \frac{R\ T\ C_w}{M_w \gamma_w P_L^0} \qquad \text{(S.6.1)}$$

where C_w is the equivalent organic aerosol mass concentration associated with the Teflon film, K_w is the gas-wall partitioning coefficient (with

saturation concentration C_w^* being the inverse) and is equal to $RT/M_w\gamma_w P_L^0$, where M_w is the mean molecular mass of the Teflon film, γ_w is the activity coefficient for the compound absorbed into the Teflon film, P_L^0 is the liquid vapour pressure of the compound, R is the ideal gas constant and T the temperature.

Wall loss of organics occurs in competition with gas-particle partitioning. Assuming all SOA is absorbing so that C_{SOA} simply becomes [SOA] and using the parameterisation of Pankow (1994).

$$\frac{[X]_{SOA}}{[X]_g} = K_{SOA}C_w = \frac{C_{SOA}}{{C_{SOA}}^*} = \frac{R\ T\ [SOA]}{M_{SOA}\gamma_{SOA}P_L^0} \quad \text{(S.6.2)}$$

The fraction of an organic compound X remaining in the gas-phase at equilibrium (F_g) relative to its total concentration can therefore be given by:

$$F_g = \frac{[X]_g}{[X]_{total}} = \frac{[X]_g}{[X]_g + [X]_w + [X]_{SOA}} = \frac{1}{1 + \frac{C_w}{C_w^*} + \frac{[SOA]}{{C_{SOA}}^*}} \quad \text{(S.6.3)}$$

For simplicity aerosol that is lost to the walls continues to be considered as constituting the aerosol phase.

Activity coefficients for ozonolysis products of α-phellandrene in SOA generated from its decomposition were calculated using the method discussed in the main manuscript, with values ranging from 0.1 – 4. The mean molecular weight of the SOA is assumed to be 200 g mol^{-1} in this work. With no available constraining information the activity coefficient of compounds absorbed into Teflon walls is assumed as 1 for simplicity (Matsunaga and Ziemann, 2010; Krechmer et al., 2016). The mean molecular mass of the Teflon film is assumed to be 250 g mol^{-1} based on the masses of $-[CF_2CF_2]_n-$ and $-[CF_2CF(CF_3)]_n-$ subunits. Using these values, and given that R, T and P_L^0 are the same irrespective of the medium the vapour is partitioning into, the fraction of an organic compound in the gas-phase at equilibrium can be equated to:

$$F_g = \frac{1}{1 + \frac{{}^4/_5\, C_w + [SOA]}{{C_{SOA}}^*}} \quad \text{(S.6.3)}$$

assuming a value of γ_{SOA} = 1. The value of C_w is therefore an important parameter in determining the fraction of an organic compound that remains in the gas-phase and thus available for detection."

References Added:

Matsunaga, A. and Ziemann, P. J.: Gas-Wall Partitioning of Organic Compounds in a Teflon Film Chamber and Potential Effects on Reaction Product and Aerosol Yield Measurements, Aerosol Scie. Technol., 44, 881-892, 2010.

Yeh, G. K. and Ziemann, P. J.: Gas-Wall Partitioning of Oxygenated Organic Compounds: Measurements, Structure-Activity Relationships, and Correlation with Gas Chromatographic Retention Factor, Aerosol Sci. Technol., 49, 727-738, 2015.

Krechmer, J. E., Pagonis, D., Ziemann, P. J., and Jimenez, J. L.: Quantification of Gas-Wall Partitioning in Teflon Environmental Chambers Using Rapid Bursts of Low-Volatility Oxidized Species Generated in Situ, Environ. Sci. Technol., 50, 5757-5765, 2016.

La, Y. S., Camredon, M., Ziemann, P. J., Valorso, R., Matsunaga, A., Lannuque, V., Lee-Taylor, J., Hodzic, A., Madronich, S., and Aumont, B.: Impact of chamber wall loss of gaseous organic compounds on secondary organic aerosol formation: explicit modeling of SOA formation from alkane and alkene oxidation, Atmos. Chem. Phys., 16, 1417-1431, 2016.

Zhang, X., Cappa, C. D., Jathar, S. H., McVay, R. C., Ensberg, J. J., Kleeman, M. J., and Seinfeld, J. H.: Influence of vapor wall loss in laboratory chambers on yields of secondary organic aerosol, Proc. Natl. Acad. Scie. U.S.A., 111, 5802-5807, 2014.

2. Page 6, 32–35: Are NO3 radicals formed under the conditions of these experiments, and if so how might that chemistry affect the results?

Nitrate radicals are expected to form to some extent in experiment 11, where NO_2 is added along with O_3 to the reactor. However formation is only small because the reaction resulting in its formation ($NO_2 + O_3 \rightarrow NO_3$, $k = 3.2 \times 10^{-17}$ cm^3 $molecule^{-1}$ s^{-1}) competes against the much faster reaction of O_3 with α-phellandrene (3.0×10^{-15} cm^3 $molecule^{-1}$ s^{-1}) and its first-generation products (1.0×10^{-16} cm^3 $molecule^{-1}$ s^{-1}). If excess O_3 had been added to the reactor then NO_3 production would be expected to have a much more significant impact. Likewise if O_3 and NO_2 had been added to the reactor first and allowed to mix, the nitrate radical would have had a large impact. Reference to the nitrate radical has been added to the manuscript in response to Referee #1 (page 4 of this document).

3. Page 7, lines 21–23: Are you certain that organic nitrates would be observed with the PTR-MS? It seems likely that these compounds could lose HNO3.

The following change has been made to the manuscript.

p.7 l.21: "Addition of NO_2 to the system in experiment 11 resulted in significantly reduced yields, with overall distribution remaining similar and no new peaks or evidence of nitrate containing compounds observed. Nonetheless alkyl nitrates are known to readily lose HNO_3 after protonation in the PTR-TOF resulting in the formation of bare alkyl ions (D'Anna et al., 2005; Aoki et al., 2007; Duncianu et al., 2016)."

References added:

Aoki, N., Inomata, S., and Tanimoto, H.: Detection of C_1–C_5 alkyl nitrates by proton transfer reaction time-of-flight mass spectrometry, Int. J. Mass Sepctrom., 263, 12-21, 2007.

D'Anna, B., Wisthaler, A., Andreasen, Ø., Hansel, A., Hjorth, J., Jensen, N. R., Nielsen, C. J., Stenstrøm, Y., and Viidanoja, J.: Atmospheric chemistry of C_3-C_6 cycloalkanecarbaldehydes., J. Phys. Chem. A, 109, 5104-5118,

2005.
Duncianu, M., David, M., Kartigueyane, S., Cirtog, M., Doussin, J,-F., and Picquet-Varrault, B.: Measurement of alkyl and multifunctional organic nitrates by Proton Transfer Reaction Mass Spectrometry, Atmos. Meas. Tech. Discuss., in review, 2016.

4. Page 10, lines 1–25: No mention is made of the possible effect of particle-phase reactions of O3 with first-generation products. These reactions would be very fast (re-active uptake coefficient about 0.001) and could form a variety of low volatility products.

The parameterisation on p.10 purely investigates gas-phase chemistry. However it is true that an oversight exists in the manuscript with the possibility of heterogeneous process not discussed. This phenomenon will be explored further in the follow up publication that investigates the collected filter samples, however mention of it is now made on page 12.

p.12 l.5: "It is therefore evident that the simple mechanistic overview provided to explain formation of gas-phase products in Section 3.1.1 and in Mackenzie-Rae et al. (2016) is insufficient to account for aerosol observations, with more complex reactions or reaction processes such as autooxidation, oligomerisation and/or heterogeneous oxidation required to develop species of sufficiently low vapour pressure for both particle nucleation and growth (Hallquist et al., 2009)."

5. Page 12, lines 26–27: Please provide a reference for the proposed relationship between density and phase state.

Reference to the work of Kostenidou et al. (2007) has been provided.

Kostenidou, E., Pathak, R. K., and Pandis, S. N.: An algorithm for the calculation of secondary organic aerosol density combining AMS and SMPS data, Aerosol Sci. Tehnol., 41, 1002-1010, 2007.

6. Page 12, lines 26–27: How well do the measured densities compare with those expected from measured O//C/H composition. Parameterizations have been developed for this (e.g. Kuwata et al. ES&T, 2011).

The manuscript is updated to include a short discussion of SOA density parameterisation.

p.15 l.33: "SOA density predictions from elemental ratios using the parameterisation of Kuwata et al. (2012) show some agreement with measured values (Supplementary Information S.8)."

With the following added to the Supplementary Information.

"S.8 SOA Density Parameterisation

This study used the same method for measuring particle density and particle composition as Kuwata et al. (2012); namely comparing AMS and SMPS measurements of vacuum and mobility diameters respectively for the density and using an AMS with Aiken et al. (2008) calibration factors to measure elemental composition. The parameterisation developed by Kuwata et al. (2012) for predicting densities from elemental composition is therefore expected to be applicable. Using the Kuwata et al. (2012) parameterisation densities were predicted using elemental compositions averaged over entire experiments, with results compared to measured values in the Fig. S.8.1. Results are agreeable for most experiments except for those where the densest aerosol was produced (ρ_{org} > 1.5 g cm^{-3}). For these, predicted density is under predicted signaling either incorrect compositional measurements or that the parameterisation is not applicable. The majority of training data for the Kuwata et al. (2012) parameterisation is for SOA with ρ_{org} < 1.5 g cm^{-3}, with validation experiments also utilising aerosol seed particles – a notable difference compared to experiments conducted in this work. With respect to experimental measurements, the elemental ratio calibration factors of Aiken et al. (2008) do carry significant errors and recently have been superseded by Canagaratna et al. (2015). Further testing of density parameterisations is therefore recommended.

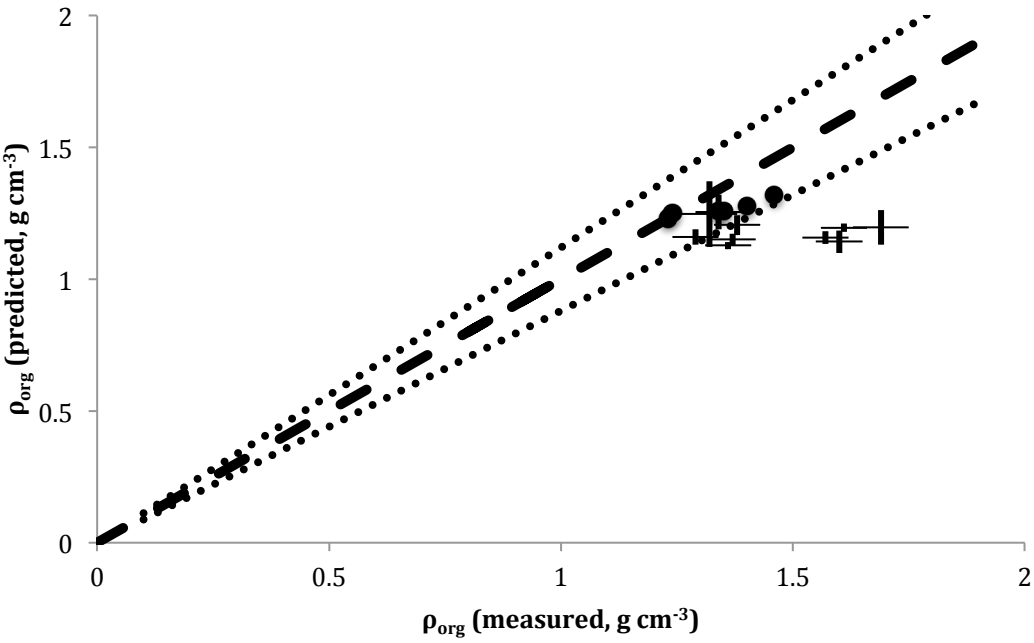

Figure S.8.1. Comparison of predicted to measured organic material density for α-phellandrene measured in this work (crosses, size reflect uncertainty) and α-pinene measured by Kuwata et al. (2012) (black circles). Predictions are made based on elemental composition using the parameterisation of Kuwata et al. (2012). Dashed line represents 1:1, whilst dotted lines show ±12% error representing the prediction accuracy envelope claimed by Kuwata et al. (2012). "

References added:

Kuwata, M., Zorn, S. R., and Martin, S. T.: Using elemental ratios to

predicted the density of organic material composed of carbon, hydrogen, and oxygen, Environ. Sci. Technol., 46, 787-794, 2012.
Canagaratna, M. R., Jimenez, J. L., Kroll, J. H., Chen, Q., Kessler, S. H., Massoli, P., Hildebrandt Ruiz, L., Fortner, E., Williams, L. R., Wilson, K. R., Surratt, J. D., Donahue, N. M., Jayne, J. T., and Worsnop, D. R.: Elemental ratio measurements of organic compounds using aerosol mass spectrometry: characterization, improved calibration, and implications, Atmos. Chem. Phys., 15, 253-272, 2015.

7. Page 13, lines 5–6: The reported wall loss rates for particles seem to be much higher than those measured by others, especially for such a large chamber. Any idea why?

The wall loss rates are higher than a lot of reported values. However many of these, especially ones reported during chamber characterisation experiments, use inert inorganic particles such as ammonium sulfate. These wall loss rates are not necessarily suitable for reactive organic aerosol (Wang et al., 2014). Wall loss rates are also dependent on turbulence inside the reactor, with two-fans operating simultaneously inside the GIG-CAS reactor during these experiments. The wall loss rates are consistent with those measured during α-pinene ozonolysis inside the chamber (Wang et al., 2014) suggesting the large loss rates are not related to specific aerosol formed but rather the GIG-CAS chamber as a whole. Meanwhile in using the same method to determine SOA wall loss rates, Pathak et al. (2007) measured wall loss rates as high as 0.48 h^{-1} for α-pinene ozonolysis SOA, Pierce et al. (2008) reported SOA loss rates of up to 0.5 h^{-1} for the ozonolysis of limonene and photooxidation of toluene, and Tasoglou and Pandis (2015) reported wall losses of up to 0.46 h^{-1} in their study on β-caryophyllene oxidation. The values reported in this work, whilst high, are thus not thought to be unreasonable.

References:
Wang et al. Atmos. Meas. Tech., 7, 301-313, 2014.
Pathak et al. J. Geophys. Res., 112, D03201, 2007.
Pierce et al. Aerosol Sci. Technol., 42, 1001-1015, 2008.
Tasoglou and Pandis, Atmos. Chem. Phys., 15, 6035-6046, 2015.

8. Page 13, lines 25–26: I would have expected that for a four-parameter fit would give a set a four different values. Doesn't this result imply that a two-parameter fit is as good as a four-parameter fit?

See response to the first referee regarding the fitted parameters on page 15 of this document.

9. Because of the large rate constant for reaction of a-phellandrene with O3 it seems likely that these experiments were conducted under conditions where RO2-RO2 reactions dominate the radical chemistry. In a clean atmosphere where this reaction might be thought to play a role in nucleation, it is likely that autoxidation may be important, or RO2-HO2 reactions. Some discussion of this would be useful.

The following was added to the manuscript.

p.5 l.23: "A focus is on RO_2–RO_2 radical chemistry which, due to the large rate constant of α-phellandrene with ozone and lack of competing radical termination channels, dominate under the considered reaction conditions."

p.14 l.16: "Indeed the reaction conditions used in these experiments better reflects this clean environment, where reactions of RO_2 with HO_2 and other RO_2 radicals dominates along with unimolecular rearrangements. Such conditions favour the formation of low-volatility compounds, with the highest SOA yields for monoterpenes found under low-NO_x conditions (Presto et al., 2005; Ng et al., 2007; Capouet et al., 2008; Eddingsaas et al., 2012). Under these conditions ozonolysis reactions remain important (Perraud et al. 2012; Zhao et al., 2015), which is conducive to autooxidation processes and therefore nascent SOA formation and growth due to enhanced propensity for intramolecular re-arrangements (Ehn et al., 2014; Jokinen et al., 2015). SOA yields measured in Experiment 11 however were consistent with the other ozonolysis experiments in this study (Fig. 12), suggesting that the impact of NO_x on SOA yields for ozonolysis driven chemistry of α-phellandrene are limited, with sufficient condensable products still produced (Draper et al. (2015). Nonetheless the reduction in aerosol number concentration in the initial stages of experiment 11 does suggest that formation pathways of ELVOC species (i.e. oligomerisation, autooxidation) are suppressed by the inclusion of NO_2 (Perraud et al. 2012). Detailed modeling studies are required to establish the relative importance of α-phellandrene in different environments, although evidence suggests that it is likely a contributor to nucleation events and aerosol growth in regions where it is emitted."

References Added:

Presto, A. A., Huff Hartz, K. E., Donahue, N. M.: Secondary organic aerosol production from terpene ozonolysis. 2. Effect of NOx concentration, Environ. Sci. Technol., 39, 7046-7054, 2005.

Ng, N. L., Chhabra, P. S., Chan, A. W. H., Surratt, J. D., Kroll, J. H., Kwan, A. J., McCabe, D. C., Wennberg, P. O., Sorooshian, A., Murphy, S. M., Dalleska, N. F., Flagan, R. C., and Seinfeld, J. H.: Effect of NOx level on secondary organic aerosol (SOA) formation from the photooxidation of terpenes, Atmos. Chem. Phys., 7, 5159-5174, 2007.

Capouet, M., Müller, J.-F., Ceulemans, K., Compernolle, S., Vereecken, L., and Peeters, J.: Modeling aerosol formation in alpha-pinene photo-oxidation experiments, J. Geophys. Res., 113, D02308, 2008.

Eddingsaas, N. C., Loza, C. L., Yee, L. D., Chan, M., Schilling, K. A., Chhabra, P. S., Seinfeld, J. H., and Wennberg, P. O.: a-pinene photooxidation under controlled chemical conditions-Part 2: SOA yield and composition in low-and high-NOx environments, Atmos. Chem. Phys., 12, 7413-7427, 2012.

Zhao, D. F., Kaminski, M., Schlag, P., Fuchs, H., Acir, I. H., Bohn, B., Häseler, R., Kiendler-Scharr, A., Rohrer, F., Tillmann, R., Wang, M. J., Wegener, R., Wildt, J., Wahner, A., and Mentel, T. F.: Secondary organic aerosol formation from hydroxyl radical oxidation and ozonolysis of monoterpenes, Atmos. Chem. Phys., 15, 991-1012, 2015.

Technical Comments
None.

Ozonolysis of α-phellandrene, Part 1: Gas- and particle-phase characterisation

Felix A. Mackenzie-Rae[1], Tengyu Liu[2,3,*], Wei Deng[2,4], Sandra M. Saunders[1], Zheng Fang[2,3], Yanli Zhang[2,4], and Xinming Wang[2,4]

[1]School of Molecular Sciences, The University of Western Australia, Crawley WA 6009, Australia
[2]State Key Laboratory of Organic Geochemistry and Guangdong Key Laboratory of Environmental Protection and Resources Utilization, Guangzhou Institute of Geochemistry, Chinese Academy of Sciences, Guangzhou 510640, China
[3]University of Chinese Academy of Sciences, Beijing 100049, China
[4]Center for Excellence in Regional Atmospheric Environment, Institute of Urban Environment, Chinese Academy of Sciences, Xiamen 361021, China
[*]now at: City University of Hong Kong

Correspondence to: X. Wang (wangxm@gig.ac.cn)

Abstract.

The ozonolysis of α-phellandrene, a highly reactive conjugated monoterpene largely emitted by Eucalypt species, is characterised in detail for the first time using a smog chamber at the Guangzhou Institute of Geochemistry, Chinese Academy of Sciences. Gas-phase species were monitored by a proton-transfer-reaction time-of-flight mass spectrometer (PTR-TOF), with yields from a large number of products obtained, including formaldehyde (5 – 9%), acetaldehyde (0.2 – 8%)~~.~~, glyoxal (6 – 23%), methyl glyoxal (2 – 9%), formic acid (22 – 37%) and acetic acid (9 – 22%). Higher *m/z* second-generation oxidation products were also observed, with products tentatively identified according to a constructed degradation mechanism. OH yields from α-phellandrene and its first-generation products were found to be 35 $\pm$ 12 % and 15 $\pm$ 7 % respectively, indicative of prominent hydroperoxide channels. An average first-generation rate coefficient was determined as 1.0 $\pm$ 0.7 $\times 10^{-16}\,\mathrm{cm^3\,molecule^{-1}\,s^{-1}}$ at 298 K, showing ozonolysis as a dominant loss process for both α-phellandrene and its first-generation products in the atmosphere. Endocyclic conjugation in α-phellandrene was also found to be conducive to the formation of highly condensible products ~~,~~with a large fraction of the carbon mass partitioning into the aerosol phase, which was monitored with a scanning mobility particle sizer (SMPS) and a high-resolution time-of-flight aerosol mass spectrometer (AMS). Nucleation was observed almost instantaneously upon ozonolysis, indicating the rapid formation of extremely low volatility compounds. Particle nucleation was found to be suppressed by the addition of either NO_2 or a Criegee scavenger, ~~suggesting~~ with it proposed that stabilised Criegee intermediates are important for new particle formation in the system. Aerosol yields ranged from 25 – 174% dependant on mass loadings, with both first- and second-generation products identified as large contributors to the aerosol mass. ~~Effective density ranged from 1.29 – 1.90 . The aerosol oxidation state was also found to be dependent on mass loadings, with parametrisation of the bulk mass indicating a large contribution of highly functionalised low- and semi-volatile organic compounds to the aerosol phase. With a~~ In short, with a high chemical reactivity and aerosol forming propensity, α-phellandrene is expected to have an immediate impact on the local environment to which it is emitted,

with ozonolysis ~~therefore~~ likely to be an important contributor to the significant blue haze and frequent nocturnal nucleation events observed over Eucalypt forests.

1 Introduction

Biogenic sources dominate the global emission budget of volatile organic compounds into the atmosphere, with monoterpenes accounting for a significant fraction of nonmethane hydrocarbons emitted (Guenther et al., 1995; Schurgers et al., 2009; Guenther et al., 2012; Lathière et al., 2006; Sindelarova et al., 2014). Considering source strength, estimated to be 30 - 127 $\mathrm{Tg\,C\,year^{-1}}$, along with high chemical reactivity (Calvert et al., 2000; Atkinson and Arey, 2003), monoterpenes are thought to play an important role in the chemistry of the atmosphere; influencing its oxidative capacity, the tropospheric ozone budget and by producing secondary organic aerosol (SOA) with impacts to both health and climate (Hoffmann et al., 1997; Griffin et al., 1999a; Chung and Seinfeld, 2002; Hallquist et al., 2009; Pye et al., 2010). Indeed the ozonolysis of monoterpenes is thought to be one of the major sources of organic SOA in the atmosphere (Griffin et al., 1999b; Ortega et al., 2012).

Consequently the gas-phase reaction of ozone with monoterpenes has been the focus of numerous studies, both experimental, with focus on gas-phase kinetics and particle formation, properties and composition (e.g. Bateman et al., 2009; Berndt et al., 2003; Griffin et al., 1999a; Herrmann et al., 2010; Lee et al., 2006; Ma et al., 2007; Pathak et al., 2007; Saathoff et al., 2009; Shilling et al., 2008, 2009; Walser et al., 2008); and theoretical, utilising state-of-the-art computational methods (Zhang and Zhang, 2005; Nguyen et al., 2009). Collectively, research has gone a long way to understanding the mechanism and product distributions of monoterpene ozonolysis, and provided important insights into SOA precursors and production. Accurate chemical mechanisms for the reaction of specific monoterpenes with ozone have since been developed (Camredon et al., 2010; Jenkin, 2004; Leungsakul et al., 2005), whilst more general parameterisations for gas-phase reactions (Jenkin et al., 1997; Saunders et al., 2003) and SOA formation (Odum et al., 1996; Donahue et al., 2006; Stanier et al., 2008) have been implemented into chemical transport models.

~~Nevertheless research shows, when~~ Ozonolysis is generally agreed to occur through a concerted cycloaddition of ozone to the olefin bond, forming a 1,2,3-trioxolane intermediate species referred to as a primary ozonide (POZ) (Calvert et al., 2000; Johnson and Marst
Addition of ozone is highly exothermic with excess energy retained in the POZ structure, resulting in rapid decomposition through homolytic cleavage of the C–C and one of the O–O bonds, which forms, in the case of asymmetrically substituted alkenes, a pair of products containing a carbonyl and reactive Criegee Intermediate (CI). Sufficient vibrational and rotational excitation exists in the CI to permit further unimolecular decomposition which typically occurs through one of two channels; firstly excited CIs can cyclise to a dioxirane, which then decomposes to a carboxylic acid, ester or lactone depending on neighbouring substituents in what is known as the ester or 'hot' acid channel, or secondly, when available, excited CIs can isomerise via a 1,5-hydrogen shift to form a vinylhydroperoxide, which subsequently decomposes into a vinoxy radical and a hydroxyl radical in what is known as the hydroperoxide channel. Alternatively, excited CIs can be collisionally stabilised such that bimolecular reactions with trace species (e.g. $\mathrm{H_2O}$, $\mathrm{NO_2}$, CO, aldehydes, acids) become important (Johnson and Marston, 2008).

The relative prevalence of these competing channels is strongly linked to the structure and conformation of the CI (Vereecken et al., 2015), with the various mechanistic pathways summarised in Fig. 1.

When considered as a whole, research shows significant variability in gas-phase ~~oxidation~~ ozonolysis products and SOA yields between different monoterpenes due to their structural differences, highlighting the unique impact different monoterpenes can have on regional atmospheric chemistry. It is therefore important that individual monoterpene variability be accounted for in developing accurate gas- and particle-phase models. Nonetheless current literature has predominantly focussed on a small number of ~~major monoterpenes (*e.g.*~~ the more commonly emitted monoterpenes (e.g. α-pinene, β-pinene, limonene). One monoterpene for which ~~respectively~~ relatively little is known is α-phellandrene ~~.~~ (structure provided in Fig. 1). One of the most reactive monoterpenes, α-phellandrene ~~(Fig. 1)~~ has been identified as a major constituent of extracts (Li et al., 1995; Brophy and Southwell, 2002; Pavlova et al., 2015; Maghsoodlou et al., 2015) and in emissions (He et al., 2000; Maleknia various Eucalypt species~~(??Pavlova et al., 2015; Maghsoodlou et al., 2015),~~ ; the world's most widely planted hardwood ~~trees~~ tree (Myburg et al., 2014). During day-to-day activities and processes ~~these Eucalypt species~~Eucalypts, such as *Eucalyptus microtheca*~~and~~ , *Eucalyptus viminalis* and *Eucalyptus dives*, emit α-phellandrene into the atmosphere, with α-phellandrene likely contributing to the intense and frequent particle nucleation events observed over Eucalypt forests–a ~~process~~ phenomenon already believed to be caused by monoterpene oxidation (Suni et al., 2008; Lee et al., 2008; Ortega et al., 2009, 2012). In the indoor environment α-phellandrene can be found as an additive to household cleaning products, detergents and air fresheners (e.g. Eucalypt themed products), with the European EPHECT project reporting α-phellandrene at a concentration of 16.7 $\mu g\,m^{-3}$ in a study of a passive air freshener in a 1 m^3 room after 5 hours (Stranger, 2013). Maisey et al. (2013) reported similar maximum concentrations of α-phellandrene in Australian dwellings.

The rate constant of α-phellandrene with ozone has been measured in a number of studies with results spanning an order of magnitude (Grimsrud et al., 1975; Atkinson et al., 1990; Shu and Atkinson, 1994), with a rate constant of 3.0×10^{-15} ($\pm 35\%$) $cm^3\,molecule^{-1}\,s^{-1}$ favoured (Calvert et al., 2000). High chemical reactivity likely makes ozonolysis a dominant loss process for α-phellandrene in the atmosphere~~, however~~; however, experimental information regarding reaction products is limited to OH radical yields, measured by Herrmann et al. (2010) to be 26 – 31% and 8 – 11% for the ozonolysis of the two double bonds, and acetone yields, which were reported by Reissell et al. (1999) to be minor ($< 2\%$). Recently ~~however~~ the reaction mechanism was investigated theoretically for the first time by Mackenzie-Rae et al. (2016), who mapped the potential energy surface to first-generation products. A basic overview of the reaction pathways is provided in Fig. 1, with a comprehensive discussion of the reaction mechanism of α-phellandrene with ozone based on findings of Mackenzie-Rae et al. (2016) pertinent to this study provided in the Supplementary Information (S.1).

~~With a theoretical foundation, this study~~ This study aims to experimentally characterise the reaction of α-phellandrene with ozone in detail for the first time by exploring and characterising both the gaseous- and particle-phases, with the impact of Criegee scavengers and NO_2 on the system ~~also~~ addressed. In doing so the impact of a highly reactive and potentially important monoterpene will be parametrised.

2 Materials and Method

2.1 Experimental set-up and procedure

Eleven dark α-phellandrene ozonolysis experiments were conducted using the indoor smog chamber facility at the Guangzhou Institute of Geochemistry, Chinese Academy of Sciences (GIG-CAS). A complete description of the facility and chamber setup is given in Wang et al. (2014). Briefly, the GIG-CAS smog chamber consists of a 30 m^3 fluorinated ethylene propylene (FEP) reactor housed inside a temperature controlled room. The reactor was flushed with purified dry air for at least 48 hours prior to each experiment, until no residual hydrocarbons, O_3, NO_x or particles were detected, with the impact of off-gassing of radicals from the reactor walls during experiments under the dark, dry conditions used negligible (Wang et al., 2014). Two Teflon-coated fans located inside the reactor ensure rapid ~~homogenization~~ homogenisation of introduced species. Liquid reactants were vaporised via injection into a heating system similar to that of gas chromatography, before being carried by nitrogen gas through FEP Teflon lines into the reactor. Ozone was generated using a commercial ozone generator (VMUS-4, Azco Industries Ltd), with pure oxygen feed gas. Initial mixing ratios of the reactants varied between 10 and 175 ppb for α-phellandrene (Aldrich Chemical Company, Inc., USA) and between 56 and 500 ppb for O_3~~, with all experiments conducted under dry conditions (Table 1)~~. α-phellandrene was injected prior to admission of O_3 into the chamber, with O_3 added ~~stepwise~~ through two separate additions in experiments 7 and ~~10.~~ 10 to facilitate the identification of detected species as either first- or second-generation products. Anhydrous cyclohexane (Sigma-Aldrich, 99.5%) was added in sufficient quantity in all but two experiments ~~, in sufficient quantity~~ to scavenge $>$ 95% of OH radicals (Aschmann et al., 1996; Hermann et al., 2010), ~~whilst formic~~ with the remaining experiments used to asses the impact of cyclohexane's inclusion. Formic acid (J&K Scientific Ltd., 98%) was added to experiments 6 and 7 ~~to ascertain the role of stabilised Criegee Intermediates (CIs) (Bonn et al., 2002; Winterhalter et al., 2009)~~as a stabilised Criegee Intermediate (sCI) scavenger to better understand the impact of sCIs on gas-phase species distribution and importantly particle-phase formation and growth, for which it has been identified as a significant precursor (Bonn et al., 2002; Bateman et al., 2009; Sakamoto et al., 2013; Wang et al., 2016). Prior to O_3 addition in experiment 11, 385 ppb of NO_2 was added through a septum installed in one of the injection ports using a gas-tight syringe, with the inclusion providing an alternative representation of tropospheric nocturnal chemistry in a polluted environment. All experiments had 2.5 µL of acetonitrile injected as a dilution tracer, with the top frame of the reactor periodically lowered to maintain a positive pressure differential inside the reactor. Experimental run times ranged from 205 – 305 minutes~~.~~, with a final reactor volume typically between 6 – 8 m^3. The starting conditions for each experiment are listed in Table 1. The high reactivity of α-phellandrene towards ozone results in reaction half lives that are similar to the mixing time of the reactor. Consequently only a lower bound of the ozone concentration is known.

2.2 Characterisation of gas- and particle-phases

Volatile organic compounds (VOCs) were measured online with a commercial proton-transfer-reaction time-of-flight mass spectrometer (PTR-TOF 2000, Ionicon Analytik GmbH, Austria) (Jordan et al., 2009; Graus et al., 2010), using H_3O^+ reagent ions. For data collected in the first 7 experiments in Table 1, the PTR-TOF drift tube was operated at 2.2 mbar and 60°C,

with a drift tube field of 600 $\mathrm{V\,cm^{-1}}$ (E/N = 136 Td). Significant fragmentation was observed under this regime, with a drift tube voltage of 484 $\mathrm{V\,cm^{-1}}$ (E/N = 112 Td) found to be optimal (Supplementary Information S.2,3). The refined operating conditions were then used for experiments 8 – 11. PTR-TOF spectra were collected at a time resolution of 2 seconds. Data were processed using the PTR-TOF Data Analyzer (Müller et al., 2013), with 30 spectra averaged to improve counts of trace species. A generic $\mathrm{H_3O^+}$ rate constant of 2×10^{-9} $\mathrm{cm^3\,s^{-1}}$ was used for conversion into ppb, except for those species where experimental or theoretical data exists (Cappellin et al., 2012; Tani, 2013).

Gas-phase $\mathrm{O_3}$ and $\mathrm{NO_x}$ were measured online using dedicated monitors (EC9810 and 9841T, Ecotech, Australia), which were calibrated regularly using a Thermo Scientific Model 146i multi-gas calibrator unit. In all experiments, excluding number 11 where it is added, $\mathrm{NO_x}$ concentrations were negligible (< 1 ppb). The $\mathrm{O_3}$ analyser experienced significant interference (had a false bias) from α-phellandrene, which was corrected for using PTR-TOF measurements.

Particle number size distributions were measured online with a scanning mobility particle sizer (SMPS; TSI Incorporated, USA) (Wang and Flagan, 1990), consisting of an electrostatic classifier (TSI 3080) fitted with a TSI 3081 differential mobility analyser (DMA) and condensation particle counter (CPC, TSI 3775). Sheath and aerosol flow rates were 3.0 and 0.3 $\mathrm{L\,min^{-1}}$ respectively, with voltage inside the DMA varied exponentially from -10 V to -9950 V every 240 seconds to provide a mobility spectrum over particle diameters 14 – 750 nm. Higher moment size distributions were calculated by assuming spherical particles (Wiedensohler et al., 2012).

A high-resolution time-of-flight aerosol mass spectrometer (AMS; Aerodyne Research Incorporated, USA) was used to measure particle chemical composition in real-time (Jayne et al., 2000; DeCarlo et al., 2006). The AMS was operated in the high sensitivity V-mode and high resolution W-mode, switching between modes every 2 minutes. AMS data were analysed in Igor Pro 6.2 (Wavemetrics) using the ToF-AMS data analysis toolkits Peak Integration by Key Analysis (PIKA) and Sequential Igor Data Retrieval (SQUIRREL). Updates were made to the fragmentation table following a similar method to Chen et al. (2011), with a detailed discussion provided in the Supplementary Information (S.5). Conductive silicon tubes were used as sampling lines for the SMPS and AMS to reduce electrostatic losses of particles, whilst all other instruments had FEP Teflon feed lines. Losses of VOCs and particles in the transfer lines are estimated to be less than 5% (Liu et al., 2015).

3 Results and Discussion

~~The starting conditions for each experiment are listed in Table 1. The high reactivity of α-phellandrene towards ozone results in reaction half lives that are similar to the mixing time of the reactor. Consequently only a lower bound of the concentration of ozone is known.~~

3.1 Gas-phase Analysis

3.1.1 Peak Identification and Yields

Significant fragmentation was observed in the PTR-TOF upon injection of starting materials into a clean reactor. α-phellandrene was detected at *m/z* 137 at 32 – 34% depending on drift tube conditions, consistent with fragmentation observed in the PTR-MS studies of Misztal et al. (2012) and Tani (2013) (Supplementary Information S~~.1~~.2). Acetonitrile was found exclusively at *m/z* 42, and remained constant throughout all experiments indicating that dilution effects in the reactor are negligible~~(e. g. Fig. 2).~~ . Despite having a lower proton affinity than water, cyclohexane was detected at *m/z* 85, although overall sensitivity is greatly reduced. The detection of cyclohexane is likely the result of termolecular reactions in the PTR-TOF (Smith and Španěl, 2005)~~, with observed cyclohexane fragments listed in Table 2~~. Meanwhile in a separate characterisation experiment, formic acid was found at *m/z* 47, with minor fragments at *m/z* 48, 49 and 65 ($< 2\%$).

Observed interferences are expected to impact detection of α-phellandrene's degradation products, biasing signals to lower *m/z*. Aldehyde, ketone, alcohol, ester and acid bearing compounds are known to dehydrate following protonation to yield a $\mathrm{MH^+}(-\mathrm{H_2O})$ daughter ion (Smith and Španěl, 2005; Blake et al., 2006). Furthermore multifunctional carbonyl compounds can eject a second water molecule from nascent $\mathrm{MH^+}$ ions yielding a $\mathrm{MH^+}(-\mathrm{H_2O})_2$ daughter ion, whilst complex acid bearing molecules have been observed to fragment via the loss of formic acid to produce $\mathrm{MH^+}(-\mathrm{HCOOH})$ ions, and esters through ejection of -OR groups to yield $\mathrm{MH^+}(-\mathrm{ROH})$ (Španěl et al., 1997; Španěl and Smith, 1998). Uncertainty arising from fragmentation ~~prevents~~ limits quantitative analysis for the majority of species, with standards neither available nor prepared. Nevertheless, Table 2 lists peaks routinely detected by the PTR-TOF across the 11 experiments. Note that *m/z* includes the addition of $\mathrm{H^+}$.

Figure 2 shows ~~that~~ time profiles of major species detected by the PTR-TOF during the ozonolysis of α-phellandrene. For clarity peaks have been corrected for background readings recorded prior to the introduction of ozone. Upon injection of ozone, α-phellandrene is rapidly oxidised ~~upon ozonolysis,~~ forming a number of product ions at low concentrations ~~.~~ that continually increase throughout the experiment. Meanwhile ozone, after rapid initial consumption, slowly decreases throughout the experiment in part due to losses to the reactor walls (Wang et al., 2014). The stability of acetonitrile and cyclohexane signals supports the finding of Wang et al. (2014) that wall losses are relatively minor for volatile organics in the GIG-CAS chamber.

Ignoring conformational isomerism, the ozonolysis of α-phellandrene can yield four unique CIs ~~(Mackenzie-Rae et al., 2016). For simplicity only the degradation of one possible CI is shown~~ (Fig. 1) (Mackenzie-Rae et al., 2016), with the degradation mechanism of CI3 provided in Fig. 3~~, with detailed~~ . Detailed schematics of the remaining CIs are provided in the Supplementary Information (S~~.4).~~ .1), and lead to products isomeric to those shown in Fig. 3. A focus is on $\mathrm{RO_2}$–$\mathrm{RO_2}$ radical chemistry which, due to the large rate constant of α-phellandrene with ozone and lack of competing radical termination channels, dominate under the considered reaction conditions.

Elucidating the mechanism of α-phellandrene, one expects initially to form a large range of first-generation products, however none of the product ions detected were observed to decrease over the course of the chamber experiments ~~, suggesting that all ions are likely~~ suggesting that detected ions in part correspond to second-generation species. For example~~from the~~

~~stabilised CIs~~ , from the sCIs one might expect an unsaturated keto-aldehyde or dialdehyde product (Figs. S~~.4~~.1~~and S.4~~.1 and S.1.2), analogous to pinonaldehyde from α-pinene and limonaldehyde from limonene, to be detected at *m/z* 169. Indeed this signal was observed, but it continued to increase in concentration after α-phellandrene was consumed, suggesting that the observed *m/z* 169 is not simply a direct product ion of α-phellandrene. Other major first-generation product ions expected include *m/z* 185, which corresponds to a range of isomeric species formed through either excited or thermalised CI re-arrangement reactions, whereby three oxygen atoms are added for no loss of carbon or hydrogen (e.g. acids, esters, epoxides, secondary ozonides) and *m/z* 155, which can be formed through radical transfer and subsequent CHO loss in the hydroperoxide channel (Mackenzie-Rae et al., 2016). Both these ions were detected in the PTR-TOF but again had concentrations which increased throughout the experiments, suggesting that they ~~instead correspond to higher generation products.~~ have large contributions from saturated species. This continual increase remained true in experiments which added a large secondary dose of ozone after commencement of the reaction (Fig. S.4.1), confirming the discussed ions as saturated.

A similar phenomenon, whereby a distinct lack of first-generation products were observed by a PTR-MS, occurred ~~in~~ when studying the ozonolysis of α-terpinene ~~(Lee et al., 2006)~~(Lee et al., 2006; Ng et al., 2006), a structurally similar endocyclic-conjugated monoterpene. In the ~~study of Lee et al. (2006)~~ studies of Lee et al. (2006) and Ng et al. (2006), first-generation products were observed using identical methods for other monoterpene species ~~,~~ including 3-carene, α-pinene, β-pinene, terpinolene and myrcene. It is possible then that for highly reactive monoterpenes such as α-terpinene and α-phellandrene, concentrations of first-generation products do not accumulate sufficiently during experiments for gas-phase detection. However, as discussed ~~in later sections~~Sections 3.1.3 and 3.2.1, a simple rate study analysis shows that residence lifetimes based on gas-phase reactions are sufficient, whilst analysis of saturation concentrations suggests that the majority of predicted first-generation products likely reside in the gas-phase. ~~It is therefore uncertain as to why~~

Recent literature has shown that functionalised organic species experience considerable losses to Teflon chamber walls through gas-wall partitioning (e.g., Matsunaga and Ziemann, 2010; Zhang et al., 2014; Yeh and Ziemann, 2015; Krechmer et al., 2016; La Observations indicate that organic compounds are not lost to the reactor walls, but rather partition between the gas-phase and Teflon walls in a reversible process that eventually reaches equilibrium, the speed of which is dependent on reactor geometry, turbulence and species diffusivity, and penetration and accommodation in the reactor walls. Based on the work of Krechmer et al. (2016) the time scale for reaching gas-wall equilibrium in these experiments is thought to be less than 600 seconds. Gas-wall partitioning therefore operates quick enough to affect the considered chamber experiments and detection of first-generation products. The relative impact of gaseous wall losses is further explored in Section 3.2.1, nonetheless partitioning is strongly dependent on volatility with losses of highly-functionalised first-generation products of α-phellandrene ~~were not detected in this work, but suggests some large loss or removal process for these functionalised, unsaturated species either in the sample lines and~~ to reactor walls and/or sample lines during transfer into and detection by the PTR-TOF expected (Yeh and Ziemann, 2015; Krechmer et al., 2016; La et al., 2016).

~~The~~ Figure 2 shows that the highest product signal concentrations were observed for low *m/z* species ($\leqslant C_3$). Whether this is an accurate representation of the system or a systematic bias from fragmentation is unknown, however anecdotally ~~,~~ increased counts of low mass species were observed as the energy of the drift tube was raised suggesting that the latter does

have some effect. Major peaks were found at *m/z* 31, 45, 47, 59, 61 and 73, corresponding to formaldehyde, acetaldehyde, formic acid, glyoxal, acetic acid and methyl glyoxal respectively. Although acetone also resides at *m/z* 59, based on the low gas-chromatographic yields reported in Reissell et al. (1999) the signal is apportioned to glyoxal. As α-phellandrene contains two double bonds, yields in this work were calculated as the slope of the least square regression between the change in concentration of the oxidation product and change in wall loss corrected ozone, as shown in Fig. 4; with ozone wall loss rates frequently characterised following the method describe in Wang et al. (2014). The average yield from sequential ozonolysis is therefore calculated ~~, however in practice~~ with results provided in Table 3. In practice however, calculations are dominated by data points measured after the consumption of α-phellandrene, with the data corresponding to the initial reaction of α-phellandrene comparably limited and often largely excluded to reduce errors associated with having a finite reactor mixing time. As discussed later, this problem is navigated for OH radicals by using a higher PTR-TOF time resolution and measuring yields against α-phellandrene consumption~~,~~; however mixing ratios of other oxidation products are too low in the initial stages of the experiment to produce reliable yield data in this regime. For experiments that had two additions of ozone (7 and 10), separate yield lines were fitted for data after each addition of ozone with the results then averaged, therefore maintaining the reported yield as an average of the entire ozonolysis system.

~~The low molecular weight acids, formic and acetic ,~~ Formic and acetic acid were both found to be produced with high yields. The fragmentation pattern of acetic acid was determined in a separate calibration experiment, with 88% residing at *m/z* 61 and the remaining mass distributed over *m/z* 43, 62 and 79, corresponding to dehydration to the acylium ion, the ^{13}C isotope and protonation by a water cluster respectively. Correcting for fragmentation, yields of formic and acetic acid were found to range from 22 – 37% and 9 – 22% respectively across the conducted experiments~~(Table 3)~~. Yields of formic acid are considerably higher than what has been reported for the ozonolysis of other terpenes, whilst acetic acid yields are consistent with species containing an endocyclic bond (Lee et al., 2006); although a subtle difference in methodology should be noted with Lee et al. (2006) calculating yields with respect to the parent hydrocarbon. The addition of NO_2 was found to reduce yields of both formic and acetic acid to 10 ± 2 % and 5 ± 1 % respectively, with O_3 losses through reaction with NO_x accounted for. The addition of NO_2 therefore acts as an inhibitor to acidic group formation, likely by scavenging acyl peroxy radicals to form peroxyacyl nitrates (PANs). Alternatively NO_2 can impact the chemistry of the system by reacting with stabilised secondary ozonides (SOZs), although no changes in acid product yields were observed in the experiments where ~~stabilised CIs~~ sCIs were scavenged, indicating that this channel is negligibly important in forming low molecular weight acids.

In characterising the PTR-TOF transmission curve, acetaldehyde and all other oxygenated VOCs in the gas-standard (Ionicon, Analytik GmbH, Austria) showed no evidence of fragmentation. Therefore, assuming no fragmentation for the remaining oxidation products ~~,~~ provides yields of formaldehyde, acetaldhyde, glyoxal and methyl glyoxal of 5 – 9%, 0.2 – 8%, 6 – 23% and 2 – 9%. Nevertheless fragmentation of methyl glyoxal through CO loss in the PTR-TOF has been reported (Müller et al., 2012), which would simultaneously reduce its own yield whilst increasing the yield of acetaldehyde. A similar phenomenon is also expected of glyoxal, nonetheless acetaldehyde yields remain low and consistent with findings reported for other terpene species. Formaldehyde yields are consistent with other terpene species containing multiple internal double bonds, e.g. α-humulene and α-terpinene (Lee et al., 2006). The addition of a ~~CI~~ sCI scavenger was found to have little impact on prod-

uct distribution or yields, suggesting that the sCI-formic acid complexes ultimately decompose to produce similar gas-phase products as sCIs that degrade through conventional channels. Whether decoupling of the sCI-acid complex occurs inside the reactor or upon protonation in the PTR-TOF remains unknown. Similarly no significant differences in yields were observed between experiment 9 and OH-scavenged experiments, with decomposition into smaller carbon species counter intuitively invariant to action by the OH radical; strengthening the argument that fragmentation inside the PTR-TOF is non-negligible. Meanwhile in experiment 11 yields of formaldehyde, ~~acetaldhyde~~acetaldehyde, glyoxal and methyl glyoxal were 1.2 ± 0.3 %, 0.41 ± 0.09 %, 7.6 ± 2 % and 2.1 ± 0.5 % respectively. ~~The~~ A comparison of rate constants of O_3 with α-phellandrene (3.0×10^{-15}cm^3 molecule^{-1} s^{-1}) and NO_2 (3.5×10^{-17}cm^3 molecule^{-1} s^{-1}) suggests that the majority of O_3 will be consumed by α-phellandrene with formation of the nitrate radical relatively minor (Calvert et al., 2000; Atkinson et al., 2004). Nevertheless NO_2 is in excess in the system, with a systematic reduction in product yields ~~upon introduction of~~ indicative of a shift towards RO_2+NO_2 ~~is consistent with a shift away from these carbonyl containing species towards more~~ dominated chemistry, producing peroxy nitrate containing products (Draper et al., 2015).

Heavier second-generation products routinely detected across experiments are listed in Table 2, with yields for a number of these products given in Table 4. The absence of a yield indicates that the peak was not detected by the PTR-TOF, which typically occurred for minor peaks in experiments with lower ~~initial~~ starting α-phellandrene concentrations. Again no fragmentation was assumed in determining yields, although some ions do differ by common fragment mass amounts, suggesting that fragmentation may be important. For example *m/z* 185 and 167, *m/z* 129 and 111 and *m/z* 115 and 97 all differ by 18 amu, suggesting that the latter masses could be dehydrated fragments. Whilst strong correlation ($R^2 > 0.99$) between these pairs of peaks is observed, it is not consistent across the entire dataset, suggesting that there exists multiple contributors to the aforementioned signals. Similar instances are also observed for peaks separated by 28 amu (e.g. *m/z* 143 and 115) and 46 amu (e.g. *m/z* 185 and 139).

Calculated yields for these larger products were in general $< 5\%$~~. Again the addition of~~ , with detected products sufficiently volatile such that gas-wall partitioning losses are thought to be minor (see Fig. 9). Again the presence of OH radicals in experiment 9 had little effect on product yields. Addition of NO_2 to the system ~~had the effect of reducing product yields, although overall distribution remained~~ in experiment 11 resulted in significantly reduced yields, with overall distribution remaining similar and no new peaks ~~were observed, indicating that ozonolysis products remain dominant~~or evidence of nitrate containing compounds observed. Nonetheless alkyl nitrates are known to readily lose HNO_3 after protonation in the PTR-TOF, resulting in the formation of bare alkyl ions (D'Anna et al., 2005; Aoki et al., 2007; Duncianu et al., 2016). Proposed structures for some of these larger second-generation products along with plausible formation mechanisms are shown in Fig. 3, although it is possible that more than one ~~product~~ species contributes to an observed oxidation product mass. A large number of products also remain unidentified, with their *m/z* unable to be transcribed to plausible, mechanistically derived ~~,~~structures.

Figure 2 shows that product signals at *m/z* 31, 59, 73 and 87 show a sharp increase upon commencement of the reaction, suggesting that these products are formed directly from α-phellandrene ozonolysis. Nevertheless a large fraction of the product mass for these ions is generated after α-phellandrene consumption, indicating that yields are largely driven by contributions from second-generation species. Slower initial production of the remaining ions suggests that their formation is linked to consumption of first-generation products. Interestingly the peaks corresponding to the heaviest ions, *m/z* 167, 169 and 185,

have relatively constant temporal profiles ~~lacking~~ which also lack an accelerated increase ~~whenever ozoneis introduced~~upon a second addition of ozone; a feature that is apparent among ~~all other~~ lighter product ions. Their unique time profiles ~~implies~~ imply that they are derived from a source secondary to ozonolysis ~~,~~ such as gas-phase accretion reactions~~(Supplementary Information S.3~~, with modelling support for this provided in the Supplementary Information (S.4).

Formation of prescribed products after the second ozonolysis is in agreement with the proposed degradation mechanism (Fig. 3), which predicts a number of both small and large species to form upon fragmentation of the carbon backbone. A large fraction of the smaller products come from decomposition of the 3-carbon system (C_1-C_2-C_7, Fig. 1) bridging the conjugated double bonds in α-phellandrene, which segments from the rest of the molecule after the second ozone addition. For example, plausible mechanisms can be traced to methyl glyoxal formation irrespective of the order of addition of ozone to the two double bonds, with the only prerequisite being that the first addition of ozone adds one carbonyl group to the C_1-C_2-C_7 system~~(e.g.~~. An example showing this from a proposed first-generation product is provided in Fig. 5~~)~~. Subsequent decomposition of the C_1-C_2-C_7 Criegee biradical fragment can yield products including formaldehyde, formic acid and acetic acid. Meanwhile functionalisation of the larger 7-carbon system bridging the conjugated bonds in α-phellandrene can give rise to a large number of heavier second-generation products. *m/z* 129 is assigned to 2-propan-2-ylbutanedial, which can be formed from a number of pathways (e.g. Fig. 3). *m/z* 115 is assigned to 2-propan-2-ylpropanedial, which is formed if a CI from either addition participates in the hydroperoxide channel resulting in CHO fragmentation. Conversely if instead of fragmentation, stabilisation occurs after a 1,5-hydrogen shift, then the product detected at *m/z* 143 shown in Fig. 3 may form. In all instances detected second-generation products can be formed from a wide variety of predicted first-generation products independent of the order of addition of ozone to the two double bonds (Supplementary Information S.~~4). So whilst the complete product distribution will likely consist of a myriad of species (Aumont et al., 2005), in practice the relatively small number of second-generation products detected likely dominate the final ozonolysis product distribution.~~ .1).

3.1.2 Determination of OH Yields

~~OH yields from the reaction of α-phellandrene and its first-generation degradation products with ozone are listed in Table 5. No OH scavenger was added in experiments 9 and 11.~~ The OH radical scavenger, cyclohexane, reacts with OH to form both cyclohexanone and cyclohexanol (Atkinson et al., 1992; Berndt et al., 2003), with cyclohexanone (*m/z* 99) used as the OH radical tracer in this study. In a characterisation experiment 98% and 85% of cyclohexanone (Sigma Aldrich, 99.8%) was found to reside at *m/z* 99 when the PTR-TOF drift tube was operated at 112 and 136 Td respectively, with the remaining mass distributed over a dehydrated and cluster peaks at *m/z* 81, 116 and 117. A minor ozonolysis product is also detected at *m/z* 99 (Section 3.1.1), however the two peaks are resolvable in the PTR-TOF.

A major uncertainty in determining OH yields is the yield of cyclohexanone formed from the reaction of cyclohexane with OH radicals. Atkinson et al. (1992) reported the combined yield of cyclohexanone and cyclohexanol to be 0.55 ± 0.09, with cyclohexanone/cyclohexanol ratios typically ranging from 0.8 – 1.4 depending on the terpene investigated. In contrast, Berndt et al. (2003) reported a cyclohexanone yield of 0.53 ± 0.06. In this study, the OH-yield is based on the average of these two findings, with a cyclohexanone yield from the reaction of OH and cyclohexane of 0.41 ± 0.14 used. Scavenging is assumed

to be 95% efficient based on the volume of cyclohexane introduced into the reactor, with the error in this assumption thought to be minimal with respect to the inherent uncertainty in cyclohexanone yields. Background interference from cyclohexane, of which a small portion is oxidised by O_2^+ to cyclohexanone in the drift tube, is corrected for (Winterhalter et al., 2009).

OH yields for the initial reaction of ozone with α-phellandrene were calculated from the slope of OH produced against α-phellandrene reacted. As both *m/z* 99 and 137 are major signals in the PTR-TOF, spectra were not averaged during analysis resulting in a 2 second time resolution. A characteristic OH-production time profile is shown in Fig. 6, which can be separated into three regions. The initial part of the experiment is characterised by a linear section, where α-phellandrene is the primary source of OH radicals. The gradient obtained from linear regression in this regime is equivalent to the OH yield from ozonolysis of the first double bond in α-phellandrene (Fig. 7a). The α-phellandrene dominated regime is short-lived with respect to total OH production time in the reactor, suggesting that first-generation products are also highly reactive and large producers of OH radicals. As the reaction proceeds, faster reacting first-generation products begin to contribute to the OH budget, whilst α-phellandrene becomes increasingly less influential. This results in a gradual curve, until ~~at which point~~ essentially all α-phellandrene has been consumed and a vertical path is traced, indicating that first-generation species are now dominating OH radical production. By plotting OH formation against O_3 consumption in the product dominated regime, the collective first-generation product OH radical yield is obtained (Fig. 7b). Naturally this method is only applicable to those experiments where the product dominated regime is attained, which is why no OH radical yields are reported for first-generation products in experiments 8 and 10. OH yields from the reaction of α-phellandrene and its first-generation degradation products with ozone are listed in Table 5.

The average OH yield for the reaction of the first double bond in α-phellandrene across the 10 experiments was found to be 35 ± 12 %, whilst the average OH yield from the ozonolysis of the second reacting double bond was 15 ± 7 %. Both these determined values are slightly higher than the values calculated in Herrmann et al. (2010), although they agree well within uncertainty limits. Whilst experimental methodology is similar, Herrmann et al. (2010) conducted their analysis under the assumption that the two double bonds in α-phellandrene react at significantly different rates, such that 95% of α-phellandrene reacts before first-generation products start to be consumed. However as Fig. 6 shows, first-generation products contribute to the OH radical budget considerably earlier than this. As a result, Herrmann et al. (2010) is likely to have under-predicted OH yields of first-generation products, inadvertently apportioning their contribution to α-phellandrene, whose OH yields would subsequently be over-predicted. The method employed in this study is thought to provide a more accurate distinction between OH radical production from α-phellandrene and its first-generation products. From the determined yields it can be concluded that the hydroperoxide channel does play an important role in the decomposition of α-phellandrene by ozone, supportive of findings from a recent theoretical study (Mackenzie-Rae et al., 2016).

3.1.3 Modelling rate constants and OH yields

The conjugated system in α-phellandrene provides two reactive sites for ozone addition. Based on analogy with rate constants from simpler alkenes, such as cyclohexene (k = 8.1 $\times 10^{-17}$ $cm^3\,molecule^{-1}\,s^{-1}$) and 1-methyl-1-cyclohexene (k = 1.66 $\times 10^{-16}$ $cm^3\,molecule^{-1}\,s^{-1}$) (Calvert et al., 2000), inductive effects are expected to make the methyl substituted double

bond the more reactive addition site. However recent theoretical results suggest the contrary (Mackenzie-Rae et al., 2016), with steric effects raising the energy barrier for entry to the more substituted double bond, resulting in addition to the less substituted double bond in α-phellandrene being favoured. This finding is consistent with experimental evidence for isoprene, where methacrolein, not methyl vinyl ketone, is the favoured first generation product (Paulson et al., 1992; Grosjean et al., 1993; Aschmann and Atkinson, 1994; Rickard et al., 1999). Nevertheless the average energy difference for addition to the two double bonds is minor, with both entry channels expected to be important.

Given the high chemical reactivity of both double bonds in α-phellandrene, it is interesting to investigate the reactivity of first-generation products. The following reaction parametrisation was therefore constructed to determine the average rate constant of ozone with all first-generation species.

$$\alpha-\text{phellandrene} + \mathrm{O_3} \xrightarrow{\mathrm{k_1}} \mathrm{FG} + \mathrm{xOH} \quad (1)$$

$$\mathrm{FG} + \mathrm{O_3} \xrightarrow{\mathrm{k_2}} \mathrm{SG} + \mathrm{yOH} \quad (2)$$

$$\mathrm{O_3} \xrightarrow{\mathrm{k_3}} \mathrm{wO_3} \quad (3)$$

where FG represents all first-generation products, SG all second-generation products, $\mathrm{wO_3}$ is ozone lost to the reactor walls and x and y are stoichiometric coefficients representing OH yields from each reaction step. The rate constant for the reaction of ozone with a-phellandrene ($\mathrm{k_1}$) was constrained to the literature value (Calvert et al., 2000), whilst a first-order ozone wall loss rate of $\mathrm{k_3}$ = 2 – 8 $\times 10^{-6}\,\mathrm{s^{-1}}$ was used based on a number of calibration experiments. Remaining parameters, namely x, y and $\mathrm{k_2}$, were varied to optimise model performance. The reaction scheme was solved using the online numerical integrator AtChem (https://atchem.leeds.ac.uk/) for all experiments, barring 9 and 11 due to the unconstrained influence of $\mathrm{NO_2}$ and/or OH radicals.

Figure 8 shows the results of the simulation of ozone consumption and OH production for three different experiments, with optimised parameters for each experiment given in Table 5. Considering simplicity the model performs surprisingly well. Based on all experiments the average simulated rate constant for the reaction of first-generation products with ozone was $\mathrm{k_2}$ = $1.0 \pm 0.7 \times 10^{-16}\,\mathrm{cm^3\,molecule^{-1}\,s^{-1}}$. Although the ozonolysis of first-generation products is around 30 times slower than that of α-phellandrene, it is still faster than the ozonolysis of ~~the monoterpenes~~ numerous monoterpenes including α-pinene, β-pinene, sabinene, 3-carene and β-phellandrene (Calvert et al., 2000). Using a typical background tropospheric ozone mixing ratio of 30 ppb, atmospheric lifetimes (τ) of α-phellandrene and its first-generation products can be estimated by:

$$\tau_i = \frac{1}{k_i[O_3]} \quad (4)$$

The atmospheric lifetime of α-phellandrene is therefore $\tau_1 \sim 7.5$ minutes, whilst the average lifetime of first-generation products is calculated to be $\tau_2 \sim 3.75$ hours. Both α-phellandrene and its first-generation products therefore have a relatively short atmospheric lifetime with respect to ozone and are unlikely to be involved in long-range transport phenomena. Instead complete saturation likely occurs in the chemical environment to which α-phellandrene is emitted, thus impacting the local radical, acid and SOA budgets. Interestingly, increasing the ozone concentration to conditions found in chamber experiments results

in first-generation product lifetimes of the order of tens of minutes, which is more than sufficient for gas-phase detection. The inability to detect first-generation products is therefore indicative of an underlying sampling or detection issue.

OH production is additionally included in the model to assist in parametrising yields from α-phellandrene and the average of its first-generation products. Experimental assessment of OH yields carries an inherent uncertainty, in that linear regression was used to fit data belonging to a segment of a curve (Fig. 5), with information in the 'combination' section notionally discarded. ~~The parametrisation employed therefore~~ Model parametrisation allows for a more complete description, although mechanistic simplicity renders the results far from quantitative. Instead its purpose is to both validate experimental findings and allow further constraints to be placed on OH production from the α-phellandrene system.

The average modelled OH yields are ~~54~~ 53 $\pm$ 10 % and 13 $\pm$ 5 % for α-phellandrene and its average first-generation products respectively. The model suggests α-phellandrene makes a greater contribution to the OH budget than what was calculated experimentally, whilst yields from ~~all~~ first-generation products are consistent with experimental measurements. Overall net OH radical production is greater from the model than experimental ~~results suggest~~measurements. The source of this discrepancy is likely the limited data used in calculating α-phellandrene's OH yields, with a large proportion of α-phellandrene consumed in the 'combination' section. Given the α-phellandrene dominated regime generally lasted around 2–3 minutes, which is comparable to the mixing time of the reactor, it is entirely possible that OH production in this regime was not characterised well. The experimental finding for OH radical production from α-phellandrene of 35 $\pm$ 12 % is therefore recommended as a lower bound.

3.2 Particle-phase Analysis

3.3 ~~Particle-phase Chemistry~~

3.2.1 SOA Formation

First- and second-generation ozonolysis products are highly functionalised, polar species with high molecular weights. It is therefore expected that they should make a significant contribution to the aerosol phase through gas-particle partitioning (Pankow, 1994; Odum et al., 1996). To assess this, the saturation vapour concentration (C^*, $\mu g\,m^{-3}$) (Donahue et al., 2006, 2012) of each species was calculated. Vapour pressures were estimated using the Extended Aerosol Inorganic Model (E-AIM) (Clegg et al., 2008), using the structure based estimator of Nannoolal et al. (2004) for boiling points coupled with Moller et al. (2008) for vapour pressures. This method has been compared extensively with other estimation techniques (Barley and McFiggans, 2010; O'Meara et al., 2014). Activity coefficients were calculated using the UNIversal Functional Activity Coefficient (UNIFAC) method (Fredenslund et al., 1975). The saturation vapour concentrations calculated are shown in two-dimensional volatility oxidation space in Fig. 9.

Gas-particle partitioning occurs in competition with gas-wall partitioning, a process that is also dependent on species saturation vapour concentrations (Supplementary Information S.6). In parameterising gas-wall partitioning, the Teflon film is often considered to have an equivalent organic aerosol mass concentration (C_w). Values for C_w vary significantly in the literature, with Ziemann and co-workers reporting values of $C_w \sim 2-40\ mg\,m^{-3}$ (Matsunaga and Ziemann, 2010; Yeh and Ziemann, 2015

Zhang et al. (2014) reporting C_w values from 0.0004 – 300 $mg\,m^{-3}$ and Krechmer et al. (2016) showing values of C_w to vary with C^*, from C_w = 0.016 $mg\,m^{-3}$ for $C^* < 1$ up to 30 $mg\,m^{-3}$ for $C^* > 10^4$. The reasons for the large discrepancies between studies are unknown, however are likely due to differing deformation and activities of the Teflon walls (Krechmer et al., 2016). Nonetheless comparing reported values to SOA loadings generated during the chamber experiments reported in this work, it is evident that gas-wall partitioning is at least competitive, if not dominant compared to gas-particle partitioning. The impact is shown in Fig. 9 by plotting the fraction of an organic species that remains in the gas-phase over different saturation vapour concentrations using C_w = 5 $mg\,m^{-3}$ and an SOA loading of 200 $\mu g\,m^{-3}$. Under this scenario gas-wall partitioning dominates, with compounds having $C^* < 10^2$ $\mu g\,m^{-3}$ predominantly residing in the walls with a small fraction in the aerosol phase after equilibrium is established, whereas species with $C^* > 10^6$ $\mu g\,m^{-3}$ remain almost entirely in the gas-phase. Compounds with $10^2 < C^* < 10^6$ $\mu g\,m^{-3}$ will partition to varying extents depending on their volatility and functional group composition between the wall, gas- and particle-phases (Krechmer et al., 2016). However no corrections for gas-particle partitioning are made in the present study, given that no product vapour loss rate measurements were made for the GIG-CAS chamber and the large variability in literature values of C_w. Without correcting for vapour wall losses, SOA yields are likely to be underestimated (Matsunaga and Ziemann, 2010; Zhang et al., 2014; La et al., 2016).

The majority of predicted first-generation and detected second-generation gas-phase products are classified as intermediate volatility compounds (IVOCs) (Donahue et al., 2012). As IVOCs, they are considered to have quite low vapour pressures ~~,~~ but nonetheless reside almost exclusively in the gas-phase. Of the proposed species, only the first-generation acids (e.g. Fig. 3) are classified as semi-volatile organic compounds (SVOCs), a classification given to those species which are expected to have sizeable mass fractions in ~~both the gaseous and~~ the aerosol phase.

Nevertheless rapid aerosol formation is observed upon reaction of α-phellandrene and ozone ~~, as shown by~~ as shown in Fig. 10, with sharp increases in particle number (dN/dlogDp) and volume (dV/dlogDp) concentrations ~~(Fig. 10).~~ observed. With no aerosol seed, nucleation must be driven by supersaturation of condensible species ~~. Donahue et al. (2013) argues~~ formed in the initial stages of the reaction. Donahue et al. (2013) argue that nucleation occurs through compounds that have extremely low volatility (ELVOC, $C^* < 3 \times 10^{-4}$ $\mu g\,m^{-3}$). For the ozonolysis of other monoterpenes, ELVOC formation has been proposed to occur through gas-phase accretion reactions (Bateman et al., 2009; Heaton et al., 2009; Camredon et al., 2010) and autoxidation processes (Ehn et al., 2014; Jokinen et al., 2015). Meanwhile to condense onto fresh aerosol, but not homogeneously nucleate, vapours need to have saturation concentrations in the 10^{-3} – 10^{-2} $\mu g\,m^{-3}$ range (Donahue et al., 2011; Pierce et al., 2011), placing them in the low volatility organic compound bin. Formation of these compounds can be explained through conventional gas-phase chemistry (Donahue et al., 2011). It is therefore evident from Fig. 9 that the simple mechanistic overview provided to explain formation of gas-phase products in Section 3.1.1 and in Mackenzie-Rae et al. (2016) is insufficient to account for aerosol observations, with more complex reactions or reaction processes such as autoxidation, oligomerisation and/or heterogeneous oxidation required to develop species of sufficiently low vapour pressure for both particle nucleation and growth (Hallquist et al., 2009).

The maximum number of particles inside the reactor occurs within the first few minutes of the reaction commencing (time resolution of the SMPS), with a small average particle diameter (~40 nm). Rapid nucleation is consistent with the findings of

Jokinen et al. (2015) who, based on limonene and α-pinene, concluded that endocyclic biogenic VOCs are efficient ELVOC producers upon ozonolysis. Coagulation of the newly-formed aerosol decreases the number of particles, whilst further partitioning of low volatility oxidation products increases the volume, with maximum aerosol concentration attained around 30 minutes into each experiment. After this point, irreversible wall losses supersedes gains from partitioning, with the volume, and hence mass of aerosol decreasing inside the reactor.

In the early stages of experiments, the number concentration is a useful proxy for measuring the amount of nucleation occurring in the system (Bonn et al., 2002). As Fig. 11 shows, the addition of a Criegee scavenger systematically reduces initial particle number concentrations, concurrent with a shift of SOA to larger diameters. These changes suggest a reduction in the number of SOA nucleating agents~~(Bonn et al., 2002)~~, implying that the reaction of α-phellandrene ~~stabilised CIs, whether uni- or bi-molecular,~~ sCIs are important in forming ELVOC and IVOC compounds, whilst ruling out the reaction of ~~stabilised CIs~~ sCIs with formic acid as a nucleating mechanism. This finding is consistent with experimental literature that is now building around ~~stabilised CIs~~ sCIs as a source of new particle formation; whether through intramolecular SOZ formation (Bonn et al., 2002), bimolecular reaction with first-generation products (Bateman et al., 2009), or oligomer formation through reaction with peroxy radicals (Sadezky et al., 2006, 2008) or hydroperoxides (Sakamoto et al., 2013). Processes such as these would all be precluded by the addition of formic acid to the system. Similarly there is a reduction in the α-phellandrene normalised number distribution when NO_2 is added (Fig. 11). Like formic acid, NO_2 can also react with sCIs (Johnson and Marston, 2008) and therefore potentially inhibit particle formation and growth. If this were the case then results from this ozonolysis study likely represent an upper limit to SOA formation under ambient conditions, although more experiments are necessary to confirm the impact of NO_2 on SOA formation in the α-phellandrene system.

Assuming spherical particles, effective aerosol densities were calculated by comparing distributions of vacuum aerodynamic and electric mobility diameters, using the AMS and SMPS respectively ~~(DeCarlo et al., 2004; Katrib et al., 2005; Kostenidou et al., 2007)~~(I Results are listed in Table 6. The average density across all experiments was found to be 1.49 ± 0.2 g cm^{-3}, indicating that the aerosol exists in a solid or waxy state (Kostenidou et al., 2007). This value is consistent with the SOA density found in the ozonolysis of other monoterpenes under similar conditions, which typically range from 1.15 – 1.73 g cm^{-3} (Bahreini et al., 2005; Kostenidou et al., 2007; Saathoff et al., 2009; Shilling et al., 2009). Because the particles are potentially non-spherical, the quoted effective density represents a lower bound of the true α-phellendrene SOA density, with error from assuming spherical particles expected to be less than 10% (DeCarlo et al., 2004; Bahreini et al., 2005). It is noted that the densest aerosol was produced in experiment 11, which had NO_2 added, although one experiment is insufficient for reliable conclusions. The aerosol density was found to be insensitive to a range of other experimental parameters, including starting α-phellandrene and ozone concentrations, aerosol loading, aerosol oxidation state and the presence of CI scavengers. These findings are in contrast to studies conducted on α-pinene (Shilling et al., 2009) and β-caryophyllene (Chen et al., 2012), in which particle density was found to decrease as chamber aerosol loadings increased in accordance with changes in aerosol oxidation state.

Aerosol densities were used to convert SMPS volume concentrations into mass loadings (μg m^{-3}). Wall loss effects were corrected for by assuming a size-independent first-order loss process (Pathak et al., 2007), by modelling data at the end of each experiment, after gas-aerosol partitioning had reached equilibrium. Calculated wall loss rate constants, which ranged from 0.32

– 0.79 h^{-1}, were then applied to correct mass loading data for respective experiments. This way, differences between individual chamber simulations are accounted for. Determined wall loss rates are consistent with those found for α-pinene ozonolysis in the chamber (Wang et al., 2014).

The same method was used to correct V-mode AMS data, with results given in the Supplementary Information (S~~.6~~.7). Clustering of points around the 1:1 line in Fig. S~~.6~~.7.1 indicates general agreement between mass loadings calculated using the AMS and SMPS (Shilling et al., 2008). Nevertheless density corrected SMPS data is preferred in this work, primarily because the AMS is known to suffer from transmission losses caused by particles bouncing off the vapouriser, and to a lesser extent, shape dependent collection losses whilst focussing the particle beam (Matthew et al., 2008; Slowik et al., 2004; Huffman et al., 2005). Whilst it is noted that the SMPS does not measure particles with diameters larger than 750 nm, as shown in Fig. 10, this shortcoming is expected to have minimal impact on reported yields in this work (Wiedensohler et al., 2012).

Wall loss corrected mass loadings for each experiment are given in Table 6, along with fractional aerosol yields (Y). The fractional aerosol yield is defined as the amount of organic particulate matter that is produced (ΔM_o, $\mu g\,m^{-3}$) for a given amount of precursor VOC reacted (ΔHC, $\mu g\,m^{-3}$) (Odum et al., 1996), and provides a convenient way of assessing the bulk aerosol-forming potential of an individual VOC. Utilising the gas/particle partitioning framework, aerosol yield can be described as a function of organic aerosol mass concentration (Pankow, 1994; Odum et al., 1996):

$$Y = \frac{\Delta M_o}{\Delta HC} = \Delta M_o \sum_i \frac{\alpha_i K_{om,i}}{1 + K_{om,i}\Delta M_o} \quad (5)$$

where α_i is the stoichiometric factor and $K_{om,i}$ the temperature-dependent equilibrium partitioning constant of product i.

A characteristic yield plot is given in Fig. 12. Whilst a large number of products are expected to contribute to the particle phase, ~~in general a two-product model provides a satisfactory fit, with higher orders found to be superfluous (Odum et al., 1996; Griffin et al~~

~~A characteristic yield plot is given in Fig. 12.~~ SOA yield is best fit using the parameters ~~, $\alpha_1 = \alpha_2 = 0.60 \pm 0.09$ and $K_{om,1} = K_{om,2} = 0.022 \pm 0.01$~~ $\alpha_1 = 1.2 \pm 0.2$ and $K_{om,1} = 0.022 \pm 0.02$ $m^3\,\mu g^{-1}$, with higher order fits found to be superfluous. The fitted constants offer little physical insight, other than perhaps the average of all α and K_{om} values, but nonetheless can be used in regional and global modelling ~~(Chung and Seinfeld, 2002)~~(Chung and Seinfeld, 2002; Tsigaridis and Kanakidou, 2003; Henze and

Figure 12 shows α-phellandrene produces a large amount of aerosol upon ozonolysis compared to other monoterpenes (Wang et al., 2014; Saathoff et al., 2009; von Hessberg et al., 2009). Formation of the necessary semi-volatile organic compounds is likely driven by the presence of two highly reactive endocyclic double bonds, with functionalisation rather than fragmentation dominating for the first addition (Lee et al., 2006). Both experiments ~~,~~ where a CI scavenger was added ~~,~~ lie below the fitted yield curve, strengthening the argument for ~~stabilised CIs~~ sCIs as a source of condensible products. Nevertheless yields from the two experiments differ by almost a factor of two despite having similar starting conditions, with further experiments necessary to better quantify the impact of sCIs on yields. Cyclohexane has been shown to reduce SOA yields in ozonolysis experiments (Bonn et al., 2002; Keywood et al., 2004; Saathoff et al., 2009), although no such effects were observed in this study.

The second addition of ozone ~~to first-generation products~~ in general fragments the molecule, but in doing so increases relative oxygen content. Thus the relative contribution of first- and second-generation products to SOA is empirically difficult

to predict. Figure 13 shows SOA mass as a function of α-phellandrene reacted, producing time-dependent aerosol growth curves. In all experiments where α-phellandrene was completely consumed, dominant vertical growth profiles are traced. This increase in aerosol mass after complete consumption of parent hydrocarbon is characteristic of compounds with more than one double bond (Ng et al., 2006), and suggests that when formed, second-generation products make an important contribution to the total aerosol mass. It is therefore likely that a large number of second-generation species fall in the IVOC or SVOC category in Fig. 9.

Whilst concentrations of precursors are somewhat elevated in experiments compared to ambient conditions, results nonetheless show α-phellandrene ozonolysis products to be heavily involved in both particle nucleation and growth processes. In polluted environments (e.g. inner city forests, consumer products) a high SOA yield results in a large fraction of α-phellandrene partitioning into the particle phase irrespective of gas-phase loadings. ~~For example at the current World Health Organisation $PM_{2.5}$ air quality guideline (25 , World Health Organization (2006)), aerosol yield from α-phellandrene ozonolysis would be ~43%.~~ Meanwhile a strong nucleation potential makes α-phellandrene ozonolysis a strong candidate to help explain the intense and frequent nocturnal nucleation events observed in Eucalypt forests (Lee et al., 2008; Suni et al., 2008), which is already believed to be caused by monoterpene oxidation products (Ortega et al., 2009, 2012). ~~Currently aerosol formation from gas-phase precursors in clean environments is a globally important , yet poorly-quantified phenomenon.~~ Indeed the reaction conditions used in these experiments better reflect this clean environment, where reactions of RO_2 with HO_2 and other RO_2 radicals dominates along with unimolecular rearrangements. Such conditions favour the formation of low-volatility compounds, with the highest SOA yields for monoterpenes found under low-NO_x conditions (Presto et al., 2005; Ng et al., 2007; Capouet et al., 2008; Eddin Under these conditions ozonolysis reactions remain important (Perraud et al., 2012; Zhao et al., 2015), which is conducive to autooxidation processes and therefore nascent SOA formation and growth due to enhanced propensity for intramolecular re-arrangements (Ehn et al., 2014; Jokinen et al., 2015). SOA yields measured in Experiment 11 are consistent however with the other ozonolysis experiments in this study (Fig. 12), suggesting that the impact of NO_x on SOA yields during the ozonolysis of α-phellandrene is limited, with sufficient condensible products still able to be produced (Draper et al., 2015). Nonetheless the reduction in aerosol number concentration in the initial stages of experiment 11 does suggest that formation pathways of ELVOC species (i.e. oligomerisation, autooxidation) are suppressed by the inclusion of NO_2 (Perraud et al., 2012). Detailed modelling studies are required to establish the relative importance of α-phellandrene in ~~these scenarios, although preliminary evidence suggests~~ different environments, although evidence suggests that it is likely a contributor to nucleation events and aerosol growth in regions where it is emitted.

3.2.2 SOA Composition

Resolution in the W-mode of the AMS is sufficient to unambiguously identify chemical formulae of detected ions (DeCarlo et al., 2006; Aiken et al., 2007)~~, with a typical mass spectra shown in Fig. **??**. For clarity only major peaks are depicted (relative intensity 0.001).~~ . Ions are formed ~~in the AMS using~~ however using high-energy electron impact ionisation (70 eV)~~. The high-energy collisions result in a large amount of fragmentation, although charge location and fragmentation patterns can generally be predicted from the functional groups present (McLafferty and Turecek, 1993). Examples are shown for a detected~~

first- and second-generation gas-phase products containing acid, aldehyde and ketone functionality, with proposed fragment ions labelled in the mass spectra. However the , resulting in significant fragmentation. The complexity of aerosol produced, along with an unknown number of fragmentation pathways , including the possibility of charge migration and other internal rearrangements, makes it exceedingly difficult to obtain clear structural information about SOA constituents from the AMS. For this reason it is useful to use the AMS data to analyse the filter samples were collected and analysed to identify SOA constituents, with results to be published in a companion paper. Nevertheless the AMS remains useful for analysing bulk properties of aerosol, the aerosol to gain further insight into the system.

Two ions commonly used as markers for oxidation of OA are (m/z 44) and (m/z 43) (Takegawa et al., 2007; Kroll et al., 2009; Chhabra et
In general, low-volatility oxygenated organic aerosol (LV-OOA) produces mass spectra dominated by the mass fragment ,
whilst semi-volatile oxygenated organic aerosol (SV-OOA) produce spectra with as the dominant ion. These ions are thought to
be produced by organic acids and carbonyls respectively, with the ratio of to therefore providing a useful metric for assessing the
degree of functionalisation in OA. During the chamber ozonolysis of α-phellandrene, it was found that the relative importance
of is greatest at the start of the experiment, with its fractional contribution with respect to decreasing as aerosol mass loadings
increase (Fig. **??**). A small shift back to is then observed in the latter stages of experiments.

The observed trend is unsurprising, as without any aerosol seed the nucleating species would likely be highly functionalised,
featuring a large amount of acidic groups. As the experiment proceeds and aerosol mass increases, more volatile species start to
contribute to the growing OA mass (Pankow, 1994; Odum et al., 1996), which increases the relative amount of . Once growth
has ceased and SOA loadings decrease (e.g. wall loss, evaporation), a small shift back to the less volatile species, and so , is
observed. The ratio of m/z 43/44 was found to be dependent on total aerosol mass inside the reactor, with the highest ratios
found in those experiments with the greatest aerosol loadings. This trend is visible in the three experiments shown in Fig. **??**,
supporting the notion of increased contribution of less volatile species at higher aerosol mass loadings.

Bulk elemental composition can be estimated by averaging ion contributions across the entire mass spectrum (Aiken et al., 2007). Raw measured atomic ratios are converted to estimated ratios using the calibration factors of Aiken et al. (2008), namely 0.91 $\pm$ 10% for hydrogen-to-carbon (H/C), 0.75 $\pm$ 31% for oxygen-to-carbon (O/C) and 0.96 $\pm$ 22% for nitrogen-to-carbon ratios respectively, thus accounting for chemical biases in fragmentation.

Temporal trends in elemental ratios (e.g. Fig. 14) are consistent with the narrative constructed by the m/z 43/44 ratioFigure 14 shows the typical temporal profile of aerosol composition observed over an experiment. Initial aerosol formation and growth is driven by highly oxygenated species, however, as the OA medium grows and less functionalised species begin to partition, the overall oxidation state rapidly decreases, as seen by a drop in O/C and respective rise in H/C ratios. Once gas-particle partitioning slows and aerosol-loss processes dominate, there is a shift in equilibrium with the more volatile aerosol constituents evaporating back into the gaseous-phase. It can therefore be concluded that many of the SOA products generated during the chamber ozonolysis of α-phellandrene in this study are semi-volatile (Donahue et al., 2012). Nitrogen containing species were found to make little contribution to the aerosol formed in experiment 11, with an average N/C $\approx$ 0.002 during the experiment. Nitrate and PAN functionality is believed to significantly reduce the vapour pressure of constituents (Capouet and Müller, 2006; Pankow and Asher, 2008), with the result implying a small gas-phase concentration.

Nevertheless there exists evidence that organic nitrate contribution to SOA may be kinetically, rather than volatility driven (Perraud et al., 2012).

The average oxidation state of carbon ($\overline{OS}_c$) in aerosol comprising of carbon, hydrogen and oxygen was parameterised by Kroll et al. (2011) as:

$$\overline{OS}_c \approx 2O/C - H/C \quad (6)$$

~~The~~ Although the definition ignores the effects of peroxides, whose oxygen atoms carry an oxidation state of -1, ~~nevertheless~~ it nonetheless serves as a useful metric for representing the degree of oxidation of organic species in complex aerosol mixtures. Figure 15 shows that $\overline{OS}_c$ decreases from -0.61 to -1.00 as the particle loading increases from 21.5 to 658.1 $\mu g\,m^{-3}$, ~~again~~ suggesting a strong link between mass loading and degree of functionalisation ~~(Shilling et al., 2009)~~consistent with the findings of Shilling et al. (2009) for the ozonolysis of α-pinene. The fastest change in $\overline{OS}_c$ is observed to occur at lower mass loadings. Calculated $\overline{OS}_c$ classifies the aerosol formed throughout the campaign as semi-volatile oxygenated organic aerosol (SV-OOA) (Kroll et al., 2011), consistent with numerous monoterpene + O_3 chamber experiments (Bateman et al., 2009; Aiken et al., 2008; Shilling et al., 2009; Chhabra et al., 2010; Chen et al., 2011). SOA density predictions from elemental ratios using the parameterisation of Kuwata et al. (2012) show some agreement with measured values (Supplementary Information S.8).

~~The average elemental composition across all experiments was found to be . The high oxygen content with little respective loss of hydrogen is consistent with the ozonolysis mechanism, and indicates a large contribution from organic acids, alcohols and/or peroxides. As products only contain carbon, hydrogen and oxygen with triple bonds unlikely, the double bond index (DBE) can be used to further parameterise the OA (Bateman et al., 2009):~~

$$DBE = 1 - H/2 + C$$

~~The DBE is equal to the total number of C=C bonds, C=O bonds and rings in the molecule. Assuming 10 carbons, the DBE value for the average SOA composition is 3.2. This value is consistent with hypothesised first-generation products (Figs. S.4.1 and S.4.2), which typically retain a double bond and have at least two oxygen-containing functional groups. For the larger second-generation species, which are thought to have 6 – 7 carbons, the DBE from the average elemental composition is 2.3 – 2.5. Assuming products are non-cyclic and saturated, the DBE indicates that second-generation species contributing to the SOA have on average 2 – 3 bonds. Of course the impact of heterogeneous reactions, oligomerisation and many more complex processes thought to occur inside SOA cannot be discounted (Hallquist et al., 2009).~~

A Van Krevelen plot of the entire dataset is given in Fig. 16. The impact of CI scavengers, cyclohexane and NO_2 on OA in Van Krevelen space is observed to be minor. The important parameter ~~, again,~~ was found to be aerosol mass loadings~~. The impact of SOA loadings on bulk aerosol metrics must now be stressed, with caution advised when translating chamber results that operate under relatively high aerosol loadings to an ambient setting, for which lower mass loadings are much more typical. With respect to Van Krevelen space, changes in aerosol mass loading results in vertical shifts~~, with changes resulting in vertical shifts consistent with a change in oxidation state. Ozonolysis reactions are unique ~~,~~ as oxygen can be added, and condensible products formed, with no loss (and possibly gain) of hydrogen. Because of this, generic functionalisation lines used to characterise reactions in Van Krevelen space (Heald et al., 2010; Chhabra et al., 2011) are not applicable.

It is evident from Fig. 16 that the majority of ~~gas-phase species detected using the PTR-TOF (Table 2)~~ predicted species have a lower O/C ratio compared to what is measured for the bulk of the aerosol~~, further confirming their primary residence in the gas-phase~~. It is therefore unlikely that any of the detected gas-phase species are substantially contributing to the generated aerosol, which instead is dominated by more functionalised products. Whilst it is likely that species comprising the OA are also present in the gas-phase, they ~~just exist below~~ exist below the detection threshold of, or are lost in detection by the PTR-TOF. Indeed the presence of a filter prior to the PTR-TOF inlet may hinder detection of less volatile species, as elevated levels of OA on the filter may coax species into partitioning (Turpin et al., 2000; Kirchstetter et al., 2001).

The carbon mass balance for each experiment ~~(~~is shown in Fig. 17~~)~~. It was calculated by summing the gas-phase yields of all product ions, assuming a carbon number of 6 for unidentified products, with SOA yields, whose carbon content was determined from elemental ratios measured in each experiment. The carbon balance ranged from 25 – 131%. General losses in the system, such as vapour losses to the Teflon walls, affect the ability to close the carbon mass balance for most experiments, with performance worse in those experiments with lower starting α-phellandrene concentrations due to an inability to detect minor gas-phase products~~(Table 4)~~. It is evident from Fig. 17 that, despite having lower yields, heavier gas-phase products make a larger contribution to the carbon mass balance than lighter species such as formaldehyde, glyoxal, formic acid and acetic acid, whose nominal yields are higher. Meanwhile experiment 4 had a carbon mass balance exceeding 100%, which is thought to be the result of an erroneously high SOA yield (Fig. 12). It is immediately obvious from the carbon mass ~~balance that in all experiments,~~ balances that a large fraction of α-phellandrene partitions into the aerosol phase upon ozonolysis, exemplifying the impact α-phellandrene can have on SOA ~~growth upon introduction into an environment~~formation and growth. Currently the species comprising SOA generated from α-phellandrene ozonolysis remain unidentified, however a complete analysis of filter samples collected during these experiments is underway, in preparation for a follow-on publication.

4 Conclusions

The reaction of α-phellandrene with ozone was studied in depth for the first time through 11 chamber experiments. In the gas-phase, only signals with increasing temporal profiles were detected by the PTR-TOF, indicative of second-generation products. Of these, small species ($\leq C_3$) were found to be produced in the highest yields, namely formaldehyde (5 – 9%), acetaldehyde (0.2 – 8%)~~.~~, glyoxal (6 – 23%), methyl glyoxal (2 – 9%), formic acid (22 – 37%) and acetic acid (9 – 22%), with yields of all products suppressed by the addition of NO_2. Despite having lower yields, heavier second-generation products were found to make a larger contribution to the carbon mass balance. A small number of second-generation products were tentatively identified based on a constructed gas-phase mechanism, ~~with some evidence for gas-phase dimers existing~~including 2-propan-2-ylpropanedial and 2-propan-2-ylbutanedial. Experimental OH-radical yields of 35 $\pm$ 12 % and 15 $\pm$ 7 % for α-phellandrene and its first-generation products are in good agreement with those reported in Herrmann et al. (2010) and show the hydroperoxide channel to be an important pathway, with model output from a simple reaction parametrisation suggesting ~~the yield from α-phellandrene~~ experimental yields to be a lower bound. Meanwhile modelling provides a rate coefficient of 1.0 $\pm$ 0.7 $\times 10^{-16}$ cm^3 molecule^{-1} s^{-1} for the average reaction of first-generation products with ozone at 298 K. This equates to

an atmospheric lifetime of around 3.75 hours, higher than many other monoterpenes, and suggests that complete saturation of α-phellandrene likely occurs in the environment to which it is emitted.

α-phellandrene was found to form a large amount of aerosol upon reacting with ozone. A homogeneous nucleation burst of fresh aerosol was observed in all experiments within the first few minutes of the reaction, indicating a rapid formation of ELVOC species. Addition of a CI scavenger inhibited nucleation, suggesting that ~~stabilised CIs~~ sCIs are important precursors in forming compounds of low volatility in the system. The mechanism behind this remains unknown, although numerous pathways have been proposed in the literature for CIs from other alkenes ~~.~~ with more experiments required. Addition of NO_2 was found to reduce initial nucleation, although overall yields remained the same. The average effective SOA density was determined to be 1.49 $\pm$ 0.2 $\mathrm{g\,cm^{-3}}$ with an oxidation state varying from 0.56 to 1.02 depending on mass loadings~~,~~ ~~with the highly functionalised aerosol therefore existing in a solid or waxy state~~. SOA growth curves show both first- and second-generation species contribute to the particulate phase, driving aerosol growth through to completion of the reaction. ~~Using a two-product model, the~~ SOA yield is best fit by ~~parameters, $\alpha_1 = \alpha_2 = 0.60 \pm 0.09$ and $K_{om,1} = K_{om,2} = 0.022 \pm 0.01$~~ a one-product model with $\alpha_1 = 1.2 \pm 0.2$ and $K_{om,1} = 0.022 \pm 0.02$ $\mathrm{m^3\,\mu g^{-1}}$, with the SOA forming potential from α-phellandrene ozonolysis greater than other monoterpenes previously investigated in the literature.

High radical, acid and SOA yields, coupled with a high reactivity, results in α-phellandrene having an immediate and significant impact on its local environment. Indeed it appears likely that ozonolysis of α-phellandrene contributes to the significant blue haze, and intense and frequent nocturnal nucleation events observed over Eucalypt forests. Characterisation and parametrisation of both the gaseous- and particle-phases formed from the ozonolysis of α-phellandrene therefore betters our understanding ~~on~~ of the impact of biogenic emissions, and begins to enable the inclusion of this potentially important monoterpene in future atmospheric models.

5 Data availability

A website dedicated to the smog chamber is currently under construction, which will include all chamber data. For the meantime original data pertaining to this work can be obtained upon request from Xinming Wang (wangxm@gig.ac.cn).

Competing interests. The authors declare that they have no conflict of interest.

Acknowledgements. Experiments were made possible through funding by the Strategic Priority Research Program of the Chinese Academy of Sciences (Grant No. XDB05010200); Ministry of Science and Technology of China (Grant No. 2016YFC0202204); and National Natural Science Foundation of China (Grant No. 41530641/41571130031). The authors would also like to extend their thanks to Antoinette Boreave (IRCELYON) for assistance with operating the AMS.

References

Aiken, A. C., DeCarlo, P. F., and Jimenez, J. L.: Elemental analysis of organic species with electron ionization high-resolution mass spectrometry, Anal. Chem., 79, 8350–8358, doi:10.1029/2010GL042737., 2007.

Aiken, A. C., Decarlo, P. F., Kroll, J. H., Worsnop, D. R., Huffman, J. A., Docherty, K. S., Ulbrich, I. M., Mohr, C., Kimmel, J. R., Sueper, D., Sun, Y., Zhang, Q., Trimborn, A., Northway, M., Ziemann, P. J., Canagaratna, M. R., Onasch, T. B., Alfarra, M. R., Prévôt, A. S. H., Dommen, J., Duplissy, J., Metzger, A., Baltensperger, U., and Jimenez, J. L.: O/C and OM/OC ratios of primary, secondary, and ambient organic aerosols with high-resolution time-of-flight aerosol mass spectrometry, Environ. Sci. Technol., 42, 4478–4485, doi:10.1021/es703009q, 2008.

Aoki, N., Inomata, S., and Tanimoto, H.: Detection of C_1–C_5 alkyl nitrates by proton transfer reaction time-of-flight mass spectrometry, Int. J. Mass Spectrom., 263, 12–21, doi:10.1016/j.ijms.2006.11.018, 2007.

Aschmann, S. M. and Atkinson, R.: Formation yields of methyl vinyl ketone and methacrolein from the gas-phase reaction of O_3 with isoprene, Environ. Sci. Technol., 28, 1539–1542, doi:10.1021/es00057a025, 1994.

Aschmann, S. M., Arey, J., and Atkinson, R.: OH radical formation from the gas-phase reactions of O_3 with methacrolein and methyl vinyl ketone, Atmos. Environ., 30, 2939–2943, doi:10.1016/1352-2310(96)00013-1, 1996.

Atkinson, R. and Arey, J.: Gas-phase tropospheric chemistry of biogenic volatile organic compounds: A review, Atmos. Environ., 37, S197–S219, doi:10.1016/S1352-2310(03)00391-1, 2003.

Atkinson, R., Hasegawa, D., and Aschmann, S. M.: Rate constants for the gas-phase reactions of O_3 with a series of monoterpenes and related compounds at 296 $\pm$ 2 K, Int. J. Chem. Kinet., 22, 871–887, doi:10.1002/kin.550220807, 1990.

Atkinson, R., Aschmann, S. M., Arey, J., and Shorees, B.: Formation of OH radicals in the gas phase reactions of O_3 with a series of terpenes, J. Geophys. Res., 97, 6065–6073, doi:10.1029/92JD00062, 1992.

Atkinson, R., Baulch, D. L., Cox, R. a., Crowley, J. N., Hampson, R. F., Hynes, R. G., Jenkin, M. E., Rossi, M. J., and Troe, J.: Evaluated kinetic and photochemical data for atmospheric chemistry: Part 1 - gas phase reactions of Ox, HOx, NOx and SOx species, Atmos. Chem. Phys., 4, 1461–1738, doi:10.5194/acpd-3-6179-2003, 2004.

Aumont, B., Szopa, S., and Madronich, S.: Modelling the evolution of organic carbon during its gas-phase tropospheric oxidation: development of an explicit model based on a self generating approach, Atmos. Chem. Phys., 5, 2497–2517, doi:10.5194/acpd-5-703-2005, 2005.

Bahreini, R., Keywood, M. D., Ng, N. L., Varutbangkul, V., Gao, S., Flagan, R. C., Seinfeld, J. H., Worsnop, D. R., and Jimenez, J. L.: Measurements of secondary organic aerosol from oxidation of cycloalkenes, terpenes, and *m*-xylene using an aerodyne aerosol mass spectrometer, Environ. Sci. Technol., 39, 5674–5688, doi:10.1021/es048061a, 2005.

Barley, M. H. and McFiggans, G.: The critical assessment of vapour pressure estimation methods for use in modelling the formation of atmospheric organic aerosol, Atmos. Chem. Phys., 10, 749–767, doi:10.5194/acp-10-749-2010, 2010.

Bateman, A. P., Nizkorodov, S. A., Laskin, J., and Laskin, A.: Time-resolved molecular characterization of limonene/ozone aerosol using high-resolution electrospray ionization mass spectrometry, Phys. Chem. Chem. Phys., 11, 7931–7942, doi:10.1039/b916865f, 2009.

Berndt, T., Böge, O., and Stratmann, F.: Gas-phase ozonolysis of α-pinene: gaseous products and particle formation, Atmos. Environ., 37, 3933–3945, doi:10.1016/S1352-2310(03)00501-6, 2003.

Blake, R. S., Wyche, K. P., Ellis, A. M., and Monks, P. S.: Chemical ionization reaction time-of-flight mass spectrometry: Multi-reagent analysis for determination of trace gas composition, Int. J. Mass Spectrom., 254, 85–93, doi:10.1016/j.ijms.2006.05.021, 2006.

Bonn, B., Schuster, G., and Moortgat, G. K.: Influence of water vapor on the process of new particle formation during monoterpene ozonolysis, J. Phys. Chem. A, 106, 2869–2881, doi:10.1021/jp012713p, 2002.

Brophy, J. J. and Southwell, I. A.: Eucalyptus Chemistry. In, Eucalyptus: The Genus Eucalyptus., Taylor & Francis, London, UK, 2002.

Calvert, J. G., Atkinson, R., Kerr, J. A., Madronich, S., Moortgat, G. K., Wallington, T. J., and G., Y.: The Mechanisms of Atmospheric Oxidation of the Alkenes, Oxford University Press, Oxford, UK, 2000.

Camredon, M., Hamilton, J. F., Alam, M. S., Wyche, K. P., Carr, T., White, I. R., Monks, P. S., Rickard, A. R., and Bloss, W. J.: Distribution of gaseous and particulate organic composition during dark α-pinene ozonolysis, Atmos. Chem. Phys., 10, 2893–2917, doi:10.5194/acpd-9-27837-2009, 2010.

Capouet, M. and Müller, J.-F.: A group contribution method for estimating the vapour pressures of α-pinene oxidation products, Atmos. Chem. Phys., 6, 1455–1467, doi:10.5194/acp-6-1455-2006, 2006.

Capouet, M., Müller, J.-F., Ceulemans, K., Compernolle, S., Vereecken, L., and Peeters, J.: Modeling aerosol formation in alpha-pinene photo-oxidation experiments, J. Geophys. Res., 113, D02 308, doi:10.1029/2007JD008995, 2008.

Cappellin, L., Karl, T., Probst, M., Ismailova, O., Winkler, P. M., Soukoulis, C., Aprea, E., Märk, T. D., Gasperi, F., and Biasioli, F.: On quantitative determination of volatile organic compound concentrations using proton transfer reaction time-of-flight mass spectrometry., Environ. Sci. Technol., 46, 2283–90, doi:10.1021/es203985t, 2012.

Chen, Q., Liu, Y., Donahue, N. M., Shilling, J. E., and Martin, S. T.: Particle-phase chemistry of secondary organic material: Modeled compared to measured O:C and H:C Elemental ratios provide constraints, Environ. Sci. Technol., 45, 4763–4770, doi:10.1021/es104398s, 2011.

Chen, Q. Q., Li, Y. L., McKinney, K. A., Kuwata, M., and Martin, S. T.: Particle mass yield from β-caryophyllene ozonolysis, Atmos. Chem. Phys., 12, 3165–3179, doi:10.5194/acp-12-3165-2012, 2012.

Chhabra, P. S., Flagan, R. C., and Seinfeld, J. H.: Elemental analysis of chamber organic aerosol using an aerodyne high-resolution aerosol mass spectrometer, Atmos. Chem. Phys., 10, 4111–4131, doi:10.5194/acp-10-4111-2010, 2010.

Chhabra, P. S., Ng, N. L., Canagaratna, M. R., Corrigan, A. L., Russell, L. M., Worsnop, D. R., Flagan, R. C., and Seinfeld, J. H.: Elemental composition and oxidation of chamber organic aerosol, Atmos. Chem. Phys., 11, 8827–8845, doi:10.5194/acp-11-8827-2011, 2011.

Chung, S. H. and Seinfeld, J. H.: Global distribution and climate forcing of carbonaceous aerosols, J. Geophys. Res., 107, 4407, doi:10.1029/2001JD001397, 2002.

Clegg, S. L., Kleeman, M. J., Griffin, R. J., and Seinfeld, J. H.: Effects of uncertainties in the thermodynamic properties of aerosol components in an air quality model — Part 2: Predictions of the vapour pressures of organic compounds, Atmos. Chem. Phys., 8, 1087–1103, doi:10.5194/acp-8-1057-2008, 2008.

D'Anna, B., Wisthaler, A., Andreasen, Ø., Hansel, A., Hjorth, J., Jensen, N. R., Nielsen, C. J., Stenstrøm, Y., and Viidanoja, J.: Atmospheric chemistry of C_3–C_6 cycloalkanecarbaldehydes., J. Phys. Chem. A, 109, 5104–5118, doi:10.1021/jp044495g, 2005.

DeCarlo, P. F., Slowik, J. G., Worsnop, D. R., Davidovits, P., and Jimenez, J. L.: Particle morphology and density characterization by combined mobility and aerodynamic diameter measurements. Part 1: Theory, Aerosol Sci. Technol., 38, 1185–1205, doi:10.1080/02786826.2004.10399462, 2004.

DeCarlo, P. F., Kimmel, J. R., Trimborn, A., Northway, M. J., Jayne, J. T., Aiken, A. C., Gonin, M., Fuhrer, K., Horvath, T., Docherty, K. S., Worsnop, D. R., and Jimenez, J. L.: Field-deployable, high-resolution, time-of-flight aerosol mass spectrometer, Anal. Chem., 78, 8281–8289, doi:8410.1029/2001JD001213.Analytical, 2006.

Donahue, N. M., Robinson, A. L., Stanier, C. O., and Pandis, S. N.: Coupled partitioning, dilution, and chemical aging of semivolatile organics, Environ. Sci. Technol., 40, 2635–2643, doi:10.1021/es052297c, 2006.

Donahue, N. M., Trump, E. R., Pierce, J. R., and Riipinen, I.: Theoretical constraints on pure vapor-pressure driven condensation of organics to ultrafine particles, Geophys. Res. Lett., 38, L16 801, doi:10.1029/2011GL048115, 2011.

Donahue, N. M., Henry, K. M., Mentel, T. F., Kiendler-Scharr, A., Spindler, C., Bohn, B., Brauers, T., Dorn, H. P., Fuchs, H., Tillmann, R., Wahner, A., Saathoff, H., Naumann, K.-H., Möhler, O., Leisner, T., Müller, L., Reinnig, M.-C., Hoffmann, T., Salo, K., Hallquist, M., Frosch, M., Bilde, M., Tritscher, T., Barmet, P., Praplan, A. P., DeCarlo, P. F., Dommen, J., Prévôt, A. S. H., and Baltensperger, U.: Aging of biogenic secondary organic aerosol via gas-phase OH radical reactions, Proc. Natl. Acad. Sci. U. S. A., 109, 13 503–13 508, doi:10.1073/pnas.1115186109, 2012.

Donahue, N. M., Ortega, I. K., Chuang, W., Riipinen, I., Riccobono, F., Schobesberger, S., Dommen, J., Baltensperger, U., Kulmala, M., Worsnop, D. R., and Vehkamaki, H.: How do organic vapors contribute to new-particle formation?, Faraday Discuss., 165, 91, doi:10.1039/c3fd00046j, 2013.

Draper, D. C., Farmer, D. K., Desyaterik, Y., and Fry, J. L.: A qualitative comparison of secondary organic aerosol yields and composition from ozonolysis of monoterpenes at varying concentrations of NO_2, Atmos. Chem. Phys., 15, 12 267–12 281, doi:10.5194/acp-15-12267-2015, 2015.

Duncianu, M., David, M., Kartigueyane, S., Cirtog, M., Doussin, J.-F., and Picquet-Varrault, B.: Measurement of alkyl and multifunctional organic nitrates by Proton Transfer Reaction Mass Spectrometry, Atmos. Meas. Tech. Discuss., in review, doi:10.5194/amt-2016-318, 2016.

Eddingsaas, N. C., Loza, C. L., Yee, L. D., Chan, M., Schilling, K. A., Chhabra, P. S., Seinfeld, J. H., and Wennberg, P. O.: α-pinene photooxidation under controlled chemical conditions-Part 2: SOA yield and composition in low-and high-NO_x environments, Atmos. Chem. Phys., 12, 7413–7427, doi:10.5194/acp-12-7413-2012, 2012.

Ehn, M., Thornton, J. A., Kleist, E., Sipilä, M., Junninen, H., Pullinen, I., Springer, M., Rubach, F., Tillmann, R., Lee, B., Lopez-Hilfiker, F., Andres, S., Acir, I.-H., Rissanen, M., Jokinen, T., Schobesberger, S., Kangasluoma, J., Kontkanen, J., Nieminen, T., Kurtén, T., Nielsen, L. B., Jørgensen, S., Kjaergaard, H. G., Canagaratna, M., Maso, M. D., Berndt, T., Petäjä, T., Wahner, A., Kerminen, V.-M., Kulmala, M., Worsnop, D. R., Wildt, J., and Mentel, T. F.: A large source of low-volatility secondary organic aerosol, Nature, 506, 476–479, doi:10.1038/nature13032, 2014.

Fredenslund, A., Jones, R. L., and Prausnitz, J. M.: Group-contribution estimation of activity coefficients in nonideal liquid mixtures, AIChE J., 21, 1086–1099, doi:10.1002/aic.690210607, 1975.

Graus, M., Müller, M., and Hansel, A.: High resolution PTR-TOF: Quantification and formula confirmation of VOC in real time, J. Am. Soc. Mass Spectrom., 21, 1037–1044, doi:10.1016/j.jasms.2010.02.006, 2010.

Griffin, R. J., Cocker, D. R., Flagan, R. C., and Seinfeld, J. H.: Organic aerosol formation from the oxidation of biogenic hydrocarbons, J. Geophys. Res., 104, 3555–3567, doi:10.1029/1998JD100049, 1999a.

Griffin, R. J., Cocker, D. R., Seinfeld, J. H., and Dabdub, D.: Estimates of global atmospheric organic aerosol from oxidation of biogenic hydrocarbons, Geophys. Res. Lett., 26, 2721–2724, doi:10.1029/1999GL900476, 1999b.

Grimsrud, E. P., Westberg, H. H., and Rasmussen, R. A.: Atmospheric reactivity of monoterpene hydrocarbons, NO, photooxidation and ozonolysis, Int. J. Chem. Kinet. Symp., 1, 183–195, 1975.

Grosjean, D., Williams, E. L., and Grosjean, E.: Atmospheric chemistry of isoprene and of its carbonyl products, Environ. Sci. Technol., 27, 830–840, doi:10.1021/es00042a004, 1993.

Guenther, A., Hewitt, C. N., Erickson, D., Fall, R., Geron, C., Graedel, T., Harley, P., Klinger, L., Lerdau, M., McKay, W. A., Pierce, T., Scholes, B., Steinbrecher, R., Tallamraju, R., Taylor, J., and Zimmerman, P.: A global model of natural volatile organic compound emissions, J. Geophys. Res., 100, 8873–8892, doi:10.1029/94JD02950, 1995.

Guenther, A. B., Jiang, X., Heald, C. L., Sakulyanontvittaya, T., Duhl, T., Emmons, L. K., and Wang, X.: The Model of Emissions of Gases and Aerosols from Nature version 2.1 (MEGAN2.1): an extended and updated framework for modeling biogenic emissions, Geosci. Model Dev., 5, 1471–1492, doi:10.5194/gmd-5-1471-2012, 2012.

Hallquist, M., Wenger, J. C., Baltensperger, U., Rudich, Y., Simpson, D., Claeys, M., Dommen, J., Donahue, N. M., George, C., Goldstein, A. H., Hamilton, J. F., Herrmann, H., Hoffmann, T., Iinuma, Y., Jang, M., Jenkin, M. E., Jimenez, J. L., Kiendler-Scharr, A., Maenhaut, W., McFiggans, G., Mentel, T. F., Monod, A., Prévôt, a. S. H., Seinfeld, J. H., Surratt, J. D., Szmigielski, R., and Wildt, J.: The formation, properties and impact of secondary organic aerosol: current and emerging issues, Atmos. Chem. Phys., 9, 5155–5236, doi:10.5194/acp-9-5155-2009, 2009.

He, C., Murray, F., and Lyons, T.: Monoterpene and isoprene emissions from 15 Eucalyptus species in Australia, Atmos. Environ., 34, 645–655, doi:10.1016/S1352-2310(99)00219-8, 2000.

Heald, C. L., Kroll, J. H., Jimenez, J. L., Docherty, K. S., Decarlo, P. F., Aiken, A. C., Chen, Q., Martin, S. T., Farmer, D. K., and Artaxo, P.: A simplified description of the evolution of organic aerosol composition in the atmosphere, Geophys. Res. Lett., 37, L08 803, doi:10.1029/2010GL042737, 2010.

Heaton, K. J., Sleighter, R. L., Hatcher, P. G., Hall, W. A., and Johnston, M. V.: Composition domains in monoterpene secondary organic aerosol, Environ. Sci. Technol., 43, 7797–7802, doi:10.1021/es901214p, 2009.

Henze, D. K. and Seinfeld, J. H.: Global secondary organic aerosol from isoprene oxidation, Geophys. Res. Lett., 33, L09 812, doi:10.1029/2006GL025976, 2006.

Herrmann, F., Winterhalter, R., Moortgat, G. K., and Williams, J.: Hydroxyl radical (OH) yields from the ozonolysis of both double bonds for five monoterpenes, Atmos. Environ., 44, 3458–3464, doi:10.1016/j.atmosenv.2010.05.011, 2010.

Hoffmann, T., Odum, J. R., Bowman, F., Collins, D., Klockow, D., Flagan, R. C., and Seinfeld, J. H.: Formation of organic aerosols from the oxidation of biogenic hydrocarbons, J. Atmos. Chem., 26, 189–222, doi:10.1023/A:1005734301837, 1997.

Huffman, J. A., Jayne, J. T., Drewnick, F., Aiken, A. C., Onasch, T., Worsnop, D. R., and Jimenez, J. L.: Design, modeling, optimization, and experimental tests of a particle beam width probe for the aerodyne aerosol mass spectrometer, Aerosol Sci. Technol., 39, 1143–1163, doi:10.1080/02786820500423782, 2005.

Jathar, S. H., Cappa, C. D., Wexler, A. S., Seinfeld, J. H., and Kleeman, M. J.: Simulating secondary organic aerosol in a regional air quality model using the statistical oxidation model - Part 1: Assessing the influence of constrained multi-generational ageing, Atmos. Chem. Phys., 16, 2309–2322, doi:10.5194/acp-16-2309-2016, 2016.

Jayne, J. T., Leard, D. C., Zhang, X., Davidovits, P., Smith, K. A., Kolb, C. E., and Worsnop, D. R.: Development of an aerosol mass spectrometer for size and composition analysis of submicron particles, Aerosol Sci. Technol., 33, 49–70, doi:10.1080/027868200410840, 2000.

Jenkin, M. E.: Modelling the formation and composition of secondary organic aerosol from α- and β-pinene ozonolysis using MCM v3, Atmos. Chem. Phys., 4, 1741–1757, doi:10.5194/acpd-4-2905-2004, 2004.

Jenkin, M. E., Saunders, S. M., and Pilling, M. J.: The tropospheric degradation of volatile organic compounds: A protocol for mechanism development, Atmos. Environ., 31, 81–104, doi:10.1016/S1352-2310(96)00105-7, 1997.

Johnson, D. and Marston, G.: The gas-phase ozonolysis of unsaturated volatile organic compounds in the troposphere., Chem. Soc. Rev., 37, 699–716, doi:10.1039/b704260b, 2008.

Jokinen, T., Berndt, T., Makkonen, R., Kerminen, V.-M., Junninen, H., Paasonen, P., Stratmann, F., Herrmann, H., Guenther, A. B., Worsnop, D. R., Kulmala, M., Ehn, M., and Sipilä, M.: Production of extremely low volatile organic compounds from biogenic emissions: Measured yields and atmospheric implications., Proc. Natl. Acad. Sci. U. S. A., 112, 7123–7128, doi:10.1073/pnas.1423977112, 2015.

Jordan, A., Haidacher, S., Hanel, G., Hartungen, E., Märk, L., Seehauser, H., Schottkowsky, R., Sulzer, P., and Märk, T. D.: A high resolution and high sensitivity proton-transfer-reaction time-of-flight mass spectrometer (PTR-TOF-MS), Int. J. Mass Spectrom., 286, 122–128, doi:10.1016/j.ijms.2009.07.005, 2009.

Katrib, Y., Martin, S. T., Rudich, Y., Davidovits, P., Jayne, J. T., and Worsnop, D. R.: Density changes of aerosol particles as a result of chemical reaction, Atmos. Chem. Phys., 5, 275–291, doi:10.5194/acpd-4-6431-2004, 2005.

Keywood, M. D., Kroll, J. H., Varutbangkul, V., Bahreini, R., Flagan, R. C., and Seinfeld, J. H.: Secondary organic aerosol formation from cyclohexene ozonolysis: Effect of OH scavenger and the role of radical chemistry, Environ. Sci. Technol., 38, 3343–3350, doi:10.1021/es049725j, 2004.

Kirchstetter, T. W., Corrigan, C. E., and Novakov, T.: Laboratory and field investigation of the adsorption of gaseous organic compounds onto quartz filters, Atmos. Environ., 35, 1663–1671, doi:10.1016/S1352-2310(00)00448-9, 2001.

Kostenidou, E., Pathak, R. K., and Pandis, S. N.: An algorithm for the calculation of secondary organic aerosol density combining AMS and SMPS data, Aerosol Sci. Technol., 41, 1002–1010, doi:10.1080/02786820701666270, 2007.

Krechmer, J. E., Pagonis, D., Ziemann, P. J., and Jimenez, J. L.: Quantification of Gas-Wall Partitioning in Teflon Environmental Chambers Using Rapid Bursts of Low-Volatility Oxidized Species Generated in Situ, Environ. Sci. Technol., 50, 5757–5765, doi:10.1021/acs.est.6b00606, 2016.

Kroll, J. H., Smith, J. D., Che, D. L., Kessler, S. H., Worsnop, D. R., and Wilson, K. R.: Measurement of fragmentation and functionalization pathways in the heterogeneous oxidation of oxidized organic aerosol, Phys. Chem. Chem. Phys., 11, 8005–8014, doi:10.1039/b916865f, 2009.

Kroll, J. H., Donahue, N. M., Jimenez, J. L., Kessler, S. H., Canagaratna, M. R., Wilson, K. R., Altieri, K. E., Mazzoleni, L. R., Wozniak, A. S., Bluhm, H., Mysak, E. R., Smith, J. D., Kolb, C. E., and Worsnop, D. R.: Carbon oxidation state as a metric for describing the chemistry of atmospheric organic aerosol, Nat. Chem., 3, 133–139, doi:10.1038/nchem.948, 2011.

Kuwata, M., Zorn, S. R., and Martin, S. T.: Using elemental ratios to predict the density of organic material composed of carbon, hydrogen, and oxygen, Environ. Sci. Technol., 46, 787–794, doi:10.1021/es202525q, 2012.

La, Y. S., Camredon, M., Ziemann, P. J., Valorso, R., Matsunaga, A., Lannuque, V., Lee-Taylor, J., Hodzic, A., Madronich, S., and Aumont, B.: Impact of chamber wall loss of gaseous organic compounds on secondary organic aerosol formation: explicit modeling of SOA formation from alkane and alkene oxidation, Atmos. Chem. Phys., 16, 1417–1431, doi:10.5194/acp-16-1417-2016, 2016.

Lathière, J., Hauglustaine, D. A., Friend, A. D., De Noblet-Ducoudré, N., Viovy, N., and Folberth, G. A.: Impact of climate variability and land use changes on global biogenic volatile organic compound emissions, Atmos. Chem. Phys., 6, 2129–2146, doi:10.5194/acp-6-2129-2006, 2006.

Lee, A., Goldstein, A. H., Keywood, M. D., Gao, S., Varutbangkul, V., Bahreini, R., Ng, N. L., Flagan, R. C., and Seinfeld, J. H.: Gas-phase products and secondary aerosol yields from the ozonolysis of ten different terpenes, J. Geophys. Res., 111, D07 302, doi:10.1029/2006JD007050, 2006.

Lee, S.-H., Young, L.-H., Benson, D. R., Suni, T., Kulmala, M., Junninen, H., Campos, T. L., Rogers, D. C., and Jensen, J.: Observations of nighttime new particle formation in the troposphere, J. Geophys. Res., 113, D10 210, doi:10.1029/2007JD009351, 2008.

Leungsakul, S., Jaoui, M., and Kamens, R. M.: Kinetic mechanism for predicting secondary organic aerosol formation from the reaction of d-limonene with ozone, Environ. Sci. Technol., 39, 9583–9594, doi:10.1021/es0492687, 2005.

Li, H., Madden, J. L., and Potts, B. M.: Variation in volatile leaf oils of the tasmanian Eucalyptus species-1. Subgenus Monocalyptus, Biochem. Syst. Ecol., 23, 299–318, doi:10.1016/0305-1978(95)97455-6, 1995.

Liu, T., Wang, X., Deng, W., Hu, Q., Ding, X., Zhang, Y., He, Q., Zhang, Z., Lü, S., Bi, X., Chen, J., and Yu, J.: Secondary organic aerosol formation from photochemical aging of light-duty gasoline vehicle exhausts in a smog chamber, Atmos. Chem. Phys., 15, 9049–9062, doi:10.5194/acp-15-9049-2015, 2015.

Ma, Y., Willcox, T. R., Russell, A. T., and Marston, G.: Pinic and pinonic acid formation in the reaction of ozone with α-pinene., Chem. Commun., 13, 1328–1330, doi:10.1039/b617130c, 2007.

Mackenzie-Rae, F. A., Karton, A., and Saunders, S. M.: Computational investigation into the gas-phase ozonolysis of the conjugated monoterpene α-phellandrene, Phys. Chem. Chem. Phys., 18, 27 991–28 002, doi:10.1039/C6CP04695A, 2016.

Maghsoodlou, M. T., Kazemipoor, N., Valizadeh, J., Falak Nezhad Seifi, M., and Rahneshan, N.: Essential oil composition of Eucalyptus microtheca and Eucalyptus viminalis, Avicenna J. Phytomedicine, 5, 540–552, 2015.

Maisey, S. J., Saunders, S. M., West, N., and Franklin, P. J.: An extended baseline examination of indoor VOCs in a city of low ambient pollution: Perth, Western Australia, Atmos. Environ., 81, 546–553, doi:10.1016/j.atmosenv.2013.09.008, 2013.

Maleknia, S. D., Bell, T. L., and Adams, M. A.: Eucalypt smoke and wildfires: Temperature dependent emissions of biogenic volatile organic compounds, Int. J. Mass Spectrom., 279, 126–133, doi:10.1016/j.ijms.2008.10.027, 2009.

Matsunaga, A. and Ziemann, P. J.: Gas-Wall Partitioning of Organic Compounds in a Teflon Film Chamber and Potential Effects on Reaction Product and Aerosol Yield Measurements, Aerosol Sci. Technol., 44, 881–892, doi:10.1080/02786826.2010.501044, 2010.

Matthew, B. M., Middlebrook, A. M., and Onasch, T. B.: Collection efficiencies in an aerodyne aerosol mass spectrometer as a function of particle phase for laboratory generated aerosols, Aerosol Sci. Technol., 42, 884–898, doi:10.1080/02786820802356797, 2008.

McLafferty, F. W. and Turecek, F.: Interpretation of Mass Spectra, University Science Books, Sausalito, CA, 4 edn., 1993.

Misztal, P. K., Heal, M. R., Nemitz, E., and Cape, J. N.: Development of PTR-MS selectivity for structural isomers: Monoterpenes as a case study, Int. J. Mass Spectrom., 310, 10–19, doi:10.1016/j.ijms.2011.11.001, 2012.

Moller, B., Rarey, J., and Ramjugernath, D.: Estimation of the vapour pressure of non-electrolyte organic compounds via group contributions and group interactions, J. Mol. Liq., 143, 52–63, doi:10.1016/j.molliq.2008.04.020, 2008.

Müller, M., Graus, M., Wisthaler, A., Hansel, A., Metzger, A., Dommen, J., and Baltensperger, U.: Analysis of high mass resolution PTR-TOF mass spectra from 1,3,5-trimethylbenzene (TMB) environmental chamber experiments, Atmos. Chem. Phys., 12, 829–843, doi:10.5194/acp-12-829-2012, 2012.

Müller, M., Mikoviny, T., Jud, W., D'Anna, B., and Wisthaler, A.: A new software tool for the analysis of high resolution PTR-TOF mass spectra, Chemom. Intell. Lab. Syst., 127, 158–165, doi:10.1016/j.chemolab.2013.06.011, 2013.

Myburg, A. A., Grattapaglia, D., Tuskan, G. A., Hellsten, U., Hayes, R. D., Grimwood, J., Jenkins, J., Lindquist, E., Tice, H., Bauer, D., Goodstein, D. M., Dubchak, I., Poliakov, A., Mizrachi, E., Kullan, A. R. K., Hussey, S. G., Pinard, D., van der Merwe, K., Singh, P., Van Jaarsveld, I., Silva-Junior, O. B., Togawa, R. C., Pappas, M. R., Faria, D. A., Sansaloni, C. P., Petroli, C. D., Yang, X., Ranjan, P., Tschaplinski, T. J., Ye, C.-Y., Li, T., Sterck, L., Vanneste, K., Murat, F., Soler, M. M., Clemente, H. S. H. S., Saidi, N., Cassan-Wang, H., Dunand, C., Hefer, C. A., Bornberg-Bauer, E., Kersting, A. R., Vining, K., Amarasinghe, V., Ranik, M., Naithani, S., Elser, J., Boyd,

A. E., Liston, A., Spatafora, J. W., Dharmwardhana, P., Raja, R., Sullivan, C., Romanel, E., Alves-Ferreira, M., Lheim, C. K., Foley, W., Carocha, V., Paiva, J., Kudrna, D., Brommonschenkel, S. H., Pasquali, G., Byrne, M., Rigault, P., Tibbits, J., Spokevicius, A., Jones, R. C., Steane, D. A., Vaillancourt, R. E. R. E., Potts, B. M., Joubert, F., Barry, K., Pappas Jr., G. J., Strauss, S. H., Jaiswal, P., Grima-Pettenati, J., Salse, J. J., Van de Peer, Y., Rokhsar, D. S., Schmutz, J., Külheim, C., Foley, W., Carocha, V., Paiva, J., Kudrna, D., Brommonschenkel, S. H., Pasquali, G., Byrne, M., Rigault, P., Tibbits, J., Spokevicius, A., Jones, R. C., Steane, D. A., Vaillancourt, R. E. R. E., Potts, B. M., Joubert, F., Barry, K., Pappas, G. J., Strauss, S. H., Jaiswal, P., Grima-Pettenati, J., Salse, J. J., Van de Peer, Y., Rokhsar, D. S., and Schmutz, J.: The genome of Eucalyptus grandis, Nature, 510, 356–362, doi:10.1038/nature13308, 2014.

Nannoolal, Y., Rarey, J., Ramjugernath, D., and Cordes, W.: Estimation of pure component properties: Part 1. Estimation of the normal boiling point of non-electrolyte organic compounds via group contributions and group interactions, Fluid Phase Equilib., 226, 45–63, doi:10.1016/j.fluid.2004.09.001, 2004.

Ng, N. L., Kroll, J. H., Keywood, M. D., Bahreini, R., Varutbangkul, V., Flagan, R. C., and Seinfeld, J. H.: Contribution of first-versus second-generation products to secondary organic aerosols formed in the oxidation of biogenic hydrocarbons, Environ. Sci. Technol., 40, 2283–2297, doi:10.1021/es052269u, 2006.

Ng, N. L., Chhabra, P. S., Chan, A. W. H., Surratt, J. D., Kroll, J. H., Kwan, A. J., McCabe, D. C., Wennberg, P. O., Sorooshian, A., Murphy, S. M., Dalleska, N. F., Flagan, R. C., and Seinfeld, J. H.: Effect of NOx level on secondary organic aerosol (SOA) formation from the photooxidation of terpenes, Atmos. Chem. Phys., 7, 5159–5174, doi:10.5194/acpd-7-10131-2007, 2007.

Nguyen, T. L., Peeters, J., and Vereecken, L.: Theoretical study of the gas-phase ozonolysis of β-pinene ($C_{10}H_{16}$), Phys. Chem. Chem. Phys., 11, 5643–5656, doi:10.1039/B822984h, 2009.

Odum, J. R., Hoffmann, T., Bowman, F., Collins, D., Flagan, R. C., and Seinfeld, J. H.: Gas/particle partitioning and secondary organic aerosol yields, Environ. Sci. Technol., 30, 2580–2585, doi:10.1021/es950943+, 1996.

O'Meara, S., Booth, A. M., Barley, M. H., Topping, D., and McFiggans, G.: An assessment of vapour pressure estimation methods., Phys. Chem. Chem. Phys., 16, 19 453–19 469, doi:10.1039/c4cp00857j, 2014.

Ortega, I. K., Suni, T., Grönholm, T., Boy, M., Hakola, H., Hellén, H., Valmari, T., Arvela, H., Vehkamäki, H., and Kulmala, M.: Is eucalyptol the cause of nocturnal events observed in Australia?, Boreal Environ. Res., 14, 606–615, 2009.

Ortega, I. K., Suni, T., Boy, M., Grönholm, T., Manninen, H. E., Nieminen, T., Ehn, M., Junninen, H., Hakola, H., Hellén, H., Valmari, T., Arvela, H., Zegelin, S., Hughes, D., Kitchen, M., Cleugh, H., Worsnop, D. R., Kulmala, M., and Kerminen, V.-M.: New insights into nocturnal nucleation, Atmos. Chem. Phys., 12, 4297–4312, doi:10.5194/acp-12-4297-2012, 2012.

Pankow, J. and Asher, W.: SIMPOL.1: a simple group contribution method for predicting vapor pressures and enthalpies of vaporization of multifunctional organic compounds, Atmos. Chem. Phys., 8, 2773–2796, doi:10.5194/acpd-7-11839-2007, 2008.

Pankow, J. F.: An absorption model of gas/particle partitioning of organic compounds in the atmosphere, Atmos. Environ., 28, 185–188, doi:10.1016/1352-2310(94)90093-0, 1994.

Pathak, R. K., Stanier, C. O., Donahue, N. M., and Pandis, S. N.: Ozonolysis of α-pinene at atmospherically relevant concentrations: Temperature dependence of aerosol mass fractions (yields), J. Geophys. Res., 112, D03 201, doi:10.1029/2006JD007436, 2007.

Paulson, S. E., Flagan, R. C., and Seinfeld, J. H.: Atmospheric photooxidation of isoprene part II. The ozone-isoprene reaction, Int. J. Chem. Kinet., 24, 103–125, doi:10.1002/kin.550240110, 1992.

Pavlova, L. V., Platonov, I. A., Nikitchenko, N. V., and Novikova, E. A.: Evaluation of the efficiency of volatile organic compounds extraction from Eucalyptus viminalis (*Eucalypti viminalis* Labill) using subcritical extractants, Russ. J. Phys. Chem. B, 9, 1109–1115, doi:10.1134/S1990793115080084, 2015.

Perraud, V., Bruns, E. A., Ezell, M. J., Johnson, S. N., Yu, Y., Alexander, M. L., Zelenyuk, A., Imre, D., Chang, W. L., Dabdub, D., Pankow, J. F., and Finlayson-Pitts, B. J.: Nonequilibrium atmospheric secondary organic aerosol formation and growth., Proc. Natl. Acad. Sci., 109, 2836–2841, doi:10.1073/pnas.1119909109, 2012.

Pierce, J. R., Riipinen, I., Kulmala, M., Ehn, M., Petäjä, T., Junninen, H., Worsnop, D. R., and Donahue, N. M.: Quantification of the volatility of secondary organic compounds in ultrafine particles during nucleation events, Atmos. Chem. Phys., 11, 9019–9036, doi:10.5194/acp-11-9019-2011, 2011.

Presto, A. A., Huff Hartz, K. E., and Donahue, N. M.: Secondary organic aerosol production from terpene ozonolysis. 2. Effect of NOx concentration, Environ. Sci. Technol., 39, 7046–7054, doi:10.1021/es050400s, 2005.

Pye, H. O. T., Chan, A. W. H., Barkley, M. P., and Seinfeld, J. H.: Global modeling of organic aerosol: the importance of reactive nitrogen (NO_x and NO_3), Atmos. Chem. Phys., 10, 11 261–11 276, doi:10.5194/acp-10-11261-2010, 2010.

Reissell, A., Harry, C., Aschmann, S. M., Atkinson, R., and Arey, J.: Formation of acetone from the OH radical- and O_3-initiated reactions of a series of monoterpenes, J. Geophys. Res., 104, 13 869–13 879, doi:10.1029/1999JD900198, 1999.

Rickard, A. R., Johnson, D., McGill, C. D., and Marston, G.: OH yields in the gas-phase reactions of ozone with alkenes, J. Phys. Chem. A, 103, 7656–7664, doi:10.1021/jp9916992, 1999.

Saathoff, H., Naumann, K. H., Möhler, O., Jonsson, Å. M., Hallquist, M., Kiendler-Scharr, A., Mentel, T. F., Tillmann, R., and Schurath, U.: Temperature dependence of yields of secondary organic aerosols from the ozonolysis of α-pinene and limonene, Atmos. Chem. Phys., 9, 1551–1577, doi:10.5194/acp-9-1551-2009, 2009.

Sadezky, a., Chaimbault, P., Mellouki, A., Römpp, a., Winterhalter, R., Le Bras, G., and Moortgat, G. K.: Formation of secondary organic aerosol and oligomers from the ozonolysis of enol ethers, Atmos. Chem. Phys., 6, 5009–5024, doi:10.5194/acp-6-5009-2006, 2006.

Sadezky, A., Winterhalter, R., Kanawati, B., Römpp, A., Spengler, B., Mellouki, A., Le Bras, G., Chaimbault, P., and Moortgat, G. K.: Oligomer formation during gas-phase ozonolysis of small alkenes and enol ethers: new evidence for the central role of the Criegee Intermediate as oligomer chain unit, Atmos. Chem. Phys., 8, 2667–2699, doi:10.5194/acp-8-2667-2008, 2008.

Sakamoto, Y., Inomata, S., and Hirokawa, J.: Oligomerization reaction of the Criegee intermediate leads to secondary organic aerosol formation in ethylene ozonolysis, J. Phys. Chem. A, 117, 12 912–12 921, doi:10.1021/jp408672m, 2013.

Saunders, S. M., Jenkin, M. E., Derwent, R. G., and Pilling, M. J.: Protocol for the development of the Master Chemical Mechanism, MCM v3 (Part A): tropospheric degradation of non-aromatic volatile organic compounds, Atmos. Chem. Phys., 3, 161–180, doi:10.5194/acp-3-161-2003, 2003.

Schurgers, G., Arneth, A., Holzinger, R., and Goldstein, A.: Process-based modelling of biogenic monoterpene emissions combining production and release from storage, Atmos. Chem. Phys., 9, 3409–3423, doi:10.5194/acpd-9-271-2009, 2009.

Shilling, J. E., Chen, Q., King, S. M., Rosenoern, T., Kroll, J. H., Worsnop, D. R., McKinney, K. A., and Martin, S. T.: Particle mass yield in secondary organic aerosol formed by the dark ozonolysis of α-pinene, Atmos. Chem. Phys., 8, 2073–2088, doi:10.5194/acp-8-2073-2008, 2008.

Shilling, J. E., Chen, Q., King, S. M., Rosenoern, T., Kroll, J. H., Worsnop, D. R., DeCarlo, P. F., Aiken, A. C., Sueper, D., Jimenez, J. L., and Martin, S. T.: Loading-dependent elemental composition of α-pinene SOA particles, Atmos. Chem. Phys., 9, 771–782, doi:10.5194/acp-9-771-2009, 2009.

Shu, Y. and Atkinson, R.: Rate constants for the gas-phase reactions of O_3 with a series of terpenes and OH radical formation from the O_3 reactions with sesquiterpenes at 296 $\pm$ 2 K, Int. J. Chem. Kinet., 26, 1193–1205, doi:10.1002/kin.550261207, 1994.

Sindelarova, K., Granier, C., Bouarar, I., Guenther, A., Tilmes, S., Stavrakou, T., Müller, J. F., Kuhn, U., Stefani, P., and Knorr, W.: Global data set of biogenic VOC emissions calculated by the MEGAN model over the last 30 years, Atmos. Chem. Phys., 14, 9317–9341, doi:10.5194/acp-14-9317-2014, 2014.

Slowik, J. G., Stainken, K., Davidovits, P., Williams, L. R., Jayne, J. T., Kolb, C. E., Worsnop, D. R., Rudich, Y., DeCarlo, P. F., and Jimenez, J. L.: Particle morphology and density characterization by combined mobility and aerodynamic diameter measurements. Part 2: Application to combustion-generated soot aerosols as a function of fuel equivalence ratio, Aerosol Sci. Technol., 38, 1206–1222, doi:10.1080/02786826.2004.10399462, 2004.

Smith, D. and Španěl, P.: Selected ion flow tube mass spectrometry (SIFT-MS) for on-line trace gas analysis, Mass Spectrom. Rev., 24, 661–700, doi:10.1002/mas.20033, 2005.

Španěl, P. and Smith, D.: SIFT studies of the reactions of H_3O^+, NO^+ and O_2^+ with a series of volatile carboxylic acids and esters, Int. J. Mass Spectrom. Ion Process., 172, 137–147, doi:10.1016/S0168-1176(97)00246-2, 1998.

Španěl, P., Ji, Y., and Smith, D.: SIFT studies of the reactions of H_3O^+, NO^+ and O_2^+ with a series of aldehydes and ketones, Int. J. Mass Spectrom. Ion Process., 165/166, 25–37, doi:10.1016/S0168-1176(97)00166-3, 1997.

Stanier, C. O., Donahue, N., and Pandis, S. N.: Parameterization of secondary organic aerosol mass fractions from smog chamber data, Atmos. Environ., 42, 2276–2299, doi:10.1016/j.atmosenv.2007.12.042, 2008.

Stranger, M.: Emissions, exposure patterns and health effects of consumer products in the EU (EPHECT), Presented in part at Green Week 2013, Brussels, http://ec.europa.eu/environment/archives/greenweek2013, 2013.

Suni, T., Kulmala, M., Hirsikko, A., Bergman, T., Laakso, L., Aalto, P. P., Leuning, R., Cleugh, H., Zegelin, S., Hughes, D., van Gorsel, E., Kitchen, M., Hörrak, U., Mirme, S., Mirme, A., Sevanto, S., Twining, J., and Tadros, C.: Formation and characteristics of ions and charged aerosol particles in a native Australian Eucalypt forest, Atmos. Chem. Phys., 8, 129–139, doi:10.5194/acp-8-129-2008, 2008.

Takegawa, N., Miyakawa, T., Kawamura, K., and Kondo, Y.: Contribution of selected dicarboxylic and ω-oxocarboxylic acids in ambient aerosol to the *m/z* 44 signal of an aerodyne aerosol mass spectrometer, Aerosol Sci. Technol., 41, 418–437, doi:10.1080/02786820701203215, 2007.

Tani, A.: Fragmentation and reaction rate constants of terpenoids determined by proton transfer reaction-mass spectrometry, Environ. Control Biol., 51, 23–29, doi:10.2525/ecb.51.23, 2013.

Tsigaridis, K. and Kanakidou, M.: Global modelling of secondary organic aerosol in the troposphere: a sensitivity analysis, Atmos. Chem. Phys., 3, 1849–1869, doi:10.5194/acpd-3-2879-2003, 2003.

Turpin, B. J., Saxena, P., and Andrews, E.: Measuring and simulating particulate organics in the atmosphere: Problems and prospects, Atmos. Environ., 34, 2983–3013, doi:10.1016/S1352-2310(99)00501-4, 2000.

Vereecken, L., Glowacki, D. R., and Pilling, M. J.: Theoretical Chemical Kinetics in Tropospheric Chemistry: Methodologies and Applications, Chem. Rev., 115, 4063–4114, doi:10.1021/cr500488p, 2015.

von Hessberg, C., von Hessberg, P., Pöschl, U., Bilde, M., Nielsen, O. J., and Moortgat, G. K.: Temperature and humidity dependence of secondary organic aerosol yield from the ozonolysis of β-pinene, Atmos. Chem. Phys., 9, 3583–3599, doi:10.5194/acp-9-3583-2009, 2009.

Walser, M. L., Desyaterik, Y., Laskin, J., Laskin, A., and Nizkorodov, S. A.: High-resolution mass spectrometric analysis of secondary organic aerosol produced by ozonation of limonene., Phys. Chem. Chem. Phys., 10, 1009–1022, doi:10.1039/B712620D, 2008.

Wang, M., Yao, L., Zheng, J., Wang, X., Chen, J., Yang, X., Worsnop, D. R., Donahue, N. M., and Wang, L.: Reactions of Atmospheric Particulate Stabilized Criegee Intermediates Lead to High-Molecular-Weight Aerosol Components, Environ. Sci. Technol., 50, 5702–5710, doi:10.1021/acs.est.6b02114, 2016.

Wang, S. C. and Flagan, R. C.: Scanning electrical mobility spectrometer, Aerosol Sci. Technol., 13, 230–240, doi:10.1016/0021-8502(89)90868-9, 1990.

Wang, X., Liu, T., Bernard, F., Ding, X., Wen, S., Zhang, Y., Zhang, Z., He, Q., Lü, S., Chen, J., Saunders, S., and Yu, J.: Design and characterization of a smog chamber for studying gas-phase chemical mechanisms and aerosol formation, Atmos. Meas. Tech., 7, 301–313, doi:10.5194/amt-7-301-2014, 2014.

Wiedensohler, A., Birmili, W., Nowak, A., Sonntag, A., Weinhold, K., Merkel, M., Wehner, B., Tuch, T., Pfeifer, S., Fiebig, M., Fjäraa, A. M., Asmi, E., Sellegri, K., Depuy, R., Venzac, H., Villani, P., Laj, P., Aalto, P., Ogren, J. A., Swietlicki, E., Williams, P., Roldin, P., Quincey, P., Hüglin, C., Fierz-Schmidhauser, R., Gysel, M., Weingartner, E., Riccobono, F., Santos, S., Grüning, C., Faloon, K., Beddows, D., Harrison, R., Monahan, C., Jennings, S. G., O'Dowd, C. D., Marinoni, A., Horn, H. G., Keck, L., Jiang, J., Scheckman, J., McMurry, P. H., Deng, Z., Zhao, C. S., Moerman, M., Henzing, B., De Leeuw, G., Löschau, G., and Bastian, S.: Mobility particle size spectrometers: Harmonization of technical standards and data structure to facilitate high quality long-term observations of atmospheric particle number size distributions, Atmos. Meas. Tech., 5, 657–685, doi:10.5194/amt-5-657-2012, 2012.

Winterhalter, R., Herrmann, F., Kanawati, B., Nguyen, T. L., Peeters, J., Vereecken, L., and Moortgat, G. K.: The gas-phase ozonolysis of β-caryophyllene ($C_{15}H_{24}$). Part I: an experimental study, Phys. Chem. Chem. Phys., 11, 4152–4172, doi:10.1039/b817824k, 2009.

World Health Organization: WHO Air quality guidelines for particulate matter, ozone, nitrogen dioxide and sulfur dioxide: global update 2005: summary of risk assessment, WHO Press, Geneva, doi:10.1016/0004-6981(88)90109-6, 2006.

Yeh, G. K. and Ziemann, P. J.: Gas-Wall Partitioning of Oxygenated Organic Compounds: Measurements, Structure-Activity Relationships, and Correlation with Gas Chromatographic Retention Factor, Aerosol Sci. Technol., 49, 727–738, doi:10.1080/02786826.2015.1068427, 2015.

Zhang, D. and Zhang, R.: Ozonolysis of α-pinene and β-pinene: Kinetics and mechanism, J. Chem. Phys., 122, 114 308, doi:10.1063/1.1862616, 2005.

Zhang, X., Cappa, C. D., Jathar, S. H., McVay, R. C., Ensberg, J. J., Kleeman, M. J., and Seinfeld, J. H.: Influence of vapor wall loss in laboratory chambers on yields of secondary organic aerosol, Proc. Natl. Acad. Sci. U. S. A., 111, 5802–5807, doi:10.1073/pnas.1404727111, 2014.

Zhao, D. F., Kaminski, M., Schlag, P., Fuchs, H., Acir, I. H., Bohn, B., Häseler, R., Kiendler-Scharr, A., Rohrer, F., Tillmann, R., Wang, M. J., Wegener, R., Wildt, J., Wahner, A., and Mentel, T. F.: Secondary organic aerosol formation from hydroxyl radical oxidation and ozonolysis of monoterpenes, Atmos. Chem. Phys., 15, 991–1012, doi:10.5194/acp-15-991-2015, 2015.

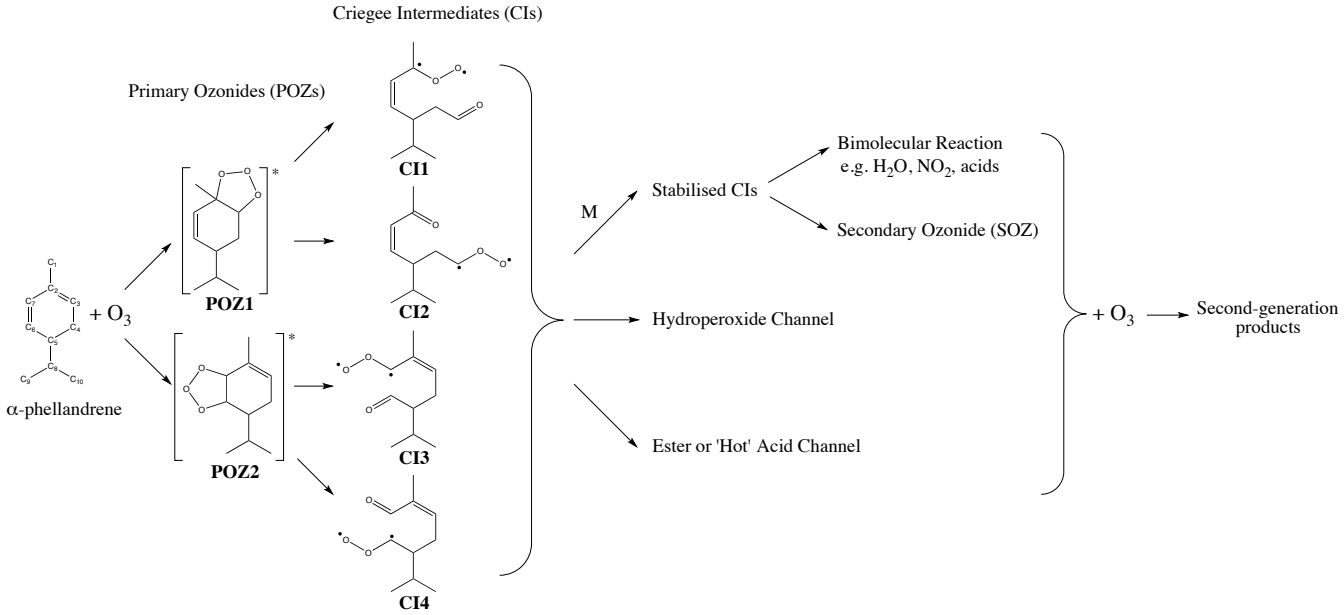

Figure 1. Simplified mechanism showing reaction processes involved during ozone addition to α-phellandrene ~~– for clarity hydrogens are not shown, carbon atom~~ within conventional frameworks (adapted from Mackenzie-Rae et al. (2016)). Carbon labels on α-phellandrene are referred to in the main text.

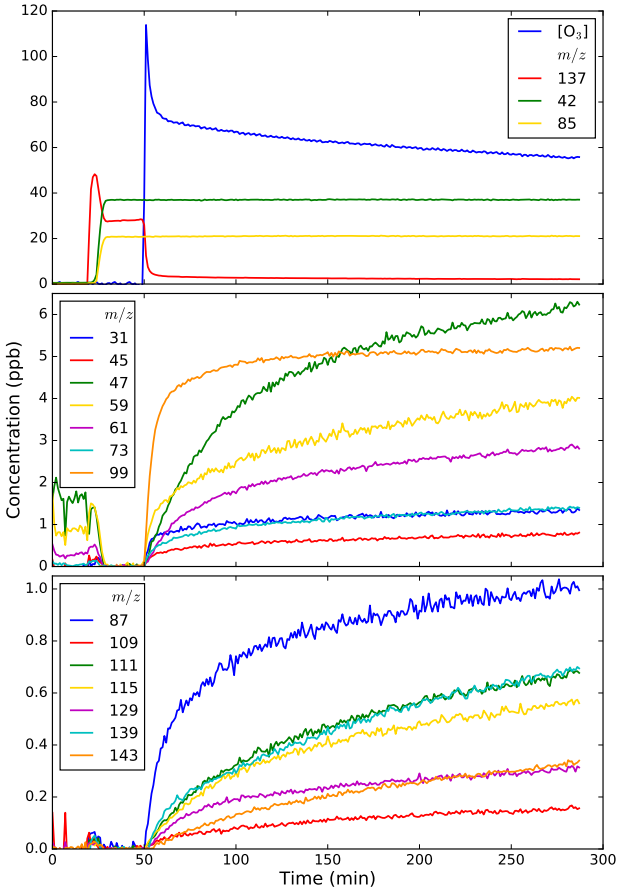

Figure 2. Time profiles of major species detected using the PTR-TOF during the ozonolysis of α-phellandrene in experiment 5. The peak of α-phellandrene observed upon its addition was the result of the reactor fans being switched on immediately prior to the introduction of acetonitrile in this experiment.

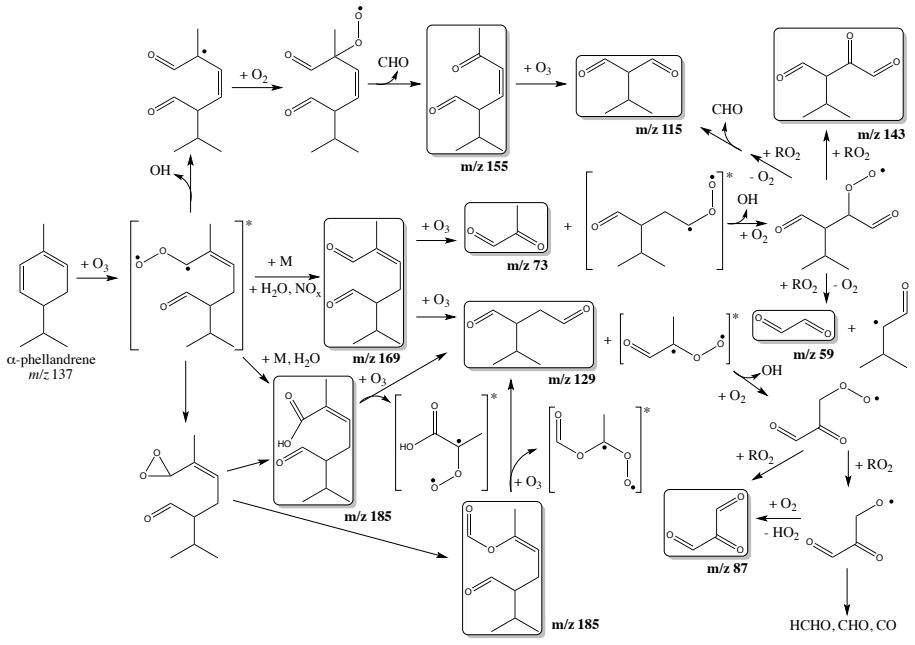

Figure 3. Partial mechanism for the ozonolysis of α-phellandrene starting from CI3, yielding product masses detected by the PTR-TOF. Similar constructs for the remaining CIs are provided in the Supplementary Information (S.1).

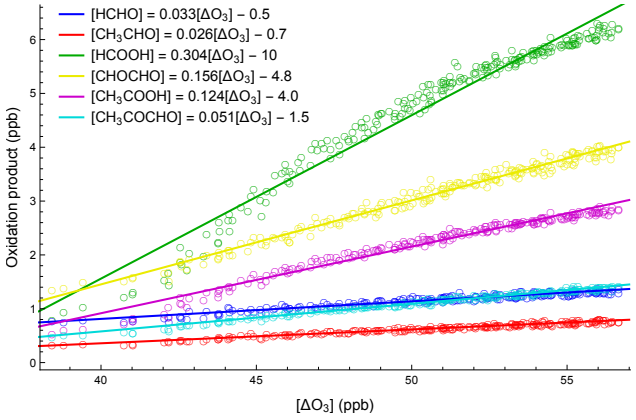

Figure 4. Determination of gas-phase product yields in experiment 5.

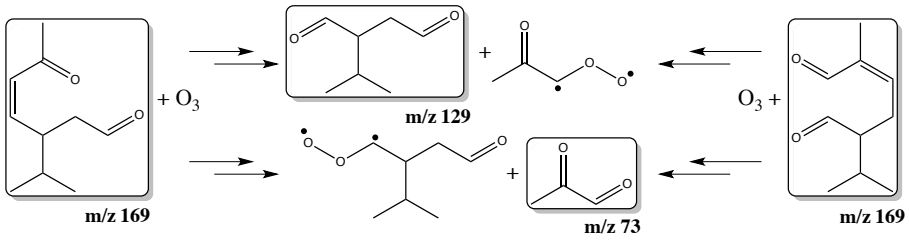

Figure 5. Mechanism of O_3 addition to the proposed *m/z* 169 structures, yielding pairs of Criegee intermediates and carbonyl containing products.

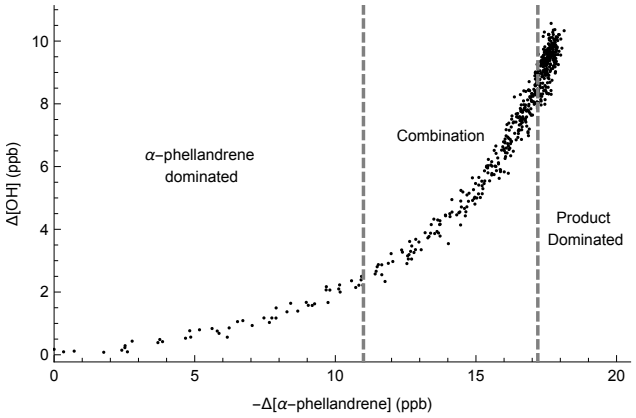

Figure 6. OH radical production versus α-phellandrene consumption for the first 18 minutes of experiment 3.

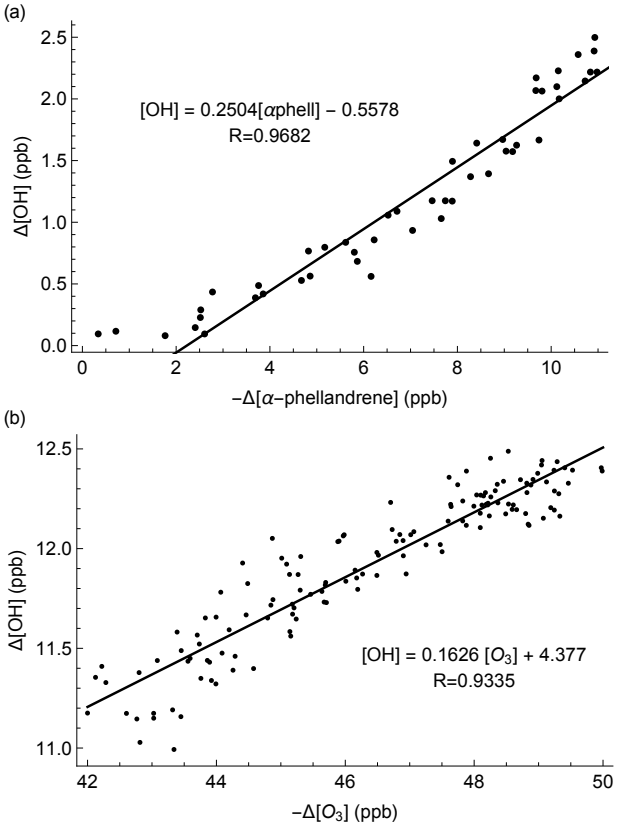

Figure 7. OH production from the (a) first and (b) second addition of ozone to α-phellandrene in experiment 3 against α-phellandrene and ozone consumption respectively.

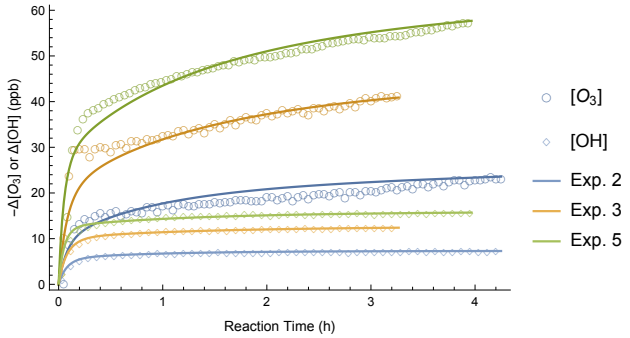

Figure 8. Plot of consumption of ozone and OH production against reaction time for experiments 2 (blue), 3 (yellow) and 5 (green). Experimental data are represented by open circles for O_3 and open diamonds for OH, whilst solid lines are modelled results using parameters listed in Table 5.

~~Mechanism of addition to the proposed *m/z* 169 structures, yielding pairs of Criegee intermediates and carbonyl containing products.~~

~~Partial mechanism for the ozonolysis of α-phellandrene yielding product masses detected by the PTR-TOF. Other CIs and reaction pathways exist but are not shown here.~~

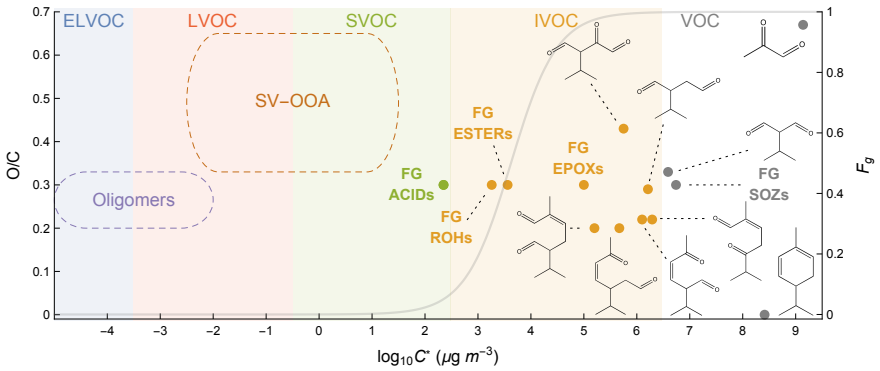

Figure 9. ~~Predicted~~ Dots show predicted first-generation and detected second-generation products from the ozonolysis of α-phellandrene in Donahue et al. (2006) space. Grey line shows the fraction of species of different saturation vapour concentrations in the gas-phase (F_g) after gas-wall and gas-particle equilibrium is reached, using C_w = 5 $\mathrm{mg\,m^{-3}}$ and an SOA loading of 200 $\mathrm{\mu g\,m^{-3}}$. Formulation of F_g is given in the Supplementary Information (S.6.).

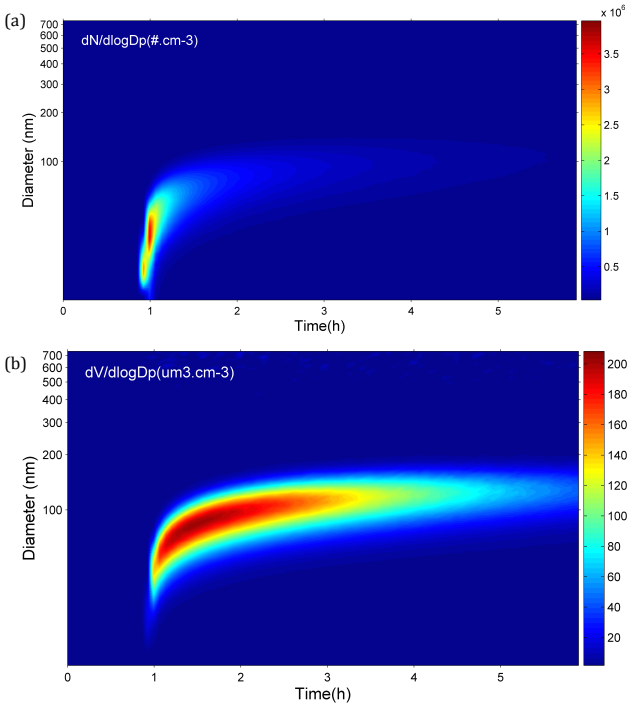

Figure 10. (a) Particle number (cm^{-3}) and (b) volume ($\mu\mathrm{m}^3\ \mathrm{cm}^{-3}$) size distributions for experiment 3.

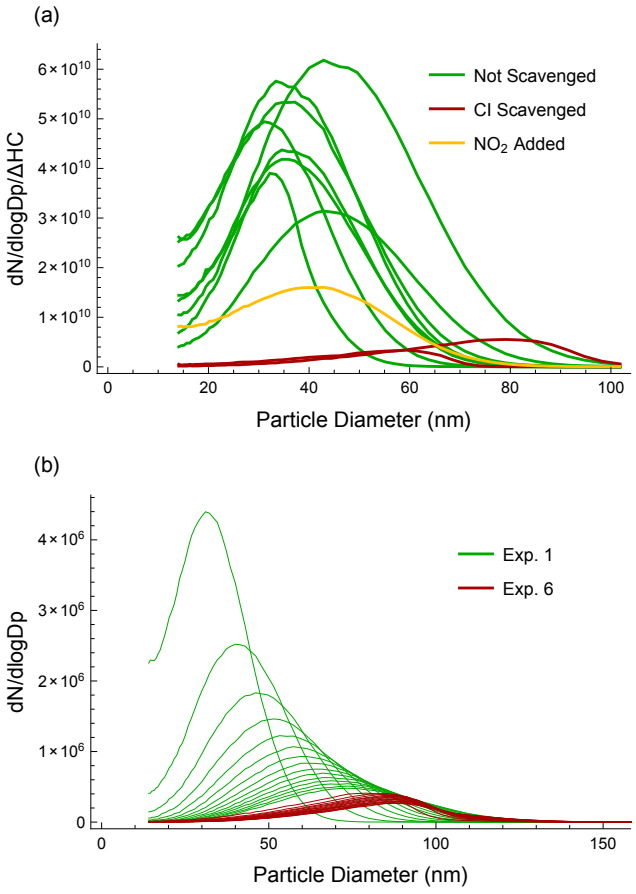

Figure 11. Impact of ~~Cl~~ sCI scavengers on particle nucleation shown by (a) peak particle number distributions scaled for the amount of α-phellandrene reacted in all experiments and (b) particle number distributions evolution over the first hour of experiments 1 and 6.

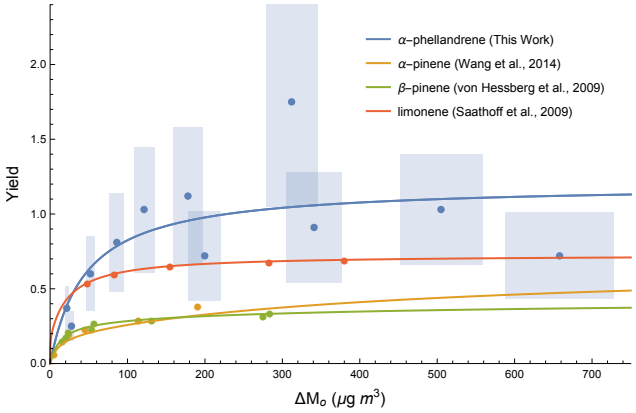

Figure 12. Comparison of SOA yield data for α-phellandrene with other monoterpene ozonolysis experiments. Lines are the best ~~two-product~~ empirical model fits ~~(see text)~~(Odum et al., 1996).

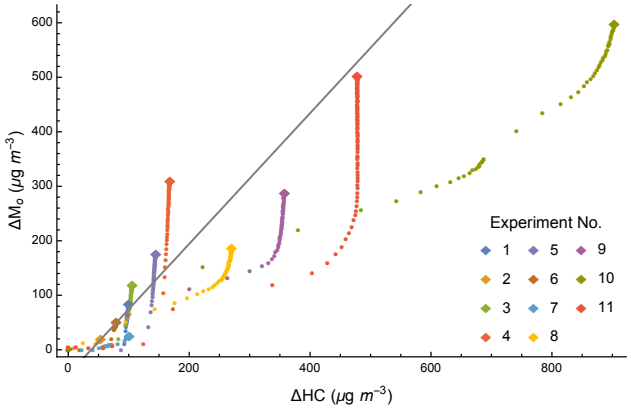

Figure 13. Time dependent SOA growth curves. Grey line is fitted one-parameter fit yield curve~~and legend refers to experiment number~~.

~~Ratio of *m/z* 43 () to *m/z* 44 () signals in AMS spectra for three α-phellandrene experiments.~~

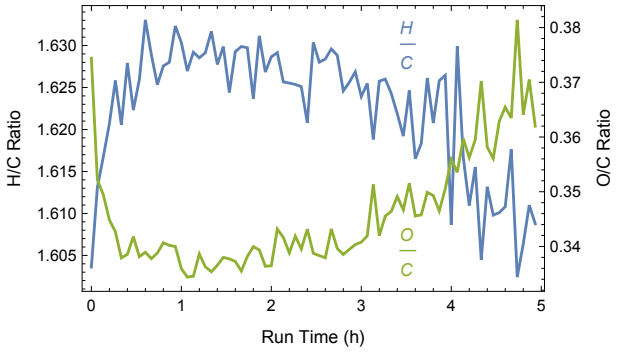

Figure 14. H/C and O/C ratios as a function of time for a typical α-phellandrene ozonolysis experiment ~~, number 4.~~(Experiment 4).

~~High-resolution AMS mass spectra at peak SOA loading from experiment 1. Inset are fragmentation routes of identified gas-phase products yielding deteeted ions.~~

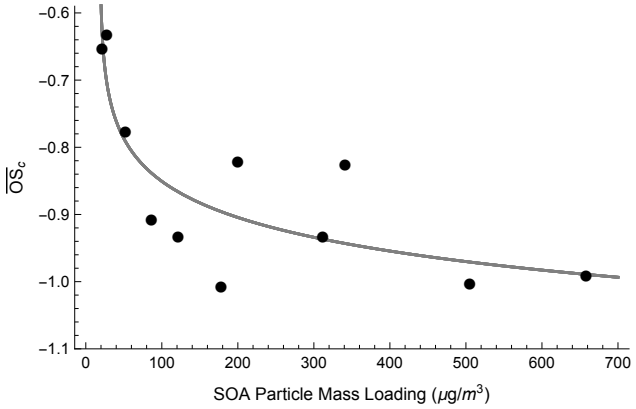

Figure 15. Average oxidation state of carbon for increasing SOA loadings generated through α-phellandrene ozonolysis experiments, with general trend shown.

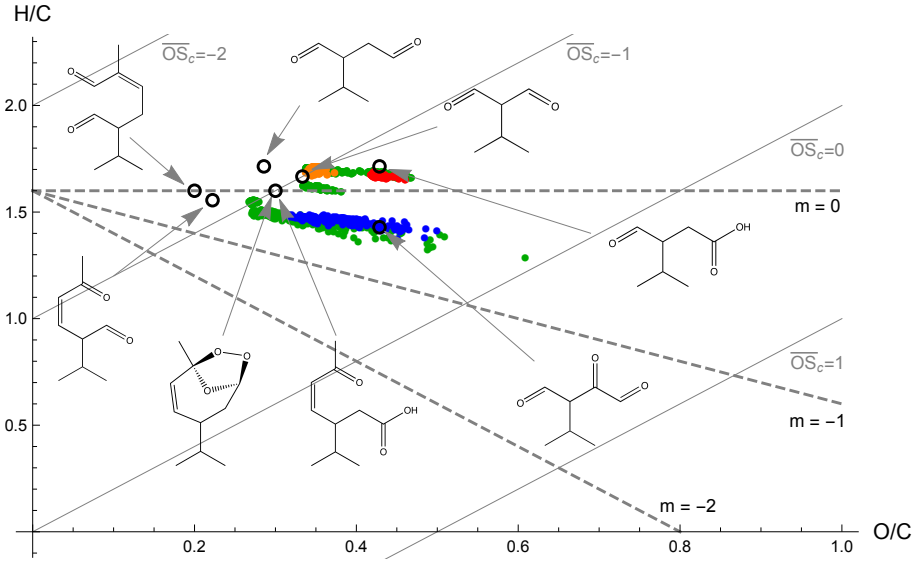

Figure 16. Van Krevelen plot. Blue dots are for experiments with a CI scavenger (6, 7), red dots for the experiment without cyclohexane (9), yellow dots for experiment with NO_2 added (11) and green dots for remaining experiments. Both predicted and detected gas-phase species are shown with open black circles.

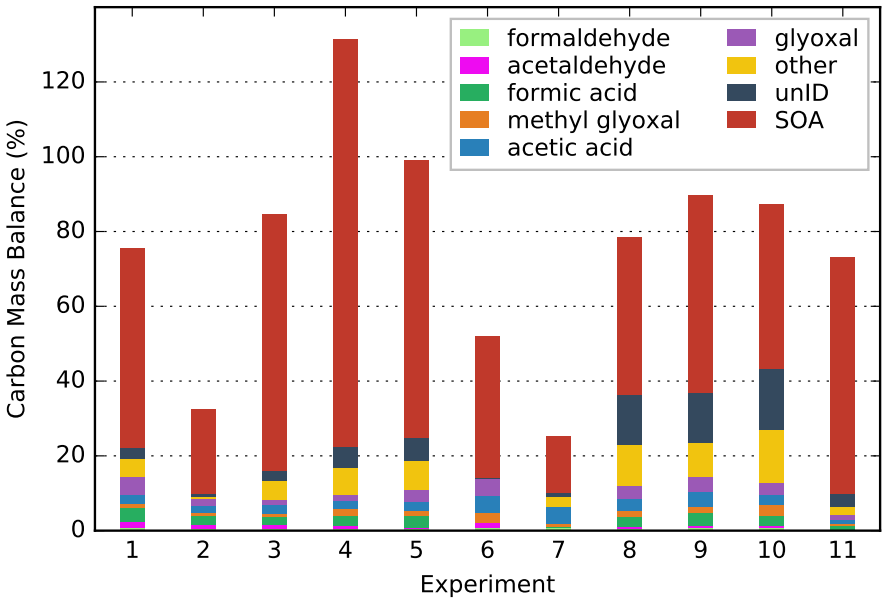

Figure 17. Carbon mass balance for each experiment.

Table 1. Starting conditions for α-phellandrene chamber ozonolysis experiments.

No.	Temperature (K)	Relative Humidity (%)	α-phellandrene (ppb)	O_3 (ppb)	Additives[a]
1	297.1 ± 0.4	2.5 ± 0.6	19 ± 7	> 259	Cyclohexane
2	297.5 ± 0.5	2.1 ± 0.7	10 ± 4	> 86	Cyclohexane
3	297.2 ± 0.2	2.3 ± 0.6	21 ± 8	> 83	Cyclohexane
4	297.4 ± 0.5	2.2 ± 0.9	32 ± 13	> 193	Cyclohexane
5	297.6 ± 0.7	1.8 ± 0.4	29 ± 11	> 114	Cyclohexane
6	298.0 ± 0.3	1.6 ± 0.1	16 ± 6	> 470	Cyclohexane Formic Acid[b]
7	298.0 ± 0.1	1.9 ± 0.2	19 ± 8	> 499	Cyclohexane Formic Acid[b]
8	298.7 ± 0.6	5.2 ± 0.2	61 ± 24	> 56	Cyclohexane
9	298.5 ± 0.4	4.9 ± 0.4	67 ± 27	> 101	–
10	298.2 ± 0.5	4.8 ± 0.3	175 ± 69	> 174	Cyclohexane
11	298.1 ± 0.4	4.5 ± 0.2	88 ± 35	> 132	NO_2[c]

~~(385 ppb)~~

[a] All experiments had acetonitrile (2.5 µL) added as a dilution tracer.

[b] 800 ± 80 ppb added prior to starting experiment.

[c] 385 ± 5 ppb added prior to starting experiment.

Table 2. Identified ions detected by the PTR-TOF. Refer to ~~Figures~~ Figure 3 for product structures.

	m/z	Formula	Assignment
Primary Signals	21	H_3O^{18+}	Hydronium ion
	37	$(H_2O)_2H^+$	Water cluster
	55	$(H_2O)_3H^+$	Water cluster
Acetonitrile	42	CH_3CNH^+	Acetonitrile
Cyclohexane	28, 39, 40, 41, 42, 43, 44, 54, 55, 56, 57, 58, 67, 68, 69, 70, 82, 83, 84, 85, 86	$C_6H_{12}H^+$	Cyclohexane and fragments
	81, 99, 100, 116, 117	$C_6H_{10}OH^+$	Cyclohexanone
	83, 101	$C_6H_{12}OH^+$	Cyclohexanol[a]
Formic Acid	47, 48, 49, 65	$CH_2O_2H^+$	Formic Acid
Acetic Acid	43, 61, 62, 79	$C_2H_4O_2H^+$	Acetic Acid
α-phellandrene	43, 67, 69, 79, 81, 82, 83, 91, 92, 93, 94, 95, 109, 119, 121, 135, 136, 137, 138, 139, 153	$C_{10}H_{16}H^+$	See Supplementary Information (S.2)
Ozonolysis Products	31	CH_2OH^+	Formaldehyde
	45	$C_2H_4OH^+$	Acetaldehyde
	47	$CH_2O_2H^+$	Formic Acid
	59	$C_2H_2O_2H^+$	Glyoxal
	61	$C_2H_4O_2H^+$	Acetic Acid
	73	$C_3H_4O_2H^+$	Methyl Glyoxal
	87	$C_3H_2O_3H^+$	
	115, 97	$C_6H_{10}O_2H^+$	Identified oxidation
	129, 111	$C_7H_{12}O_2H^+$	products[b]
	143	$C_7H_{10}O_3H^+$	
	85[c], 99, 109, 125, 139, 155	–	Unidentified oxidation products
	167, 169, 185	–	Gas-phase dimers

[a] Winterhalter et al. (2009)

[b] Refer to Fig. 3

[c] Detected in experiments 9 and 11.

Table 3. Gas-phase molar yields (%) for major α-phellandrene ozonolysis products.

No.	formaldehyde	acetaldehyde	formic acid	glyoxal	acetic acid	methyl glyoxal
1	6.9 ± 2	8.3 ± 2	37 ± 9.0	23 ± 5	13 ± 3	3.7 ± 0.9
2	5.9 ± 1	4.4 ± 1	24 ± 6	9.0 ± 2	9.0 ± 2	3.1 ± 0.7
3	5.9 ± 1	5.4 ± 1	22 ± 5	6.2 ± 1	12 ± 3	2.0 ± 0.5
4	5.0 ± 1	3.8 ± 0.9	28 ± 6	7.6 ± 2	11 ± 2	5.7 ± 1
5	3.3 ± 0.8	2.6 ± 0.6	30 ± 7	16 ± 4	12 ± 3	5.1 ± 1
6	7.0 ± 2	7.6 ± 2		24 ± 6	22 ± 5	8.5 ± 2
7	8.7 ± 2	0.2 ± 0.04			22 ± 5	3.4 ± 0.8
8	5.4 ± 1	2.3 ± 0.5	28 ± 6	17 ± 4	16 ± 4	5.2 ± 1
9	7.5 ± 2	2.5 ± 0.6	35 ± 8	21 ± 5	20 ± 5	5.3 ± 1
10	7.9 ± 2	2.2 ± 0.5	29 ± 7	17 ± 4	13 ± 3	9.2 ± 2
11	1.2 ± 0.3	0.41 ± 0.09	10 ± 2	7.6 ± 2	5.0 ± 1	2.1 ± 0.5

Table 4. Minor gas-phase molar yields (%) for α-phellandrene ozonolysis.

No.	*m/z* 87	*m/z* 97	*m/z* 109	*m/z* 111	*m/z* 115	*m/z* 129	*m/z* 139	*m/z* 143
1	2.5 ± 0.6	1.1 ± 0.3	0.58 ± 0.1	2.9 ± 0.7	3.3 ± 0.8		3.4 ± 0.8	
2	2.5 ± 0.6	0.87 ± 0.2	0.19 ± 0.04					
3	3.2 ± 0.8	1.3 ± 0.3	0.61 ± 0.1	3.6 ± 0.9	3.0 ± 0.7		2.3 ± 0.5	
4	2.5 ± 0.6	0.21 ± 0.05	0.74 ± 0.2	3.6 ± 0.9	3.0 ± 0.7	1.3 ± 0.3	4.4 ± 1	1.9 ± 0.5
5	3.5 ± 0.8	1.1 ± 0.3	0.78 ± 0.2	3.7 ± 0.9	3.0 ± 0.7	1.4 ± 0.3	3.7 ± 0.9	2.0 ± 0.5
6	0.13 ± 0.03		0.45 ± 0.1					
7	0.75 ± 0.2				2.4 ± 0.6		1.7 ± 0.4	1.5 ± 0.4
8	5.4 ± 1	2.0 ± 0.5	1.1 ± 0.3	4.8 ± 1	3.1 ± 0.7	1.4 ± 0.3	4.2 ± 1	4.4 ± 1
9	2.3 ± 0.5	0.76 ± 0.2	0.68 ± 0.2	2.2 ± 0.5	3.0 ± 0.7	1.9 ± 0.5	3.8 ± 0.9	5.1 ± 1
10	7.4 ± 2	2.7 ± 0.6	0.69 ± 0.2	4.0 ± 0.9	2.7 ± 0.6	6.0 ± 1	3.9 ± 0.9	4.4 ± 1
11	0.12 ± 0.03	0.13 ± 0.03	0.15 ± 0.03	0.09 ± 0.02	0.91 ± 0.2	0.29 ± 0.07	0.40 ± 0.09	1.7 ± 0.4

Table 5. Measured and modelled OH radical yields and modelled rate constants for α-phellandrene ozonolysis experiments.

	α-phellandrene			First-generation products		
	k_1 (10^{-15} cm^3 molecule^{-1} s^{-1})	Experimental OH Yield (%)	Modelled OH Yield (%)	k_2 (10^{-16} cm^3 molecule^{-1} s^{-1})	Experimental OH Yield (%)	Modelled OH Yield (%)
1	2.0	29 ± 8	48	0.7	10 ± 2	10
2	2.0	25 ± 8	55	2.0	27 ± 5	13
3	2.0	25 ± 8	48	1.5	16 ± 4	11
4	2.0	21 ± 7	46	0.6	10 ± 2	8
5	2.0	28 ± 8	45	1.0	11 ± 3	10
6	3.0	54 ± 14	~~67~~ 57	0.3	20 ± 4	20
7	3.0	48 ± 13	65	1.0	10 ± 3	23
8	2.0	43 ± 14	68	2.0	–	10
10	2.0	47 ± 11	46	0.3	–	15
Lit.	3.0 ± 1[a]	26 – 31[b]			8 – 11[b]	

[a] Calvert et al. (2000)

[b] Herrmann et al. (2010)

Table 6. Aerosol loadings, effective densities, oxidation states and yields for α-phellandrene ozonolysis experiments.

No.	Total SOA Mass[a] ($\mu g\,m^3$)	Density ($g\,cm^{-3}$)	$\overline{OS}_c$	Yield (Y)
1	86.1 ± 9	1.29 ± 0.05	-0.91 ± 0.3	0.81 ± 0.3
2	21.5 ± 2	1.32 ± 0.06	-0.65 ± 0.2	0.37 ± 0.2
3	121.3 ± 13	1.37 ± 0.05	-0.93 ± 0.3	1.03 ± 0.4
4	311.9 ± 33	1.57 ± 0.05	-0.93 ± 0.3	1.74 ± 0.7
5	178.0 ± 19	1.36 ± 0.05	-1.0 ± 0.3	1.11 ± 0.5
6	52.0 ± 6	1.38 ± 0.05	-0.77 ± 0.3	0.60 ± 0.2
7	27.6 ± 3	1.34 ± 0.05	-0.63 ± 0.2	0.25 ± 0.1
8	199.7 ± 21	1.69 ± 0.06	-0.82 ± 0.3	0.72 ± 0.3
9	341.0 ± 36	1.61 ± 0.05	-0.83 ± 0.3	0.90 ± 0.37
10	658.1 ± 70	1.60 ± 0.05	-0.99 ± 0.3	0.71 ± 0.3
11	504.9 ± 53	1.90 ± 0.06	-1.0 ± 0.3	1.02 ± 0.4

[a] Wall-loss corrected (Pathak et al., 2007).